This is to certify that the

dissertation entitled

TRANSFORMATION OF CARBON TETRACHLORIDE
BY MOBILE AND STATIONARY PHASE
BACTERIA IN POROUS MEDIA

presented by

Michael Erich Witt

has been accepted towards fulfillment
of the requirements for

Ph.D. degree in Environmental
Engineering

Craig S. Criddle
Major professor

Date 5/12/98

TRANSFORMATION OF CARBON TETRACHLORIDE BY MOBILE AND STATIONARY PHASE BACTERIA IN POROUS MEDIA

By

Michael Erich Witt

A DISSERTATION

Submitted to
Michigan State University
in partial fulfillment of the requirements
for the degree of

DOCTOR OF PHILOSOPHY

Department of Civil and Environmental Engineering

1998

ABSTRACT

TRANSFORMATION OF CARBON TETRACHLORIDE BY MOBILE AND STATIONARY PHASE BACTERIA IN POROUS MEDIA

By

Michael Erich Witt

Pseudomonas stutzeri KC is a motile aquifer isolate capable of transforming carbon tetrachloride (CT) to carbon dioxide, formate, and non-volatile end products under denitrifying conditions without producing chloroform (CF). The feasibility of CT removal by planktonic and attached *Pseudomonas stutzeri* KC was evaluated in model aquifer columns packed with sediments from a CT- and nitrate-contaminated aquifer near Schoolcraft, Michigan.

The removal of CT by attached cells was evaluated using two 2-m long model columns and inoculating an 8-cm-wide, pH-adjusted zone near the upstream end of both columns with groundwater containing strain KC and acetate. Both columns received weekly nutrient additions in the slug injection zone. Base and phosphate additions were performed weekly in one column and twice-weekly in the second column. A CT-transforming zone developed in the slug injection zone of both columns, with 97% removal of CT in the column receiving weekly base additions and 93% removal in the column receiving twice-weekly base additions. The results indicate that efficient CT removal without CF production is possible over extended periods. The results also suggest that microbial populations indigenous to the Schoolcraft aquifer can convert CT to CF, and that such populations may be selected by twice-weekly base additions.

Capillary assay experiments have established that strain KC is chemotactic toward nitrate. Columns packed with aquifer sediment were used to determine whether nitrate-directed motility of planktonic KC cells would influence bioremediation of CT-contaminated aquifer sediments. A "continuous flow" column was used to evaluate the effects of chemotaxis in the presence of an imposed advective flow, and a "static" column was used to isolate the effects of chemotaxis in the absence of flow. The continuous flow column was inoculated near its upstream end with strain KC, base, acetate, and phosphate. KC cells migrated through the column at a velocity exceeding the average linear groundwater velocity, removing ~55% of the total mass of CT in the aqueous phase and ~29% of the sorbed CT. The static column was inoculated near its midpoint, and was maintained thereafter as a static incubation. Motile KC cells migrated over a 30 cm distance within five days. After 26 days, over 94% of the CT in the aqueous phase had been degraded. The results support the hypothesis that localized depletion of nitrate creates nitrate gradients that trigger a chemotactic response by strain KC.

A computer model was developed to predict liquid and solid phase concentrations of CT, attached and planktonic strain KC, acetate, and nitrate as functions of time in the model column. The computer model accurately predicted strain KC migration, CT degradation, and acetate and nitrate utilization.

The ability of *Pseudomonas stutzeri* KC to colonize aquifer sediments and transform CT in the groundwater and the solids has been shown. The key to successful bioaugmentation using strain KC is to provide cells with an environment where they may successfully compete with indigenous microflora for microbial growth substrates. The use of such a technology may have widespread application in CT- and nitrate-contaminated aquifers around the United States and beyond.

For Laurie
whose life adds so much to mine
your love and companionship are truly a blessing which I will cherish forever

ACKNOWLEDGMENTS

I would like to express my sincere gratitude to all of those who made successful completion of this dissertation possible.

To my wife, Laurie, words cannot describe how much your love, support, and companionship has helped me to complete this mountainous task. Your drive and optimism on life are only surpassed by your ability to be the best friend that anyone could ever hope to have. I look forward to our bright future and am eager to spend a lifetime with you.

I would like to thank my parents for all of their support and encouragement during my educational career. Twenty-two years ago you walked me to my first kindergarten class, probably telling me that for the next seventeen years, I would acquire an education to prepare me for the whatever the future holds. Little did you know that almost a quarter-century later my educational endeavors would finally be realized. You have taught me most of what I know about life, and have prepared me well for what the future holds in store for both Laurie and me. I thank God every day for the gift of growing up and being loved as one of your children.

To my wonderful brothers and sisters, thank you all for giving me the experience of growing up with the five of you. I would not trade the experiences I had in my childhood for anything. The fun and laughter that we have all enjoyed together will stay with me for a lifetime. Thank you Deb, Laura, Bill, Julie, and Steve - what more could a brother ask for! And to our little girl Denali.....you are truly "a Great One."

To Laurie's parents, Mike and Lynne, thank you for all of your support of both Laurie and I during our college education. Your extraordinary ability to parent is manifest in the life of my wonderful wife. Your unselfish generosity helped us to complete our educational goals, and for that I am grateful.

A heart-felt thank you to my good friend, teacher, and academic adviser Craig Criddle. I cannot think of another who is so enthusiastic and so devoted to learning about science and the world around us. I greatly respect your intellect, honesty, and ability to inspire others. I sincerely wish that all of your personal and professional endeavors are accomplished.

Thank you, Michael Dybas, for providing an enjoyable atmosphere in the lab and in the field. I greatly appreciate all of your contributions to my research. Your ability to solve complex and difficult "roadblocks" is unmatched by most in the scientific field. I also appreciate your company during the many hunting and fishing trips that we made together. We still need to get the elusive "big one!"

Special thanks to my friend, David Wiggert, for his advice and counsel. I really appreciate the many inspiring discussions related to graduate studies and research. I especially enjoyed our talk about the finer aspects of life - sports and outdoor travel. I wish you nothing but the best as you prepare for your future in northern Michigan near Lake Leelanau.

I would also like to extend a thank you to Gary Klecka, a research committee member and good friend. You brought valuable insight to my research committee through your unique perspective with which to critique my research. I respect your

knowledge and expertise in the field of bioremediation and hope to continue to learn more from you. I also appreciate your assistance with my search for employment.

I appreciate the beneficial contributions to my research by my friend and professor Stephen Boyd. I am especially appreciative of your careful examination and critique of my research results. You have certainly helped to make me a better scientist and engineer by serving on my research committee.

Thank you to Linda Steinman, the "brains" of the research complex, without whom many of us graduate students would still be trying to figure out how to graduate. Our daily chats were quite enjoyable.

A number of friends and colleagues deserve praise for their assistance in the completion of this research. Thank you to Greg Tatara, Mike Szafranski, Jamie Gellner, Blake Key, Kelly Kelly, Randy Brown, Pat Radabaugh, Dave Berends, Fred Knoll, Mark Sneathen, Joel Parker, Yan Pan, and Xianda Zhao. A special thanks to Leslie Dybas for all of her insight into the wonderful world of canines, and also for her assistance in teaching me the PCR technique. And to Terry Casey, who can make a square peg fit into a round hole, thank you for all of your expert assistance for the past five years.

TABLE OF CONTENTS

LIST OF TABLES

LIST OF FIGURES

LIST OF SYMBOLS

a	chemoattractant concentration, mg/L
α	growth-related specific ATP production rate, moles ATP/mg cell-day
b	bacterial cell concentration, mg/L
b_{KC}	decay rate for strain KC, day^{-1}
β	maintenance-related specific ATP production rate from substrate degradation, moles ATP/mg substrate-day
C_a	acetate concentration in the aqueous phase, mg/L
C_{CT}	carbon tetrachloride concentration in the aqueous phase, mg/L
C_n	nitrate concentration in the aqueous phase, mg/L
χ	chemotaxis coefficient, cm^2/day
χ_o	chemotactic sensitivity coefficient, cm^2/day
$\chi_{o,eff}$	effective chemotactic sensitivity coefficient, cm^2/day
D	diffusion coefficient, cm^2/day
D_a	diffusion coefficient for acetate, cm^2/day
D_n	diffusion coefficient for nitrate, cm^2/day
D_{eff}	effective diffusion coefficient, cm^2/day
$D_{l,cell}$	hydrodynamic dispersion coefficient for a bacterial cell, cm^2/day
δ	maintenance-related specific ATP consumption rate, moles ATP/mg cell-day
f	fraction of exchange sites at equilibrium
γ	specific ATP production rate from biomass decay, moles ATP/mg cell-day
J_a	chemoattractant flux, mg/cm^2-day
J_b	bacterial flux, mg/cm^2-day
K_{at}	bacterial attachment rate, day^{-1}
K_d	partition coefficient, L/kg
K_{de}	bacterial detachment rate, day^{-1}
K_s	half-saturation coefficient for growth substrate, mg/L
$K_{s,n}$	half-saturation coefficient for nitrate, mg/L
k	substrate utilization rate, mg substrate/mg cell-day
k'	second-order rate coefficient for CT degradation, L/mg-day
k_{rc}	dissociation constant for receptor-attractant complex, mg/L
κ	first-order kinetic rate coefficient for desorption, day^{-1}
L	run length for motile bacteria
M	Monod-type saturation term
M_n	Monod-type saturation term for nitrate
M_s	Monod-type saturation term for growth substrate
M_s'	Monod-type saturation term for growth substrate (assumed to be a value of 1.0)

μ	bacterial growth rate, day^{-1}
μ_e	specific growth rate associated with no maintenance costs,day^{-1}
μ_{max}	maximum bacterial growth rate, day^{-1}
μ_{obs}	observed specific growth rate, day^{-1}
μ_{true}	true specific growth rate, day^{-1}
N_b	number of bound receptors on surface of cell
N_t	total number of receptors on surface of cell
n	sediment porosity
ω	random motility coefficient, cm^2/day
ω_{eff}	effective random motility coefficient, cm^2/day
P	model parameter
φ	variation coefficient
ψ	motility-related specific ATP consumption rate, moles ATP/mg cell-day
q_s	specific substrate utilization rate, mg substrate/mg cell-day
$q_{s,ana}$	specific substrate utilization rate for anabolism, mg substrate/mg cell-day
$q_{s,cat}$	specific substrate utilization rate for catabolism, mg substrate/mg cell-day
$q_{s,gr}$	specific substrate utilization rate for growth, mg substrate/mg cell-day
$q_{s,m}$	specific substrate utilization rate for maintenance, mg substrate/mg cell-day
R_a	retardation coefficient for acetate
R_{CT}	retardation coefficient for carbon tetrachloride
R_n	retardation coefficient for nitrate
ρ_b	soil bulk density, mg/L
S_{CT}	carbon tetrachloride concentration on the solid phase, mg/kg
σ	differential tumbling frequency, day
t	time, days
τ	tortuosity
θ	random turn angle for motile bacteria
υ	one-dimensional cell swimming speed, cm/day
V	one-dimensional swimming speed of bacterial cells, cm/day
V_{max}	maximum one-dimensional swimming speed of cells, cm/day
V_c	chemotactic velocity, cm/day
$V_{c,eff}$	effective chemotactic velocity, cm/day
W	model variable
X	bacterial cell concentration, mg/L
X_{KC}	strain KC concentration in the aqueous phase, mg/L
X_{KC}	strain KC concentration on the solid phase, mg/L
x	distance along one-dimensional length of column, cm
Y, $Y_{s,x}$	cell yield on substrate, mg cells/mg substrate
Y_a	cell yield on acetate, mg cells/mg acetate

$Y_{cat,ATP}$	ATP yield on catabolic substrate, moles ATP/mg substrate
$Y_{mot,ATP}$	ATP required for cell motility, moles ATP/mg cell-rotation
Y_n	cell yield on nitrate, mg cells/mg nitrate
Y_{nb}	cell yield on decaying biomass, mg cells/mg cells
$Y_{x,ATP}$	ATP yield from cell oxidation, moles ATP/mg cell
Z_{kc}	decay coefficient related to motility, day^{-1}
$Z_{ac,1}$	maintenance coefficient for acetate, day^{-1}
$Z_{ac,2}$	motility coefficient for acetate, mg acetate/mg cell-day
Z_{nit}	motility coefficient for nitrate, mg nitrate/mg cell-day

Chapter 1

INTRODUCTION

1.1 Halogenated solvent contamination

Halogenated organics are one of the most prevalent organic groundwater contaminants in the United States. Because of the high solubility of halogenated solvents, they tend to be mobile and migrate freely through aquifer materials. The threat that such contaminants pose to drinking water is striking, as approximately 39% of the United States' public drinking water is supplied by groundwater (Solley *et al.*, 1988).

One example of a commonly-used halogenated solvent is carbon tetrachloride (CT). Due to its non-polarity and non-flammability, CT has served as a very useful solvent in recent decades. In addition to being used as a solvent, it has also been used as a drying agent for spark plugs, a dry cleaning agent, a grain fumigant, and a fire extinguishing agent. Due of its widespread use, followed by improper disposal or accidental releases, it is now a common groundwater pollutant. Because CT is a dense non-aqueous phase liquid (DNAPL), when large quantities have contaminated an aquifer, they sink to the bottom of the aquifer and slowly solubilize into the groundwater. CT has been found in an estimated 25% of groundwater supplies at concentrations of 1 to 400 μg/L (Sittig, 1985). Estimates indicate that 20 million people are exposed to CT through drinking contaminated groundwater, and an additional 2 million are exposed to contaminated soil or landfills (Sittig, 1985). For this reason, the United States Environmental Protection Agency has classified CT as a priority toxic pollutant due to its carcinogenicity and toxic effects.

Due to large volumes of CT-contaminated media in the United States, significant amounts of money have been invested in remediating these by conventional means. Historically, the preferred method of remediating groundwater contaminated with halogenated solvents and other volatile organics has been to pump the groundwater to the surface and treat it *ex-situ* by one of a number of physical, chemical, or biological processes. Air stripping is the most common practice. This treatment simply transfers the target compound from one medium (water) and to another (air). Long-term operation of such systems can be costly because multiple plume volumes must be removed to achieve the desired removal efficiency for both solids and groundwater.

1.2 Bioremediation

An alternative to the conventional method of pump and treat is the use of bioremediation to degrade halogenated solvents *in-situ*. This method of remediation has the potential to reduce cleanup costs (Quinton *et al.*, 1997). Until recent years, many in the scientific and engineering community believed that halogenated compounds, more specifically chlorinated compounds, were resistant to degradation by microbes. This view prevailed until transformation products of chlorinated solvents were detected in groundwater, surface water, and soil samples. Many of these toxic halogenated solvents (and degradation byproducts) are biodegradable under appropriate conditions and *in-situ* bioremediation is now viewed an attractive alternative for solving subsurface contamination problems.

In-situ bioremediation involves stimulating indigenous microbes to transform a target compound (biostimulation) or adding non-indigenous microbes to the subsurface

for the purposes of transforming a target compound (bioaugmentation). The use of biostimulation to degrade a target compound is generally favored, but this approach can result in undesirable outcomes. For example, although biostimulation to remove CT in contaminated aquifers is possible, care must be taken to avoid conversion of CT to chloroform (CF) or to further degrade CF if it is produced. In the case of CT, CF is a common result of biostimulation in both the laboratory and field environments (Criddle *et al.*, 1990; Egli *et al.* 1987 and 1988; and Semprini *et al.*, 1992). Although research suggests that chloroform levels can be controlled by manipulation of redox conditions (Criddle *et al.*, 1990; Jin and England, 1997), such control may be difficult to achieve under field conditions.

The principal advantage of bioaugmentation is in attacking molecules that are generally recalcitrant to biostimulation or that are transformed to undesirable products via intrinsic bioremediation. Another advantage is that the introduced organism and the transformation mediated by the organism can be studied and optimized in the laboratory. This can facilitate pathway control, ensuring adequate detoxification of the target contaminant. However, in the case of cometabolism where growth substrate must be added to support the desired biotransformation, competition for growth substrate can be expected between indigenous microflora and the microorganisms that are introduced. This competition presents a challenge when attempting to initiate cometabolic biotransformation of a particular compound using non-indigenous microorganisms. Indigenous populations are unavoidably stimulated by carbon and nutrients added for the support of the augmented organism. For bioremediation of CT, some of the stimulated populations transform CT to CF. If the concentration of indigenous organisms is too high

or the concentration of the augmented organism too low, the rate of transformation of CT to CF may equal or exceed rates of CT degradation by desirable pathways. Methods are needed whereby non-indigenous organisms used for bioaugmentation can be maintained at concentrations that are high enough to enable control of preferred degradation pathways.

One means of reducing the resistance of a microbial community to invasion and colonization by non-indigenous organisms is the creation of a niche for the non-indigenous organism. This method of niche (or environmental) adjustment provides conditions that favor the growth of the non-indigenous microbe. Here, niche is defined as "the combined description of the physical habitat, functional role, and interactions of the microorganisms occurring at a given location" (Atlas and Bartha, 1993). Practical modifications in a habitat can create functional roles for which a non-indigenous organism is well adapted. An increase in pH to 8.0-8.3, for example, reduces the solubility (hence bioavailability) of several essential trace metals, favoring microbes with efficient mechanisms for trace metal scavenging. This appears to be the case for *Pseudomonas stutzeri* KC, which secretes several distinct siderophores capable of efficient iron-scavenging (Dybas *et al.*, 1995). This capability may explain the competitiveness of strain KC at more alkaline pH levels. For pH values less than 7.8, microflora indigenous to a Schoolcraft (Michigan) aquifer had maximum specific growth rates that exceeded those of strain KC, but for pH values greater than 8.0, strain KC had higher growth rates (Sneathen, 1996).

A second critical factor controlling the success of bioremediation is delivery of bacterial cells to regions of contamination. While pumping cell cultures into the

subsurface will provide some degree of invasion, migration of cells into micropores is needed to ensure that contaminated groundwater does not pass through the zone of remediation. Therefore, transport of bacteria to regions unavailable by hydraulic delivery is paramount in the success of such a technology.

1.3 Carbon tetrachloride transformation by *Pseudomonas stutzeri* KC

Pseudomonas stutzeri KC (DSM deposit number 7136, ATCC deposit number 55595) is a natural aquifer isolate capable of transforming CT to CO_2, formate, and an unidentified non-volatile product under denitrifying conditions without the production of CF (Criddle *et al.*, 1990; and Lewis and Crawford, 1993). Figures 1.1 and 1.2 illustrate strain KC grown under aerobic and anaerobic (denitrifying) conditions, respectively. In both photographs the 1 μm-long bacterial flagellum is clearly visible. Also, the photograph of the KC cell grown under aerobic conditions is slightly longer and approximately 50% wider than the cell grown under denitrifying conditions.

Numerous experiments have been completed to better understand the mechanism of CT transformation by KC (Tatara *et al.*, 1993, and Dybas *et al.*, 1995). The requirements for CT transformation by KC are: (1) sufficient concentrations of an electron acceptor (nitrate) and electron donor (acetate); (2) denitrifying and (3) iron-limiting conditions; and (4) presence of trace levels of copper. In iron-rich groundwater and soils inoculated with KC, CT transformation can be achieved by raising the pH of the groundwater and soil materials to 8.0-8.3 (Knoll, 1994), a range where ferric iron solubility is lowest (Stumm and Morgan, 1981). Copper is required for CT transformation but is toxic at neutral pH (Tatara *et al.*, 1993). Dybas *et al.* (1995) and

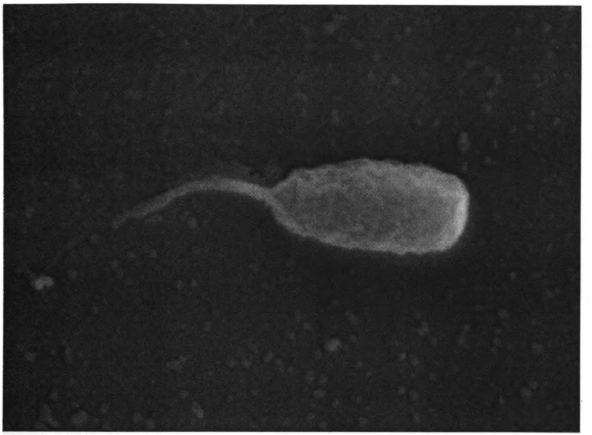

Figure 1.1 Scanning electron microscope secondary image of a fixed and critical point dried sample of *Pseudomonas stutzeri* KC grown under aerobic conditions (35,000X magnification).

Tatara (1996) investigated the complex mechanism responsible for CT transformation and determined that a plausible model involves: (1) production and export of a small biomolecule (~500 daltons) from the KC cell in response to iron limitation; (2) deactivation of the biomolecule upon transformation of CT; and (3) reactivation of the biomolecule at the cell membrane. Evidence suggests that production and export of this CT-transforming biomolecule from the cell in response to iron-limitation, along with reactivation of the factor by viable cells after transformation of CT, is the mechanism that enables strain KC to degrade CT. This factor is secreted by strain KC during periods of

rapid-growth and can be re-activated by a wide variety of organism types, including members of the Schoolcraft aquifer microflora community (Tatara, 1996). Tatara (1996) also established that the secreted biomolecule is transported freely without retardation through Schoolcraft aquifer materials.

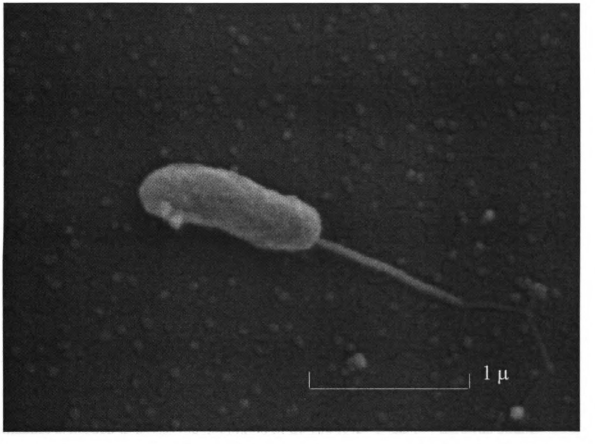

Figure 1.2 Scanning electron microscope secondary image of a fixed and critical point dried sample of *Pseudomonas stutzeri* KC grown under anaerobic (denitrifying) conditions (35,000X magnification).

1.4 Cell motility and chemotaxis

Transport of bacteria with degradative capabilities through aquifer material was first proposed in the 1980s (Lee *et al.*, 1988; and Thomas and Ward, 1989). Since then, a considerable research effort has focused on bioaugmentation using motile (and chemotactic) microorganisms. Upon injection into the subsurface, bacteria are likely to travel along preferred flow paths (macropores and fractures) through porous media. Motile bacteria may have the ability to migrate away from highly conductive macropores into regions of higher contaminant (or chemoattractant) concentration. The mechanism for this biased migration of bacterial cells in the direction of increasing chemoattractant concentration is termed chemotaxis.

The issue of bacterial transport in subsurface environments is not well understood. Many biological processes affect the transportability of microorganisms through porous media. Transport may be strongly affected by characteristics that are microbe-specific. Cell size, cell age, cell shape, cell surface chemistry, aggregating tendency, presence/absence of flagella, and polysaccharide production are examples of bacterial characteristics that affect transport. An understanding of these issues and how they interact is needed to assess the likelihood of transport for a specific bacterial strain.

Tim *et al.* (1988) were the first to identify and subdivide the microbial transport mechanisms into physical, chemical, and biological processes. The main physical processes responsible for microbial movement through porous media are advection and hydrodynamic dispersion. Advection is transport that occurs as cells are carried by the bulk flow of moving groundwater. Hydrodynamic dispersion ($D_{l,\,cell}$) occurs because of mixing during fluid advection and because of random motility of the bacterial cells.

Hydrodynamic dispersion, which causes dilution of cells, occurs because of mechanical mixing during fluid advection and because of random motility due to the energy of the cells. Therefore, bulk diffusion is one mode by which cells are able to move unimpeded through porous media.

Chemical processes that influence cell transport include adsorptive and desorptive interactions of bacterial cells and particles in the soil matrix. Harvey and Garabedian (1991) determined that bacterial transport is influenced greatly by adsorption. Adsorption is defined as the process of collecting substances that are in aqueous suspension or solution on a suitable interface (Weber, 1972). Since the surface of most bacteria are negatively charged they tend to be strongly adsorbed by anionic adsorbents (e.g. soil particles), as cations in solution bridge between charged sites on the sand surface and the cell surface (Gordon and Millero, 1984; and Mozes *et al.*, 1987). Since this is a reversible process, a cell may adsorb to one soil grain, desorb in water, then re-adsorb to a different soil grain. Adsorption of cells to soil grains may also be influenced by other physical and chemical changes, i.e. ionic strength, pH, presence/absence of extracellular polysaccharides, and temperature.

Much effort has been expended attempting to define those parameters which most affect the transportability of microbes through soil. In the absence of chemotactic transport, a number of parameters govern the extent to which microbes migrate through saturated porous media. A study by Fontes *et al.* (1991) focused on the affects of ionic strength, cell size, and grain size of the porous media. This study concluded that grain size is the most important factor controlling transport of bacteria through porous media. Cell size and ionic strength were about equal in importance and lower in importance than

grain size. A larger grain size presents bacteria with larger pores through which transport can occur. In fact, straining and surface filtration are the dominant attachment mechanism when the ratio of average soil particle size to cell size is less than 20 (McDowell-Boyer *et al.*, 1986). When this ratio exceeds 20, the attachment mechanism depends on the frequency and extent of cell-to-soil particle collision. Others have shown that straining becomes important when the average cell diameter is greater than the sizes of 5% of the soil particles in the porous media (Jang *et al.*, 1983).

The ionic strength of groundwater also affects attachment of cells to soil particles. An increase in ionic strength results in compression of the double-layer surrounding the bacterial cell. This compression in turn increases the likelihood of cell attachment to soil particles. An increase in ionic strength may also encourage cell aggregation and lead to pore clogging and poor cell transport (Scholl *et al.*, 1991). However in situations where increased bacterial transport is desired, the lowering of ionic strength could have negative physiological effects on the cells and result in cell lysis.

Gannon *et al.* (1991) studied the relationship between cell size, cell surface characteristics, and cell surface charges of 19 bacterial strains and their transport through soil. Strains shorter than one micron in length were transported better through soil than longer strains. It is obvious that smaller particles will migrate more readily through porous media consisting of pore channels of many different sizes. On the other hand, larger cells may be transported more rapidly because of size exclusion. In this case, large cells can travel through porous media faster because they only travel through larger pores whereas smaller cells travel through all pores. This principle is the basis for size exclusion chromatographic separations.

Several studies present solid evidence that bacteria have the ability to be transported significant distances in the subsurface (Gannon *et al.*, 1991; Fontes *et al*, 1991; and Harvey and Garabedian, 1991). However, many questions remain to be answered. For example, what is the capacity of bacteria to move through various types of aquifer solids? How far can cells move through saturated soil? By what mechanism do cells travel? Some researchers have postulated that bacteria are only capable of moving short distances through aquifer material (Edmonds, 1976; and Goldstein, 1985). While this generalization may be valid for certain types of bacteria in certain types of aquifer material, other evidence (Gannon *et al.*, 1991) indicates that certain cells are motile and are readily transported through aquifer material. For strain KC to be effective in CT degradation, it must be transported or migrate across a treatment zone that intercepts the plume of CT contamination. Within this treatment zone, strain KC must attach to the solid matrix, survive, and retain its CT-degrading ability. Of concern are regions where the lack of advective flow prevents cell transport. Within such regions, the capacity of KC cells to actively move or "swim" towards regions of higher nutrient and/or contaminant concentrations would be highly desirable.

Chemotaxis may play a role in the ability of subsurface microorganisms to migrate and move towards nutrient sources (Reynolds *et al.*, 1989). Chemotaxis, by definition, is the directionally-biased movement of bacteria in response to chemoattractant gradients. Chemotactic bacteria move by performing a series of "runs" and "tumbles" (Berg and Brown, 1972). Bacterial flagella rotate and cause the cell to "run" in a straight-line direction for approximately one to two seconds. At the completion of a run, the cell tumbles, reversing the rotation of its flagella, and reorients

itself in a new direction. Tumbling is characterized by chaotic motion which randomly reorients the bacterium for the next run (Corapcioglu and Haridas, 1984), and the duration of a tumble is on the order of 0.1 seconds. A series of runs, interrupted by a number of tumbles, defines a random walk. For chemotactic bacteria, the resulting direction of the random walk will be biased by the presence of an attractive chemical, or chemoattractant. When the cell senses an increasing concentration gradient of the chemoattractant, the frequency of tumbling decreases. This decrease in tumble frequency leads to an increase in run length in the direction of increasing chemoattractant concentration. Figure 1.3 shows an example of a series of runs and tumbles performed by a chemotactic bacterium in the absence of a chemoattractant gradient. Short run lengths (L) and random turn angles (θ) result in no apparent biased movement of the cell in any one direction.

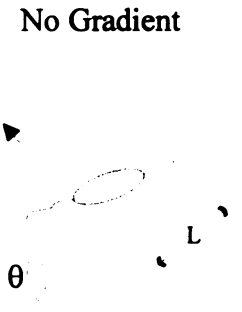

Figure 1.3. Movement of motile bacterium in the absence of a chemoattractant gradient.

Figure 1.4 shows the movement of a chemotactic bacterium in the presence of a chemoattractant gradient. The cell runs are longer in the direction of increasing

chemoattractant gradient, while the frequency of tumbling has decreased to yield a net movement in the direction of increasing chemoattractant concentration.

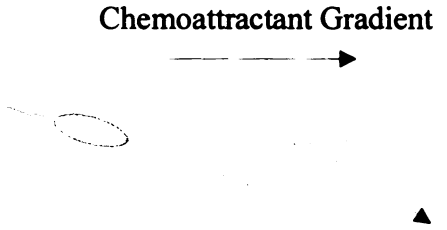

Figure 1.4. Movement of a motile bacterium in the presence of a chemoattractant gradient.

Chemotactic bacteria monitor chemical changes in their surroundings through receptor proteins located near the cell surface. These attractant-specific proteins have a very high affinity for the chemoattractant, thus allowing the chemoattractant to bind. The first step in chemotactic response is the binding of a chemoattractant by a specific protein (or binding site). The cell senses chemical gradients monitoring change in the number of bound receptors over time (Macnab and Koshland, 1972).

Chemotaxis provides a possible mechanism by which bacteria can migrate toward regions of higher chemical concentrations. In the subsurface where contamination may be isolated in zones of low advective flow, chemotaxis may enable microbes to penetrate and decontaminate pockets of contamination that would otherwise by inaccessible to remediation. The chemotactic response of some specific microorganisms have been studied (Ford *et al*, 1991; Harwood *et al.*, 1990; Reynolds *et al.*, 1989; and Widman *et al.*, 1997). Typical cell swimming speeds are on the order of 20 to 40 μm/sec (Berg and Brown, 1972; Lowe *et al.*, 1987; and Macnab and Aizawa, 1984). Considering that a

representative groundwater velocity is on the order of 1 μm/sec (equivalent to 10 cm/day), microbes that exhibit chemotaxis could conceivably "sweep" through and remediate regions of contaminated groundwater.

1.5 Development of chemotaxis model

The development of a simple, generalized model for cell population migration was presented by Rivero *et al.* (1989). This model will hereafter be referred to as the RTBL model, named for the authors who developed it. This model was simplified by approximating the experimental system as a one-dimensional sand column. The goal was to mathematically define the migration of bacteria through porous media. In a stagnant system, the conservation equations for bacterial cell density, X, and chemoattractant concentration, a, are:

$$\frac{\partial X}{\partial t} = -\frac{\partial J_b}{\partial x} \tag{1.1}$$

$$\frac{\partial a}{\partial t} = -\frac{\partial J_a}{\partial x} \tag{1.2}$$

where J_b and J_a are the bacterial and chemoattractant fluxes, respectively. Keller and Segel (1971) developed a one-dimensional expression for flux:

$$J_b = -\omega \frac{\partial X}{\partial x} + V_c X \tag{1.3}$$

where ω is the random motility coefficient (analogous to diffusion coefficient), V_c is the chemotactic velocity - a value equal to the chemotaxis coefficient, χ, multiplied by $\frac{\partial a}{\partial x}$ (Segel and Jackson, 1973), and x is the distance along the one-dimensional column. In this expression, the random motility term is essentially a diffusion term and the velocity term is essentially an advection term.

Substituting the Keller and Segel flux equation into the conservation equation for cells (Eq. 1.1) yields:

$$\frac{\partial X}{\partial t} = \omega \frac{\partial^2 X}{\partial x^2} - \frac{\partial}{\partial x}\left(V_c X\right) \tag{1.4}$$

The chemoattractant flux can be modeled according to Fickian diffusion, while the consumption of the chemoattractant can be assumed to follow Monod kinetics. With substitutions, the conservation equation for chemoattractant (Eq. 1.2) yields:

$$\frac{\partial a}{\partial t} = D\frac{\partial^2 a}{\partial x^2} - \left(\frac{\mu_{\max} a}{K_s + a}\right) X \tag{1.5}$$

where D is the diffusion coefficient, and K_s is the half-saturation coefficient for growth on chemoattractant a.

The RTBL model considers the effects of a chemical stimulus on directional change probability and an expression can be formulated for the number of bound receptors, N_b, on the surface of a cell. For a single cell receptor population, N_b is given by the following expression:

$$N_b = \frac{N_t a}{k_{rc} + a} \tag{1.6}$$

where k_{rc} is the dissociation constant for the receptor-chemoattractant complex (relates the chemoattractant concentration in the bulk to the number density of receptor-chemoattractant complexes on the cell surface) and N_t is the total number of cell receptors on the surface of the cell. Using Eq. 1.6 for a single homogeneous receptor population, the change in the number of bound receptors per change in chemoattractant concentration is:

$$\frac{dN_b}{da} = \frac{N_t k_{rc}}{(k_{rc} + a)^2} \tag{1.7}$$

Rivero *et al.* developed an equation for the chemotaxis coefficient, χ, in terms of the change in the number of bound receptors per change in chemoattractant concentration and substituted into Segel and Jackson's equation for chemotactic velocity:

$$\chi = \upsilon^2 \sigma \frac{dN_b}{da} \tag{1.8}$$

$$V_c = \upsilon^2 \sigma \frac{dN_b}{da} \frac{\partial a}{\partial x} \tag{1.9}$$

where υ is the one-dimensional swimming speed and σ is the differential tumbling frequency, representing the fractional change in cell run time per unit time change in receptor binding. Ford (1992) shows that a similar cell transport parameter, the chemotactic sensitivity coefficient, χ_o, can be defined in terms of υ, σ, and N_t:

$$\chi_o = \sigma \upsilon^2 N_t \tag{1.10}$$

Substituting Eqs. 1.7 and 1.10 into 1.9 defines an equation for the chemotactic velocity in terms of χ_o, k_{rc}, a, and x:

$$V_c = \chi_o \frac{k_{rc}}{\left(k_{rc} + a\right)^2} \frac{\partial a}{\partial x} \tag{1.11}$$

Using the equations developed in the RTBL model, Barton and Ford (1997) develop expressions for the effective random motility coefficient (ω_{eff}) and effective chemotactic velocity ($V_{c,eff}$) in porous media. Since determination of the parameters D, ω, and χ_o are typically made in bulk aqueous solution, an effective value for each parameter should be

employed to account for differences created in porous media. The effective random motility coefficient is related to the random motility coefficient measured in bulk aqueous solution by the following relationship:

$$\omega_{eff} = \frac{n}{\tau}\omega \tag{1.12}$$

where n is porosity and τ is the tortuosity of the porous media. Similarly, effective values for the diffusion coefficient, D_{eff}, and the chemotactic sensitivity coefficient, $\chi_{o,eff}$, can be determined. As a result of these derivations and substitution of Eqs. 1.11 and 1.12 into Eqs. 1.4 and 1.5, the general form of the conservation equations describing chemoattractant and cell concentration in the aqueous phase can be represented as:

$$\frac{\partial X}{\partial t} = \omega_{eff}\frac{\partial^2 X}{\partial x^2} - \left(\chi_{o,eff}\frac{k_{rc}}{\left(k_{rc}+a\right)^2}\frac{\partial a}{\partial x}\right)\frac{\partial X}{\partial x} \tag{1.13}$$

$$\frac{\partial a}{\partial t} = D_{eff}\frac{\partial^2 a}{\partial x^2} - \frac{\mu_{\max} a}{Y\left(K_s + a\right)}X \tag{1.14}$$

Equations 1.13 and 1.14 will be employed for development of a computer model to simulate chemotaxis and CT degradation in a model aquifer column. The development and execution of this computer model is presented in Chapter 5.

1.6 Measurement of bacterial transport coefficients

The transport coefficients ω and χ_o are both specific to a particular type of bacteria and are both functions of the chemoattractant concentration. These coefficients can be independently measured in the laboratory. Widman *et al.* (1997) developed the diffusion gradient chamber (DGC) assay to study microbial chemotaxis under conditions of well-characterized, steady-state gradients or multiple gradients in multiple directions. The DGC consists of a square arena bounded by reservoirs on all four sides. The arena is filled with medium containing dilute agarose gel through which the studied cells can swim. If different concentrations are maintained in the reservoirs, then a chemoattractant gradient will establish for a specified duration of time. Chemotaxis is measured by movement of the microbial population(s) in response to the chemoattractant gradients. Measurement of cell movement is achieved by monitoring from above the arena by light diffraction.

Another assay to measure motility coefficients is the stopped-flow diffusion chamber (SFDC) assay. Ford *et al.* (1991) developed this assay to determine the transport coefficients in bulk aqueous media. Within the SFDC, two solutions are contacted by impinging flow. One solution contains chemoattractant and cells, while the other contains only cells. After flow is stopped, a gradient develops as the chemoattractant in the top (or bottom) half diffuses into the bottom (or top) half of the SFDC. As bacteria respond to this gradient, a high density of cells moves upward towards the region of higher chemoattractant concentration. Redistribution of the bacterial population is recorded by capturing images of scattered light. Analysis of these images is used to determine the random motility and chemotactic sensitivity coefficients.

1.7 Motility and chemotaxis of *Pseudomonas stutzeri* KC

Pseudomonas stutzeri KC has been shown to display chemotaxis towards chemoattractants (Widman, 1997). Using a DGC, Widman established that KC exhibited chemotaxis towards acetate and nitrate under a variety of conditions. Other research has shown that KC exhibits chemotaxis towards nitrate in capillary tube assays (Witt *et al.*, 1998). Movement toward the nitrate could improve the efficiency of CT transformation in contaminated aquifer material. However, nitrate will also be consumed by indigenous populations. With this in mind, a logical question is whether strain KC will exhibit chemotaxis in a soil or sediment environment in the presence of competing microflora.

1.8 Research objectives

The research presented in this dissertation provides insight into the issue of bioremediation by bioaugmentation. The central hypothesis of this research is that biotransformation can occur at two fronts during bioaugmentation of porous media. These two fronts consist of a stationary biocurtain attached to aquifer solids and a mobile biocurtain that migrates through porous media. An additional hypothesis is that the mechanism for migration of the mobile biocurtain is a chemotactic response. There are two main objectives for this research. The first objective is to examine the effectiveness of a stationary biocurtain created by bioaugmentation. Long-term maintenance of biodegradative activity under varying conditions of nutrient and/or base addition was also evaluated. The second objective is to assess the role of chemotaxis and cell motility during and after bioaugmentation.

1.9 Literature cited

Atlas, R.M. and R. Bartha. 1993. *Microbial Ecology: Fundamentals and Applications.* The Benjamin/Cummings Publishing Company, Inc., New York, New York.

Barton, J.W. and R.M. Ford. 1997. Mathematical model for characterization of bacterial migration through sand cores. *Biotech. Bioeng.* **53**:487-496.

Berg, H.C. and D.A. Brown. 1972. Chemotaxis in *Escherichia* coli analyzed by three-dimensional tracking. *Nature.* **239**:500-504.

Corapcioglu, M.Y. and A. Haridas. 1984. Transport and fate of microorganisms in porous media: A theoretical investigation. *J. Hydrol.* **72**:149-169.

Criddle, C.S., J.T. DeWitt, D. Grbic-Galic, and P.L. McCarty. 1990. Transformation of carbon tetrachloride by *Pseudomonas* sp. strain KC under denitrification conditions. *Appl. Environ. Microbiol.* **56**:3240-3246.

Dybas, M.J., G.M. Tatara, and C.S. Criddle. 1995. Localization and characterization of the carbon tetrachloride transforming activity of *Pseudomonas* sp. strain KC. *Appl. Environ. Microbiol.* **61**:758-762.

Edmonds, R.L. 1976. Survival of coliform bacteria in sewage sludge applied to a forest clearcut and potential movement into groundwater. *Appl. Environ. Microbiol.* **32**:537-546.

Egli, C., R. Scholtz, A.M. Cook, and T. Leisinger. 1987. Anaerobic dechlorination of tetrachloromethane and 1,2-dichloromethane to degradable products by pure cultures of *Desulfobacterium* sp. and *Methanobacterium* sp. *FEMS Microbiol. Lett.* **43**:257-261.

Egli, C., T. Tschan, R. Scholtz, A.M. Cook, and T. Leisinger. 1988. Transformation of tetrachloromethane to dichloromethane and carbon dioxide by *Acetobacterium woodii*. *Appl. Environ. Microbiol.* **54**:2819-2823.

Fontes, D.E., A.L. Mills, G.M. Hornberger, and J.S. Herman. 1991. Physical and chemical factors influencing transport of microorganisms through porous media. *Appl. Environ. Microbiol.* **57**:2473-2481.

Ford, R.M., B.R. Phillips, J.A. Quinn, and D.A. Lauffenburger. 1991. Measurement of bacterial random motility and chemotaxis coefficients. I. Stopped-flow diffusion chamber assay. *Biotechnol. Bioeng.* **37**:647-660.

Ford, R.M. 1992. Mathematical modeling and quantitative characterization of bacterial motility and chemotaxis. In *Modeling the Metabolic and Physiologic Activities of Microorganisms*, by C.J. Hurst (ed.). John Wiley & Sons, Inc., New York, New York. pp. 177-215.

Gannon, J.T., V.B. Manilal, and M. Alexander. 1991. Relationship between cell surface properties and transport of bacteria through soil. *Appl. Environ. Microbiol.* **57**:190-193.

Goldstein, R.M., L.M. Mallory, and M. Alexander. 1985. Reasons for possible failure of inoculation to enhance biodegradation. *Appl. Environ. Microbiol.* **50**:977-983.

Gordon, A.S. and F.J. Millero. 1984. Electrolyte effect on attachment of an estuarine bacterium. *Appl. Environ. Microbiol.* **47**:495-499.

Harwood, C.S., R.E. Parales, and M. Dispensa. 1990. Chemotaxis of *Pseudomonas putida* toward chlorinated benzoates. *Appl. Environ. Microbiol.* **56**:1501-1503.

Harvey, R.W. and S.P. Garabedian. 1991. Use of colloid filtration theory in modeling movement of bacteria through a contaminated sandy aquifer. *Environ. Sci. Technol.* **25**:178-185.

Jang, L.K., P.W. Chang, J. Findley, and T.F. Yen. 1983. Selection of bacteria with favorable transport properties through porous rock for the application of microbial enhanced oil recovery. *Appl. Environ. Microbiol.* **46**:1066-1072.

Jin, G. and A. J. England, Jr. 1997. Biodegradation kinetics of carbon tetrachloride by *Pseudomonas cepacia* under varying oxidation-reduction potential conditions. *Water Environ. Res.* **69**:1094-1099.

Keller, E.F. and L.A. Segel. 1971. Model for chemotaxis. *J. Theor. Biol.* **30**:225-234.

Knoll, W.H. 1994. Factors influencing the competitive advantage of *Pseudomonas* sp. strain kC for subsequent remediation of a carbon tetrachloride impacted aquifer. Master's Thesis, Department of Civil and Environmental Engineering, Michigan State University, East Lansing, Michigan.

Lee, M.D., J.M. Thomas, R.C. Borden, P.B. Bedient, J.T. Wilson, and C.H. Ward. 1988. Biorestoration of aquifer contaminated with organic compounds. *CRC Crit. Rev. Environ. Control.* **18**:29-89.

Lewis, T.A. and R.L. Crawford. 1993. Physiological factors affecting carbon tetrachloride dehalogenation by the denitrifying bacterium *Pseudomonas* sp. strain KC. *Appl. Environ. Microbiol.* **59**:1635-1641.

Lowe, G., M. Meister, and H.C. Berg. 1987. Rapid rotation of flagellar bundles in swimming bacteria. *Nature* **325**:637-640.

Macnab, R.M. and S.I. Aizawa. 1984. Bacterial motility and the bacterial flagellar motor. *Annu. Rev. Biophys. Bioeng.* **13**:51-83.

Macnab, R.M. and D.E. Koshland, Jr. 1972. The gradient-sensing mechanism in bacterial chemotaxis. *Proc. Natl. Acad. Sci. USA.* **69**:2509-2512.

McDowell-Boyer, L.M., J.R. Hunt, and N. Sitar. 1986. Particle transport through porous media. *Water Resources Research.* **22**:1901-1921.

Mozes, N., F. Marchal, M.P. Hermesse, J.L. Van Haecht, L. Reuliaux, A.J. Leonard, and P.G. Rouxhet. 1987. Immobilization of microorganisms by adhesion: interplay of electrostatic and nonelectrostatic interactions. *Biotechnol. Bioeng.* **30**:439-450.

Quinton, G.E., R.J. Buchanan, Jr., D.E. Ellis, and S.H. Shoemaker. 1997. A method to compare groundwater cleanup technologies. *Remediation.* Autumn 1997.

Reynolds, P.J., P. Sharma, G.E. Jenneman, and M.J. McInerney. 1989. Mechanisms of microbial movement in subsurface materials. *Appl. Environ. Microbiol.* **55**:2280-2286.

Rivero, M.A., R.T. Tranquillo, H.M. Buettner, and D.A. Lauffenburger. 1989. Transport models for chemotactic cell populations based on individual cell behavior. *Chem. Engr. Sci.* **44**:2881-2897.

Scholl, M.A., A.L. Mills, J.S. Herman, and G.M. Hornberger. 1991. The influence of mineralogy and solution chemistry on attachment of bacteria to representative aquifer materials. *J. Contam. Hydrol.* **6**:331-336.

Segel, L.A. and J.L. Jackson. 1973. Theoretical analysis of chemotactic movement in bacteria. *J. Mechanochem. Cell Motility.* **2**:25-34.

Semprini, L., G.D. Hopkins, P.L. McCarty, and P.V. Roberts. 1992. In-situ transformation of carbon tetrachloride and other halogenated compounds resulting from biostimulation under anoxic conditions. *Environ. Sci. Technol.* **26**:2454-2461.

Sittig, M. (ed.) 1985. Handbook of Toxic and Hazardous Chemicals and Carcinogens. Second edition. Noyes Publications, New Jersey. pp. 194-196.

Sneathen, M.A. 1996. Theoretical and experimental competitiveness of *Pseudomonas stutzeri* KC. Master's thesis. Department of Civil and Environmental Engineering, Michigan State University, East Lansing, Michigan.

Solley, W.B., C.F. Merk, and R.R. Pierce. 1988. Estimated use of water in the united states in 1985. U.S. Geological Survey Circular 1004.

Stumm, W. and J.J. Morgan. 1981. *Aquatic Chemistry*, 2nd edition. John Wiley & Sons. New York, New York.

Tatara, G.M., M.J. Dybas, and C.S. Criddle. 1993. Effects of medium and trace metals on kinetics of carbon tetrachloride transformation by *Pseudomonas* sp. strain KC. *Appl. Environ. Microbiol.* **59**:2126-2131.

Tatara, G.M. 1996. Physiology of carbon tetrachloride transformation by *Pseudomonas stutzeri* strain KC. Doctoral Dissertation, Department of Microbiology, Michigan State University, East Lansing, Michigan.

Tim, U.S., S. Mostaghimi, and T.A. Dillaha. 1988. Modeling the movement and persistence of bacteria and viruses in porous media. AZO Paper Number 88-2627, St. Joseph, Michigan.

Thomas, J.M., and C.H. Ward. 1989. In situ biorestoration of organic contaminants in the subsurface. *Environ. Sci. Technol.* **23**:760-766.

Weber, W.J. 1972. *Physicochemical Processes For Water Quality Control.* John Wiley & Sons. New York, New York.

Widman, M.A. 1997. Engineering aspects of microbial chemotaxis. Doctoral Dissertation, Department of Chemical Engineering, Michigan State University, East Lansing, Michigan.

Widman, M.A., D. Emerson, C.C. Chiu, and R.M. Worden. 1997. Modeling microbial chemotaxis in a diffusion gradient chamber. *Biotech. Bioeng.* **55**:191-205.

Witt, M.E., M.J. Dybas, R.M. Worden, and C.S. Criddle. 1998. Bioremediation of carbon tetrachloride-contaminated sediments by chemotactic, denitrifying cells responding to a nitrate gradient. Submitted for publication to *Biotech. Bioeng.*

Chapter 2

DESIGN OF PROTOTYPE MODEL AQUIFER COLUMN

2.1 Background

Columns packed with aquifer material are particularly useful microcosms for research on biotransformation and microbial transport behavior because such columns provide control that cannot be achieved in the field. A critical factor is the level of hydraulic control. Columns can be designed to ensure adequate distribution of cells and nutrients. By eliminating hydraulic variabilities, it is possible to focus attention on other variables that may influence the bioremediation process, such as ecological issues. Accordingly, the results of model column studies are valuable in design, implementation, and interpretation of field-scale remediation activities.

In order to evaluate the effectiveness of different bioaugmentation protocols, a model aquifer column was developed and evaluated. The design requirements were: (1) the construction materials that do not sorb carbon tetrachloride (CT) or chloroform (CF); (2) sufficient length to permit evaluation of spatial variability; and (3) sufficient sampling ports to permit evaluation of spatial and temporal gradients. The following sections document design of a column used to assess the remediation potential of *Pseudomonas stutzeri* KC in Schoolcraft aquifer sediments.

2.2 Materials and methods

Model aquifer column

A diagram of the prototype model aquifer column is presented in Figure 2.1. Three identical columns were constructed. Each column consisted of clear Excelon polycarbonate tubing (schedule 40), 200 cm long with an inside diameter of 5.2 cm. A total of 25 holes (per column), spaced 7.6 cm apart, were tapped and threaded to serve as sampling ports. Sampling port assembly was completed by inserting brass unions (1/4-inch NPT to ¼-inch Swagelock) into all of the sampling port locations. The unions were each fitted with 10/32-inch Thermogreen GC septa to allow for sampling while keeping the internal contents of the column airtight. Female endcap fittings (polyvinyl chloride) were glued onto both ends of each column with PVC pipe glue. Uncured silicone sealant was applied to two PVC threaded male endcaps, and each male endcap was then screwed into a female endcap fitting. A stainless steel screen (40 mesh) was cut and held in place by silicone sealant on the interior portion of each endcap. This screen prevented glass beads and sand particles from exiting the model aquifer column. Both male endcaps were drilled to allow a 5/8-inch NPT to ¼-inch stainless steel reducing union to provide for entrance and exit of groundwater. From each reducing union, ¼-inch stainless steel tubing was connected to a Nupro stainless steel ball valve. Additional stainless steel tubing was used to connect the valve to the static mixing reservoir on the influent end, and to deliver effluent groundwater to a waste containment vessel.

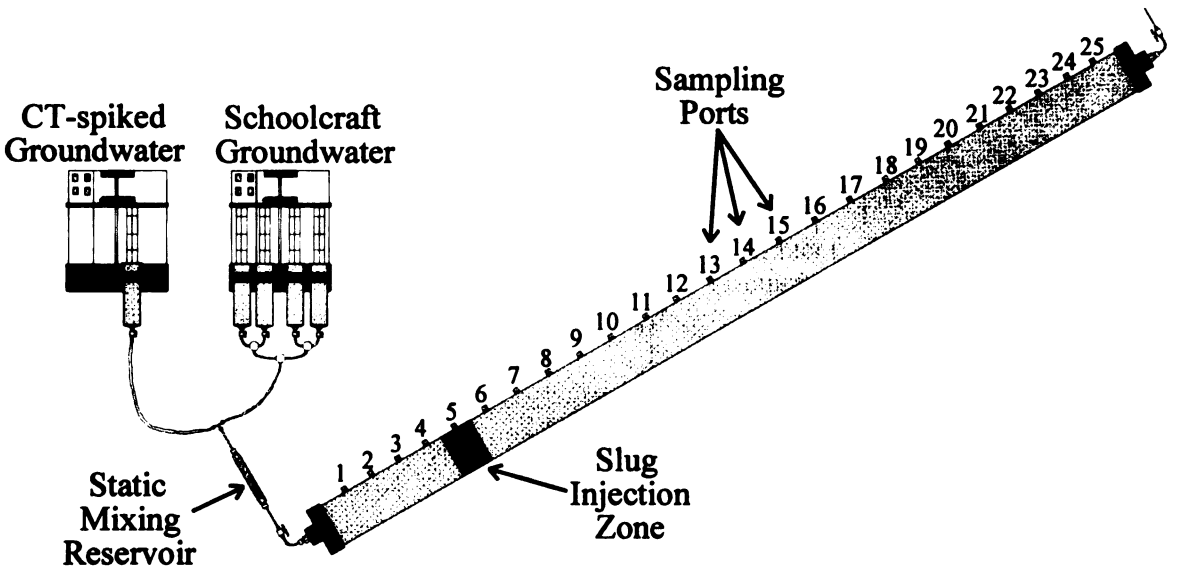

Figure 2.1. Diagram of prototype model aquifer column.

Static mixing reservoir

A static mixing reservoir (see Figure 2.2) was constructed in-line near the influent end of each column to ensure adequate mixing of CT-spiked and CT-free Schoolcraft groundwater. The mixing reservoir consisted of a six-inch section of one-inch diameter stainless steel tubing filled with 3-mm diameter glass beads. Stainless steel screen at both ends of the one-inch tubing held the glass beads in place. Both ends of the mixing reservoir were fitted with stainless steel reducing unions (one-inch to ¼-inch). Stainless steel tubing (¼-inch) connected syringes filled with CT-free and CT-spiked groundwater to the mixing reservoir. Syringe pumps pushed the CT-spiked and CT-free groundwater in the desired proportions through the tubing to a tee connection then to the mixing reservoir where mixing was accomplished by means of the tortuous flow path created by

the glass bead packing. Effluent from the static mixing reservoir was delivered to the model aquifer column via stainless steel tubing (¼-inch).

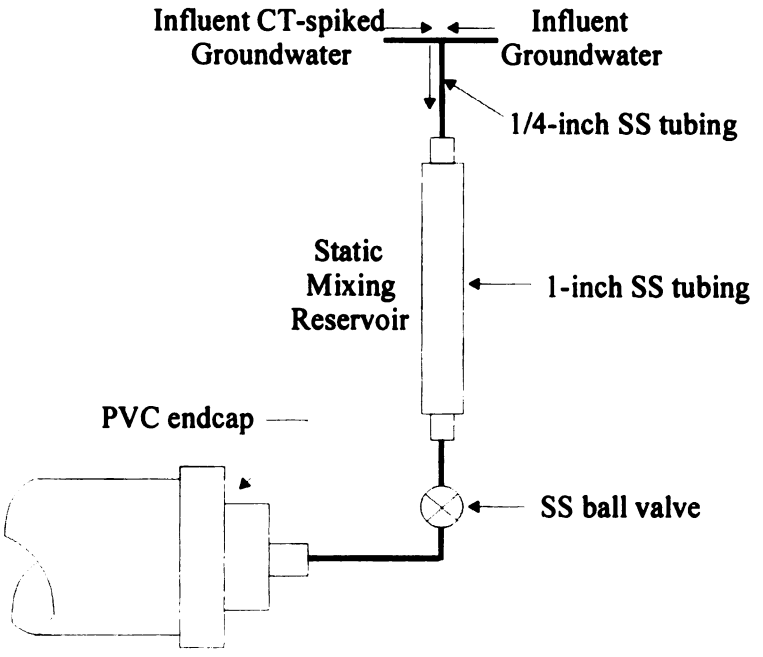

Figure 2.2. Diagram of static mixing reservoir and influent groundwater assembly.

Slug injection manifold

Both model aquifer columns were outfitted with a special slug injection zone manifold for delivery of organisms, base, and nutrients. Figure 2.3 is a photograph of the slug injection manifold. The manifold consisted of four 3/16-inch stainless steel tubes (each 8 inches long) passing completely through the center of the column and extending out from both sides of the column. The middle section of each tube (approximately 2 inches) was slotted, much like a well screen, to allow free flow of water into and out of the tube while preventing plugging by sand grains. The four tubes were connected using

additional stainless steel tubing and fittings. Two slotted tubes were used for delivering the injection solution into the column while the other two tubes were simultaneously used to withdraw groundwater.

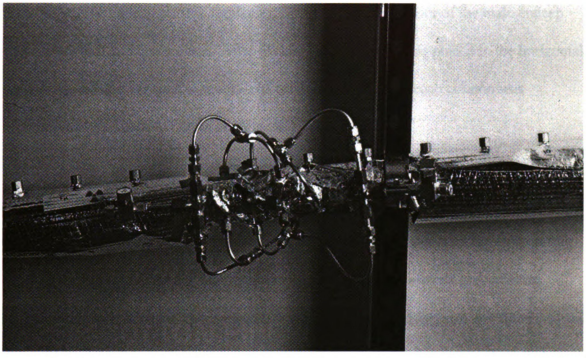

Figure 2.3. Photograph of slug injection manifold on the prototype model aquifer column.

Packing procedure

Columns were wet-packed with aquifer material from the Schoolcraft, Michigan, aquifer. Before packing, each column was placed in a vertical upright position and sanitized overnight with a 10% household bleach solution. The column was rinsed three times with DI water just prior to packing with Schoolcraft groundwater. Each column was filled approximately one-fourth full of Schoolcraft groundwater. Enough glass beads (3-mm diameter) were poured into the column to fill the bottom two inches of the column

(near the influent end). Two-hundred mL portions of saturated aquifer material were poured into the top of the column and allowed to settle. Gentle tapping on the column exterior encouraged more dense packing of the sand. The final two inches of the column were filled with 3-mm glass beads. Uncured silicone sealant was spread onto the threading of the endcap prior to tightening. Once tight, the exterior of the male endcap was sealed with silicone sealant. After packing, each column was placed in the horizontal position in the climate control room. The total mass of sand in each column was approximately 7 kg, or 4.2 liters in volume.

Climate control room

A climate control room (Figure 2.4) was constructed to maintain the temperature of model aquifer columns at a temperature close to that of Schoolcraft groundwater (12°C). A mobile 8'x8'x4' room insulated with 2-inch thick Styrofoam and fitted with an Amana-brand 7500 btu air-conditioner was constructed. Steel U-bars were installed on the back wall of the room for mounting of model aquifer columns. Shelving units were also installed to hold syringe pumps and sample acquisition materials. Packed columns were mounted horizontally.

Delivery of Schoolcraft groundwater

Groundwater from a CT-contaminated aquifer in Schoolcraft, Michigan, was obtained from a monitoring well screened 46 feet below the water table. Prior to groundwater collection, this well was purged for 30 minutes at a flow rate of 20 L/min using a Grundfus groundwater collection device. Groundwater was dispensed into pre-

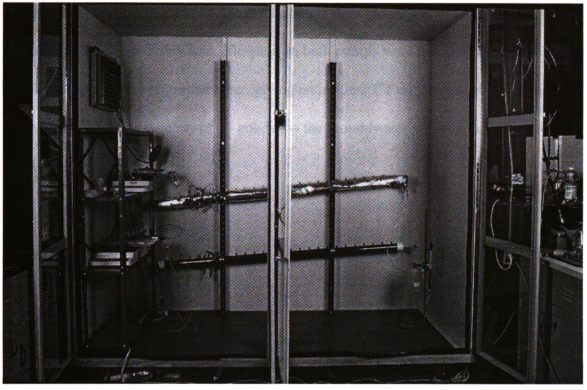

Figure 2.4. Photograph of the climate control room.

sterilized sealed Nalgene carboys and transported to the laboratory on the same day. In the laboratory, samples were stripped to remove volatile organics, then transferred to 1 L Wheaton bottles and sealed with Teflon™-lined caps. Samples were stripped by bubbling a N_2-CO_2 gas mix rapidly through each bottle for a period of 45 minutes. The pH of each groundwater sample was kept at the background level observed in the field (pH 7.2).

Two Harvard Apparatus syringe pumps (model 22) were used to pump Schoolcraft groundwater containing 100 μg/L into and through each model aquifer column. One pump drove the piston of a 100-mL glass syringe (Unimetrics Corporation) containing filter-sterilized Schoolcraft groundwater spiked with 1 mg/L CT. The second

pump drove the pistons of four 140-mL plastic syringes (Monoject Corporation) containing CT-free groundwater. Flows from both pumps were combined in a 1:10 ratio of CT-spiked to CT-free groundwater, giving an influent CT concentration of 100 μg/L and an average linear velocity of 15 cm/day -- the groundwater velocity in the Schoolcraft aquifer.

Chapter 3

USE OF BIOAUGMENTATION TO CREATE A BIOCURTAIN CAPABLE OF LONG-TERM, CONTINUOUS REMOVAL OF CARBON TETRACHLORIDE IN MODEL AQUIFER COLUMNS

3.1 Abstract

The feasibility of sustained removal of carbon tetrachloride (CT) in a biocurtain colonized by *Pseudomonas stutzeri* KC was evaluated utilizing two 2-meter long columns packed with aquifer material from a CT-contaminated aquifer at Schoolcraft, Michigan. CT-contaminated groundwater was pumped continuously through both columns until the aqueous and adsorbed CT had equilibrated. CT transformation was initiated by inoculating an 8-cm-wide, alkaline-adjusted zone near the upstream end of both columns with a slug of strain KC and acetate. CT-contaminated groundwater was then pumped continuously through the columns. Both columns received weekly acetate additions in the slug injection zone. Base (sodium hydroxide) and phosphate additions were performed weekly in one column and twice-weekly in the second column. A CT-transforming zone developed in the slug injection zone of both columns, with 97% removal of CT in the column receiving weekly base additions and 93% removal in the column receiving twice-weekly base additions. Strain KC was detected on the solids of both columns. When acetate and base additions were discontinued, CT transformation decreased, and chloroform (CF) production was observed in the column that had received twice-weekly base additions (no CF was detected in the other column). The results indicate that efficient CT removal without CF production is possible over extended periods. The results also suggest that microbial populations indigenous to the Schoolcraft

aquifer can convert CT to CF, and that such populations were selected by twice weekly base additions. Weekly base additions evidently failed to select such populations.

3.2 Introduction

Carbon tetrachloride, once widely used as a solvent, fumigant, and degreasing agent, is now a common groundwater contaminant. Bioremediation to remove CT in contaminated aquifers is possible, but care must be taken to avoid conversion of CT to CF or to degrade CF if it is formed. Under denitrifying conditions, CF is a common end product of transformation in both laboratory and field environments (Criddle *et al.*, 1990a; Egli *et al.*, 1987 and 1988; and Semprini *et al.*, 1992). Although research suggests that CF levels can be controlled by manipulation of redox conditions (Criddle *et al.*, 1990b, and Jin and England, 1997), such control may be difficult to achieve under field conditions, especially when *in-situ* remediation is desired.

A potential advantage of adding organisms for bioremediation (bioaugmentation) is pathway control. For CT remediation, bioaugmentation with *Pseudomonas stutzeri* KC is attractive because strain KC degrades CT rapidly, without CF production. Denitrifying microbial populations typically do not transform CT, or they do so slowly with CF production. Under iron-limited conditions, however, the denitrifying bacterium *Pseudomonas stutzeri* KC secretes a small biomolecule that can degrade CT rapidly, without CF production (Dybas *et al.*, 1995). The requisite iron-limiting conditions can be created by adjusting the pH of the growth medium to 8.0-8.3 (Tatara *et al.*, 1993). By adjusting pH, inoculating with strain KC, and providing sufficient electron donor,

electron acceptor, and nutrients, CT degradation can be achieved in diverse water and soil environments (Dybas *et al.*, 1995; Tatara *et al.*, 1993; and Mayotte *et al.*, 1996).

A potential drawback to bioaugmentation with strain KC is competition with indigenous microflora. Indigenous populations are unavoidably stimulated by carbon and nutrients added for the support of strain KC. Some of these populations may be capable of transforming CT to CF. If the activity of such populations is too high or the activity of strain KC too low, the rate of transformation of CT to CF may equal or exceed rates of CT degradation by desirable pathways. Methods are needed whereby non-native organisms used for bioaugmentation can be maintained at activity levels that are high enough to enable control of degradation pathways.

One means of reducing the resistance of a microbial community to invasion and colonization by non-native organisms is the creation of a niche for the non-native organism. Atlas and Bartha (1993) define a "niche" as the "combined description of the physical habitat, functional role, and interactions of the microorganisms occurring at a given location." Judicious modifications in a habitat can create functional roles for which a non-native organism is well adapted. An increase in pH to 8.0-8.3, for example, reduces the solubility (bioavailability) of several essential trace metals, favoring microorganisms with efficient mechanisms for trace metal scavenging. This appears to be the case for strain KC which secretes several distinct siderophores capable of efficient iron-scavenging (Dybas *et al.*, 1995). This capability probably explains the competitiveness of strain KC at more alkaline pH levels. For pH values less than 7.8, microflora indigenous to the Schoolcraft aquifer had maximum specific growth rates that

exceeded those of strain KC, but for pH values greater than 8, strain KC had higher rates (Sneathen, 1996).

Carbon addition also modifies a habitat, creating new "job opportunities" that may be assumed by a non-native organism. In the case of the Schoolcraft groundwater, carbon addition results in a denitrifying enrichment community that converts nitrate sequentially to nitrite and then to gaseous end products. During reduction of nitrate to nitrite, the maximum specific growth rate (μ_{max}) for strain KC is triple that of the indigenous flora at pH 8.2 (Knoll, 1994). However, the reverse situation is true for further reduction of nitrite to gaseous end products. Thus, it appears likely that within this bioaugmented denitrifying community, strain KC will be the dominant nitrate-reducer while indigenous organisms are the dominant nitrite-reducers.

In the bench-scale studies described in this report, intermittent base and acetate addition were used to sustain populations of strain KC that degraded CT without CF production in packed columns. The effects of two different base addition strategies on CT removal efficiency and potential for CF formation were evaluated, as were the effects of discontinuing weekly feeding operations. The results are helpful in interpreting results from a pilot-scale *in-situ* experiment conducted at Schoolcraft, Michigan (Dybas *et al.*, 1998) and suggest that timing of base addition may be a useful operational tool for minimization of CF production.

3.3 Materials and methods

Construction of a model aquifer column

Two laboratory-scale model aquifer columns were used to investigate the potential for bioaugmentation at a CT contaminated aquifer in Schoolcraft, Michigan. A diagram of a model aquifer column is provided in Figure 3.1. Each column consisted of a two meter length of clear polycarbonate pipe, 5.2 cm in diameter (i.d.) and outfitted with 25 sampling ports spaced at 7.6 cm intervals along the pipe. Each column was wet-packed with aquifer sediment obtained from borings MLS 2 and MLS 7 (Dybas *et al.*, 1998) at a CT-contaminated aquifer in Schoolcraft, Michigan.

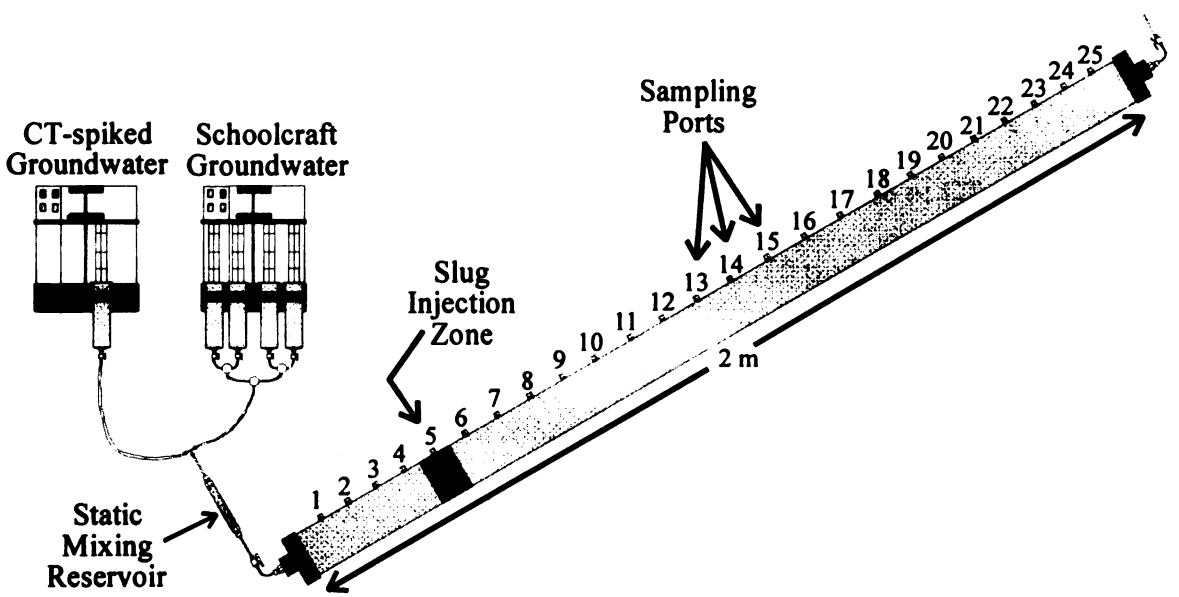

Figure 3.1. Diagram of model aquifer column system design, showing groundwater delivery, a static mixing reservoir, location of slug injection zone, and sand column.

Before constructing each model aquifer column, the possibility of CT sorption to polycarbonate tubing was investigated. A solution of CT-spiked Schoolcraft groundwater was injected into a short length of polycarbonate piping (2-inch diameter) and sealed at both ends with polyvinyl chloride endcaps. Samples were obtained from the capsule at various intervals over two weeks and analyzed for CT via gas chromatography. Only 3% of the CT in solution was sorbed by the polycarbonate side-walls and/or end-caps after 13 days, the design residence time for water in the model aquifer columns.

Two Harvard Apparatus syringe pumps (model 22) were used to pump Schoolcraft groundwater containing 100 μg/L CT into and through both model aquifer columns. One pump drove the piston of a 100-mL glass syringe (Unimetrics Corporation) containing filter-sterilized groundwater spiked with 1 mg/L CT. The second pump drove the pistons of four 140-mL plastic syringes (Monoject Corporation) containing CT-free groundwater. Flows from both pumps were combined in a 1:10 ratio of CT-spiked to CT-free groundwater, giving an influent CT concentration of 100 μg/L and an average linear velocity aquifer of 15 cm/day -- the groundwater velocity in the Schoolcraft aquifer. Both columns were incubated in a constant temperature room at the temperature of the Schoolcraft aquifer (12°C).

Construction of a slug injection zone

Each polycarbonate pipe used for construction of a model aquifer column was outfitted with a manifold for delivery of organisms, base, and nutrients into a section of each column designated the "slug injection zone." The delivery manifold (Figure 3.2) consisted of four 8-inch stainless steel pipes (3/16-inch o.d.). Each of these pipes passed

through one side of the polycarbonate pipe, through the center of the column, and out the opposite side of the polycarbonate pipe. Sections of manifold located on the inside of the polycarbonate pipe (within the column interior) were slotted to create well screens, allowing for free flow of water into and out of the pipe while preventing plugging by sand grains. Sections of the manifold located outside of the polycarbonate pipe (external to the column) were connected together to create injection and extraction lines. For chemical and organism delivery into the slug injection zone, a peristaltic pump (Watson-Marlow model 502E) was used to pump fluid at 20 mL/min from a reservoir (500-mL Erlenmeyer flask) into the manifold delivery lines.

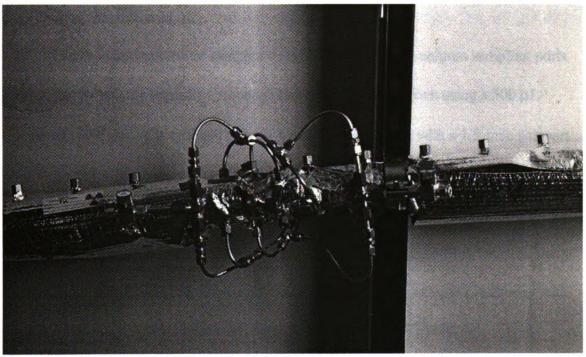

Figure 3.2. Photograph of the slug injection manifold on a model aquifer column.

Schoolcraft groundwater

Groundwater from the CT-contaminated aquifer in Schoolcraft, Michigan, was used for all column studies. Groundwater was obtained manually by bailing with a Teflon™ bailer from a two-inch steel well screened 46 feet below the water table, and was transported to the laboratory in pre-sterilized sealed Nalgene carboys. Once in the laboratory, it was stripped to remove volatiles, transferred to 1 L Wheaton bottles, and sealed with Teflon™-lined caps. Samples were stripped by bubbling a N_2-CO_2 gas mix rapidly through each bottle for a period of 45 minutes. CO_2 was used to achieve a pH equivalent to that of the field site (pH 7.1).

Carbon tetrachloride analysis

Two-hundred microliter samples were obtained from the column sampling ports for analysis of volatile organics. Aqueous samples were withdrawn using a 500 µL Pressure-Lok™ gas-tight syringe (Alltech Associates) equipped with a 1.5-inch sideport sampling needle. Both the syringe needle and sampling port septum were pre-sterilized with an ethanol-soaked cotton swab. Each 200 µL sample was dispensed into a 1.5 mL glass vial (Sun Brokers, Inc.) sealed with Teflon™-lined crimp tops (Sun Brokers, Inc.). Between sampling events, the interior of the gas-tight syringe was rinsed internally with 0.5 mL methanol, followed by 0.5 mL autoclaved deionized (DI) water.

Carbon tetrachloride was assayed by removal of 100 µL of headspace gas with a 500 µL Precision gas-tight syringe (Alltech Associates) and injecting the sample into a Perkin Elmer model 8500 gas chromatograph equipped with a 100/120-mesh column

(10% Alltech CS-10 on Chromsorb W-AW) and an electron capture detector with nitrogen carrier (40 mL/min).

External standard calibration curves were prepared by addition of a primary standard (8.22 ng of CT per μL of methanol) to secondary solutions having identical gas to water ratios and incubation temperatures as the assay samples. For each run on the gas chromatograph, a four point calibration curve was prepared to bracket the expected concentration range of the samples.

Anion analysis

Anions were assayed by ion chromatography with suppressed conductivity detection on a Dionex model 2000i/SP ion chromatograph equipped with a Dionex AS4A IonPac column and utilizing a 1.8 mM bicarbonate-1.7 mM carbonate mobile phase (3 mL/min). Chromatograms were recorded and data integrated with a Spectra Physics model SP 4270 integrator. Five-point calibration curves were prepared by diluting primary anion standards into secondary DI water standards. Two-hundred microliter samples were obtained from sampling ports for analysis on the ion chromatograph. Each sample was diluted into 400 μL of DI water, filtered through a 0.22 μm nylon filter (Scientific Resources Inc.), and dispensed into a polypropylene sample vial (Alcott Chromatography). Each sample was analyzed for acetate, bromide, nitrate, nitrite, phosphate, and sulfate.

Establishment of conditions mimicking the Schoolcraft aquifer

Denitrifying conditions were established by pumping oxygen-free Schoolcraft groundwater through the column for a period of four weeks. After this time period, random samples collected from various ports on the column contained no detectable concentrations of dissolved oxygen (less than 0.1 mg/L).

A conservative tracer study was performed to measure the porosity of the aquifer materials in each column. Tritiated water (^3H_2O) was used as the conservative tracer. Porosity determined in this manner was 0.37 for column 1 and 0.34 for column 2.

Niche adjustments

Solutions injected into the slug injection zone for niche adjustment consisted of Schoolcraft groundwater amended with 100 µg/L CT, 30 mg/L bromide, 10 mg/L phosphate, and adjusted to a pH of 8.3 using a 1 N sodium hydroxide solution. Groundwater pH was measured using a Beckman Φ11 pH meter with an Orion PerpHect 9209BN pH probe. Calibration was performed daily using pH 7.00 and 10.01 standards.

Prior to inoculation using strain KC, three injections of pH amended groundwater were introduced to both columns near the slug injection zone. Each injection consisted of 320 mL of Schoolcraft groundwater adjusted to pH 8.2 and containing 30 mg/L bromide, 100 µg/L CT, and 10 mg/L phosphate. Each 320 mL volume was four times the pore volume of the slug injection zone.

Inoculation using Pseudomonas stutzeri KC

Pseudomonas stutzeri KC (DSM deposit number 7136, ATCC deposit number 55595), derived originally from aquifer solids from Seal Beach, California, is routinely maintained in our laboratory on R2A (Difco Laboratories) agar plates. To determine the appropriate growth conditions for the inoculum, a series of laboratory experiments were conducted to evaluate the effects of media composition on the ability of strain KC to compete with native microflora and to maximize expression of CT degradation activity (Dybas *et al.*, 1998). The results indicated good growth and transformation activity in an inoculum grown with 1600 mg/L acetate and 10 mg/L phosphate in groundwater adjusted to a pH of 8.2.

A liquid KC culture was initiated by removing one colony from an R2A agar plate and placing it in an Erlenmeyer flask containing 100 mL of sterile nutrient broth. After shaking overnight, 4 mL of the resulting starter culture was transferred to 400 mL of filter-sterilized Schoolcraft groundwater (amended with 1600 mg/L acetate, 10 mg/L phosphate, and pH-adjusted to 8.2). The flask was shaken overnight and cell growth was monitored by protein using the modified Lowry method (Markwell *et al.*, 1981) and by colony forming units using R2A agar spread plates.

Inoculation with strain KC was performed a single time in each column. Column 1 was inoculated in the slug injection zone using a 320 mL volume of an aqueous strain KC culture grown for 17 hours in filter-sterilized Schoolcraft groundwater. The inoculum was augmented with CT (100 µg/L), acetate (100 mg/L), nitrate (70 mg/L), and a conservative tracer (^3H_2O). Immediately after inoculation, samples were taken for ^3H_2O, CT, and anions. ^3H_2O levels within the slug injection zone were 70% of those in

the inoculum, indicating slight mixing between the injected inoculum and the pore fluid that it replaced. The final concentrations of acetate, CT, and nitrate in the slug injection zone immediately after inoculation were 712 mg/L, 100 µg/L, and 68 mg/L, respectively. Equal concentrations of CT and nitrate were present throughout the column.

Before injecting inoculum into column 2, the ability of the inoculum to transform CT was confirmed. Two sealed test tubes, containing only water and 60 µg/L CT, were spiked with 50 µL of inoculum. After 45 minutes, 48% of the CT was removed in the inoculated tubes, with no removal in uninoculated control tubes.

Columns 1 and 2 differed in the ages and concentrations of the inoculum. The inoculum for column 1 was grown for 17 hours before injection into the slug injection zone; the inoculum for column 2 was grown for 24.5 hours before injection. A modified Lowry protein assay performed on the inoculum of column 1 indicated a protein concentration of 50 µg/mL, corresponding to a cell density of approximately 10^6-10^7 cells/mL. Plate count analyses on the inoculum for column 2 indicated a cell density of 5 × 10^7 cells/mL and a protein concentration of 100 µg/mL.

Maintenance of strain KC activity

After inoculation, nutrient slugs were added to both columns on a weekly basis. Each nutrient slug consisted of 320 mL of Schoolcraft groundwater containing 100 mg/L acetate, 30 mg/L bromide, 100 µg/L CT, and 10 mg/L phosphate. Each slug was also adjusted to a pH of 8.2 prior to injection. Nutrient injections continued for twelve weeks in column 1 and ten weeks for column 2.

Semiweekly pH modification in column 2

For column 2 only, pH 8.2 groundwater was added semiweekly in the slug injection zone. Each semiweekly injection consisted of 100 mL of Schoolcraft groundwater containing 100 µg/L CT, 10 mg/L phosphate, and adjusted to pH 8.2 with a 1 N sodium hydroxide solution.

Enumeration of planktonic and attached bacteria

For enumeration of free-swimming or planktonic bacteria, 200 microliter water samples were withdrawn from the odd-numbered ports (Figure 3.1) and dispensed into sterile culture tubes containing 1.8 mL of 50 mM phosphate buffer (pH 8.0). For six subsequent serial dilutions, 200 µL were withdrawn from the preceding dilution and mixed on a vortex mixer for five seconds with 1.8 mL phosphate buffer. A 100 µL subsample of each dilution was spread aseptically in a sterile petri dish containing R2A agar. Plates were incubated at room temperature for five days, then scored for growth of strain KC and indigenous microflora. Strain KC was differentiated from Schoolcraft flora by the unique "fried-egg" appearance of strain KC colonies after five days of incubation (Sneathen, 1996). Results were compiled as colony forming units (CFU) per mL.

Attached bacteria were enumerated by removing 200 to 600 milligrams of aquifer material from each sampling port. The samples were placed in sterile Eppendorf tubes and weighed. One mL of cell extraction buffer was added to each Eppendorf tube, and the tubes were capped and shaken vigorously for 45 minutes. Two-hundred microliter samples were then removed from each tube and serially diluted six times. One-hundred

microliter sub-samples were spread on R2A agar, and the plates were incubated for five days prior to enumeration. The dry weight of solids was determined after drying each sample at 105°C for 24 hours. Cell extraction buffer, prepared as per Warren *et al.* (1992), was used to remove bacterial cells from aquifer sediment.

3.4 Results and discussion

Model aquifer column 1

Figure 3.3 shows the aqueous-phase carbon tetrachloride concentration profile in column 1 following inoculation. Carbon tetrachloride concentrations began to drop immediately after introduction of strain KC into the column. Most of the transformation occurred in the region of ports 5 through 15, where the biologically-active zone of strain KC activity presumably existed. After 34 days, the effluent CT concentration was ~10 µg/L, and it continued to drop to a low of 3 µg/L after 63 days (CT removal efficiency of 97%).

Nutrient slug injections were stopped after 84 days and no additional acetate, phosphate, or base were added. Aqueous-phase CT concentrations began to rise gradually after this date, indicating a loss of CT transformation activity. However, the rate of increase in aqueous-phase CT was rather low, and nitrate removal persisted. No acetate remained in the column. It can therefore be inferred that the electron donor for sustained denitrification was endogenous reserves or available sediment-associated organic carbon (present at ~0.03% by weight).

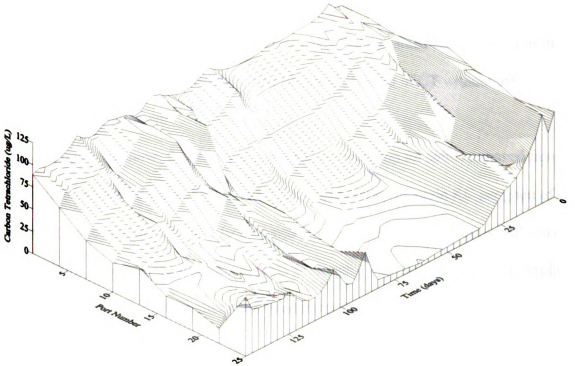

Figure 3.3. Carbon tetrachloride concentration profile in aqueous samples obtained from model aquifer column 1.

Planktonic bacterial enumeration assays were performed on days 0, 85, and 155. On the date of inoculation (day 0), planktonic strain KC was detected at a concentration of 1 x 10^7 CFU/mL was near the slug injection zone at port 5. It was not detected at any other port. This was also the only location where planktonic strain KC was detected on the day after final nutrient addition (day 85). The KC cell concentration at port 5 on day 85 was 3 x 10^3 CFU/mL. On day 155, strain KC was detected at low concentrations (~5 x 10^3 CFU/mL) in samples from ports 5 and 15. This may explain why CT concentrations downgradient from the slug injection zone were lower than the influent CT concentration. While sorption of CT onto the sediment solids may account for the

apparent removal of CT from the liquid phase after feeding was stopped, close examination of the CT concentrations near the slug injection zone show a consistent trend indicating removal of CT in this zone. It was likely that sustained KC activity near the slug injection zone was responsible for the observed removal of CT without the production of chloroform.

Figure 3.4 shows the results of strain KC enumeration for solids removed from the odd-numbered ports on days 85 and 155. The concentration of strain KC per gram of soil did not change significantly after feeding was stopped. High concentrations (10^4 cells per gram of aquifer solids) were present at ports 5 through 13 on day 155. This may explain continued CT transformation after nutrient addition stopped.

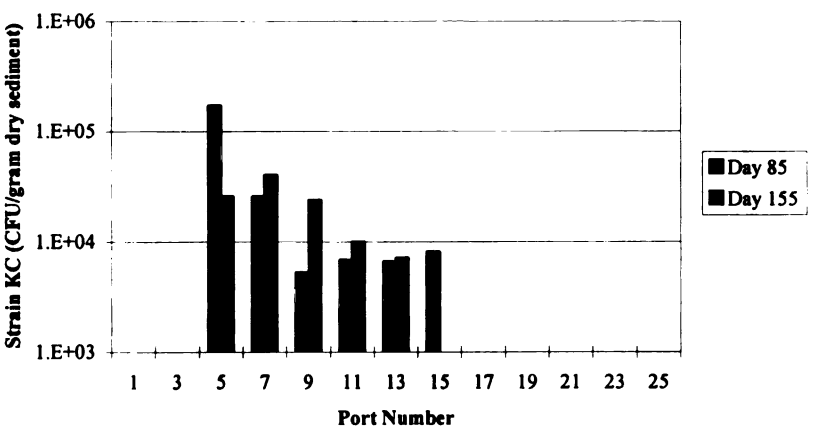

Figure 3.4. *Pseudomonas stutzeri* KC enumeration results from solid samples obtained from model aquifer column 1. Strain KC was not detected in samples obtained from port number locations where bars are not shown.

The initial slug of acetate migrated through the column at a rate similar to that of the conservative tracer bromide, but the overall mass of acetate decreased. Phosphate disappeared rapidly after addition with the inoculum and following each nutrient addition.

Model aquifer column 2

Strain KC bioaugmentation in column 2 was evaluated using an inoculum cell age of 24.5 hours, compared to 17 hours for column 1. This inoculum was active for CT transformation, but aqueous samples removed on day 3 had CT concentrations near 90 µg/L indicating loss of CT transformation activity in the slug injection zone. In an attempt to revitalize CT transformation activity, a slug of pH 8.2 groundwater containing 100 µg/L CT and 10 mg/L phosphate was injected into the slug injection zone on day 3. One day later, CT transformation was observed in the slug injection zone, with CT concentrations near 35 µg/L. On day 7, a slug of Schoolcraft groundwater (pH 8.2) containing 100 mg/L acetate, 10 mg/L phosphate, 100 µg/L CT was injected into the column. This injection scheme was continued for ten weeks: acetate, phosphate, and pH-adjusted groundwater were injected weekly (as in column 1) and an additional slug of pH-adjusted groundwater was added semiweekly.

A zone of strain KC colonization, resulting in CT removal, established close to the slug injection zone. No chloroform production was observed during the period of active operation (data not shown). The zone of colonization for column 1 differed from that of column 2. A possible explanation was the growth stage of the cells at the time of inoculation. The younger cells injected into column 1 were evidently transported with groundwater flow downstream of the slug injection zone before colonizing the sand grains in the model column. The resulting zone of KC colonization was longer than in column 2. The shorter zone of KC colonization observed in column 2 was consistent with the results of previous column studies (Witt *et al.*, 1995).

Figure 3.5 shows the aqueous-phase CT concentration profile in column 2 through day 127. A rapid initial drop in the CT concentration was observed after pH modification was included in the weekly injection scheme. A rapid drop in CT concentration occurred in the region of ports 5 and 6. By day 55 the effluent CT concentration was 7 μg/L, a CT removal efficiency of 93%. Although this CT removal efficiency was slightly lower than that of column 1, it should be noted that the semiweekly slug addition of base included 100 μg/L CT, and this "extra" CT may account for the lower removal efficiency. The final slug of nutrients was added to column 2 ten weeks after inoculation with strain KC. Subsequently, CT concentrations gradually increased over a 70-day time period to approximately 70 μg/L (70% of the influent CT concentration). Thus, low level CT transformation apparently continued for weeks after the final nutrient injection. A possible explanation is residual strain KC activity. On day 140, strain KC was detected on solids removed from ports 5, 7, 9, and 15 (see Figure 3.6). The higher mean concentrations of strain KC in column 2 versus column 1 may have resulted from the more frequent base additions to column 2. Growth of strain KC is known to be favored at pH levels close to 8.0 (Sneathen, 1996).

There was no evidence of CF production during the first ten weeks of active operation. All the added carbon was rapidly consumed by KC in the biocurtain, as is evidenced by the rapid depletion of acetate and nitrate in the slug injection zone following nutrient addition (data not shown).

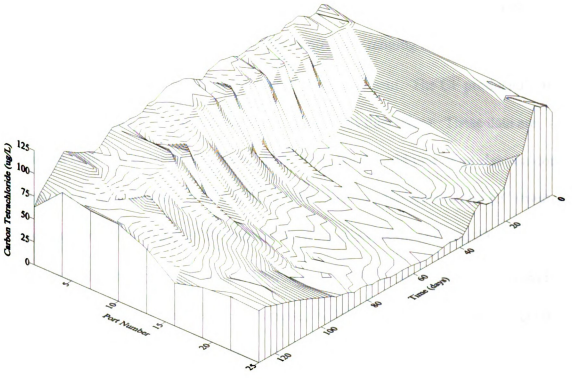

Figure 3.5. Carbon tetrachloride concentration profile in aqueous samples obtained from model aquifer column 2.

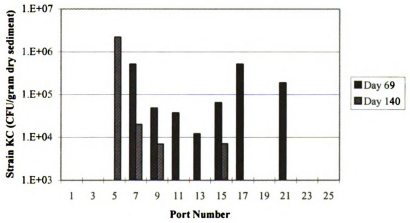

Figure 3.6. *Pseudomonas stutzeri* KC enumeration results from solid samples obtained from model aquifer column 2. Strain KC was not detected in samples obtained from port number locations where bars are not shown.

Chloroform was detected in ports 8 through 25 beginning two weeks after the final nutrient addition. Figure 3.7 shows concentrations ranging from 1 to 20 µg/L were detected in these samples for the remainder of the experiment. The CF produced was most likely a result of CT transformation by indigenous microflora. These data are consistent with earlier laboratory results indicating that the addition of an electron donor (acetate) to saturated Schoolcraft aquifer sediments in the absence of strain KC resulted in the production of 10-20 µg/L CF (data not shown). Conversion of CT to CF is a reductive dechlorination requiring an electron donor. The likely source of electrons in model aquifer column 2 was decaying biomass. A die-off of strain KC was evident by the decrease in solid-phase cell densities between days 69 and 140.

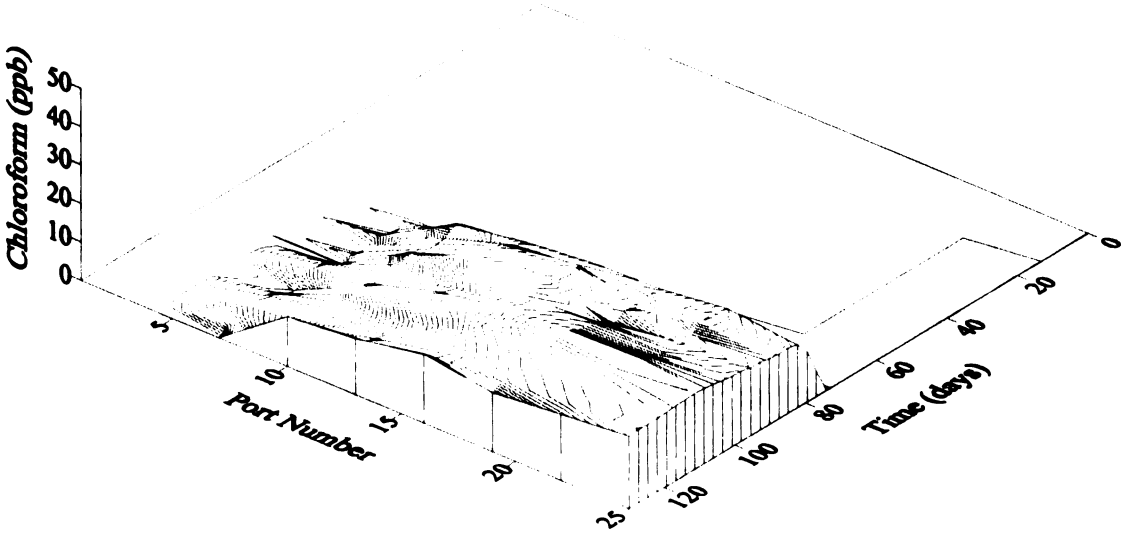

Figure 3.7. Chloroform concentrations measured in samples obtained from model aquifer column 2. No chloroform was ever detected in samples obtained from model aquifer column 1.

In column 1, no CF was produced after nutrient addition was halted. Evidently, twice-weekly pH amendments, performed only in column 2, selected for indigenous populations capable of degrading CT to CF.

Comparison to pilot-scale study

The bench-scale studies detailed in this report were designed and operated to simulate operations in a field-scale bioaugmentation experiment (Dybas *et al.*, 1998). The chemical components and respective concentrations in the slug additions for the field-scale experiment were similar to those used in the laboratory-scale experiments. Phosphorus and pH levels within a small test zone of the Schoolcraft aquifer were increased to a favorable range using pulses of pH and phosphate-amended groundwater. Strain KC was grown in an above-ground reactor and introduced into the test zone along with acetate and phosphate. In situ microbial activity was sustained with periodic pulses of extracted groundwater amended with acetate, base, and phosphate. In the weeks following inoculation of the test zone, strain KC spread throughout the grid and nitrate and CT concentrations dropped. At those wells where base and acetate were delivered effectively, strain KC was detected in the groundwater, nitrate levels decreased by 85%, and CT levels decreased by 65% without significant CF production. As in the column studies, shifts in microbial community structure were observed with indigenous flora eventually gaining dominance in the aqueous phase as strain KC partitioned to the solid phase. Samples obtained weeks after the final nutrient addition in both columns indicated that strain KC was able to colonize aquifer materials and assimilate into the aquifer community. Similar results were also found in the field experiment (Dybas *et al.*, 1998).

A critical difference between the pilot-scale experiment and the model aquifer columns was the level of hydraulic control. In the laboratory-scale experiments, establishing hydraulic control in a two-meter long column was not difficult, enabling adequate coverage of KC cells, delivery of nutrients, and efficient removal of CT. In the field test grid, however, establishing hydraulic control was considerably more difficult. Of the six monitoring wells in the test grid, two had good overall hydraulic communication with the injection well, three had marginal communication, and one had very little communication. Evidence of CT removal was most apparent in the wells in good hydraulic communication with the injection well. Carbon tetrachloride transformation, although lower in efficiency, was also observed in those wells having marginal communication with the injection well. It was apparent from the field results that CT removal was dependent on the degree to which KC cells were moved and allowed to colonize the solids near the monitoring wells.

We conclude that bioaugmentation can be used to establish a biocurtain capable of long-term sustained bioremediation activity. Bioaugmentation with strain KC effectively removed CT from contaminated groundwater in laboratory-scale model aquifer systems over extended periods. The results also indicate that microbes indigenous to the Schoolcraft, Michigan, aquifer can convert CT to CF under certain conditions. A key to successful bioaugmentation is establishment of an environment that selects for the added microorganism while avoiding selection for competitor populations, especially those capable of mediating undesirable transformations.

3.5 Acknowledgments

This work was supported by the State of Michigan, Department of Environmental Quality. Additional funding for this research was also provided by the National Institute of Environmental Health Sciences and the U.S. Environmental Protection Agency under Grant R-819605 to the Great Lakes and Mid-Atlantic Hazardous Substance Research Center.

3.6 Literature cited

Atlas, R.M. and R. Bartha. 1993. *Microbial Ecology: Fundamentals and Applications*. The Benjamin/Cummings Publishing Company, Inc., New York, New York.

Criddle, C.S., J.T. DeWitt, D. Grbic-Galic, and P.L. McCarty. 1990a. Transformation of carbon tetrachloride by *Pseudomonas* sp. strain KC under denitrification conditions. *Appl. Environ. Microbiol.* **56**:3240-3246.

Criddle, C. S., J. T. DeWitt, and P. L. McCarty, 1990b. Reductive dehalogenation of carbon tetrachloride by *Escherichia coli* k-12. *Appl. Environ. Microbiol.* **56**:3247-3254.

Dybas, M.J., G.M. Tatara, and C.S. Criddle. 1995. Localization and characterization of the carbon tetrachloride transforming activity of *Pseudomonas* sp. strain KC. *Appl. Environ. Microbiol.* **61**:758-762.

Dybas, M.J., M. Barcelona, S. Bezborodnikov, S. Davies, L. Forney, H. Heuer, O. Kawka, T. Mayotte, L. Sepulveda-Torres, K. Smalla, M. Sneathen, J. Tiedje, T. Voice, D.C. Wiggert, M.E. Witt, and C.S. Criddle. 1998. Pilot-scale evaluation of bioaugmentation for in-situ remediation of a carbon tetrachloride-contaminated aquifer. Submitted for publication to *Environ. Sci. Technol.*

Egli, C., R. Scholtz, A.M. Cook, and T. Leisinger. 1987. Anaerobic dechlorination of tetrachloromethane and 1,2-dichloromethane to degradable products by pure cultures of *Desulfobacterium* sp. and *Methanobacterium* sp. *FEMS Microbiol. Lett.* **43**:257-261.

Egli, C., T. Tschan, R. Scholtz, A.M. Cook, and T. Leisinger. 1988. Transformation of tetrachloromethane to dichloromethane and carbon dioxide by *Acetobacterium woodii*. *Appl. Environ. Microbiol.* **54**:2819-2823.

Jin, G. and A. J. England, Jr. 1997. Biodegradation kinetics of carbon tetrachloride by *Pseudomonas cepacia* under varying oxidation-reduction potential conditions. *Water Environ. Res.* **69**:1094-1099.

Knoll, W.H. 1994. Factors influencing the competitive advantage of *Pseudomonas* sp. strain KC for subsequent remediation of a carbon tetrachloride impacted aquifer. Master's Thesis, Department of Civil and Environmental Engineering, Michigan State University, East Lansing, Michigan.

Markwell, M.A., S.M. Haas, N.E. Tolbert, and L.L. Bieber. 1981. Protein determination in membrane lipoprotein samples: manual and automated procedures. *Methods Enzymol.* **72**:296-301.

Mayotte, T.J., M.J. Dybas, and C.S. Criddle. 1996. Bench-scale evaluation of bioaugmentation to remediate carbon-tetrachloride-contaminated aquifer materials. *Ground Water.* **34**:358-367.

Semprini, L., G.D. Hopkins, P.L. McCarty, and P.V. Roberts. 1992. In-situ transformation of carbon tetrachloride and other halogenated compounds resulting from biostimulation under anoxic conditions. *Environ. Sci. Technol.* **26**:2454-2461.

Sneathen, M.A. 1996. Theoretical and experimental competitiveness of *Pseudomonas stutzeri* KC. Master's Thesis, Department of Civil and Environmental Engineering, Michigan State University, East Lansing, Michigan.

Tatara, G.M., M.J. Dybas, and C.S. Criddle. 1993. Effects of medium and trace metals on kinetics of carbon tetrachloride transformation by *Pseudomonas* sp. strain KC. *Appl. Environ. Microbiol.* **59**:2126-2131.

Warren, T.M., V. Williams, and M. Fletcher. 1992. Influence of solid surface, adhesive ability, and inoculum size on bacterial colonization in microcosm studies. *Appl. Environ. Microbiol.* **58**:2954-2959.

Witt, M.E., M.J. Dybas, R.L. Heine, S. Nair, C.S. Criddle, and D.C. Wiggert. 1995. Bioaugmentation and transformation of carbon tetrachloride in a model aquifer. *Bioaugmentation for Site Remediation.* Battelle Press, Columbus, Ohio.

Chapter 4

BIOREMEDIATION OF CARBON TETRACHLORIDE-CONTAMINATED SEDIMENTS BY CHEMOTACTIC, DENITRIFYING CELLS RESPONDING TO A NITRATE GRADIENT

4.1 Abstract

Pseudomonas stutzeri KC is a motile aquifer isolate that is capable of transforming carbon tetrachloride (CT) to carbon dioxide, formate, and non-volatile end products under denitrifying conditions. Capillary experiments have established that strain KC is chemotactic toward nitrate. Columns packed with aquifer sediment were used to determine whether nitrate-directed motility would influence bioremediation of CT in CT-contaminated aquifer sediments. A "continuous flow" column was used to evaluate the effects of chemotaxis in the presence of an imposed advective flow, and a "no-flow" column was used to isolate the effects of chemotaxis in the absence of flow. Both columns were packed with sediments from a CT- and nitrate-contaminated aquifer near Schoolcraft, Michigan, and groundwater was pumped continuously through the columns until the aqueous and sorbed CT had equilibrated. The continuous flow column was inoculated near its upstream end with strain KC, base, acetate, and phosphate. CT-contaminated groundwater was then pumped continuously through the column. Cells migrated through the column at a velocity exceeding the average linear groundwater velocity, removing ~55% of the total mass of CT in the aqueous phase and ~29% of the sorbed CT. The no-flow column was inoculated near its midpoint, and was maintained thereafter as a static incubation. Motile KC cells migrated over a 0.3 m distance within five days. After 26 days, over 94% of the CT in the aqueous phase had degraded. The

results support the hypothesis that localized depletion of nitrate creates nitrate gradients that trigger a chemotactic response. The results also indicate that motile KC cells are capable of CT transformation.

4.2 Introduction

In earlier work, we reported that biocurtains capable of long-term, continuous removal of CT can be created in columns packed with aquifer sediments by bioaugmentation with *Pseudomonas stutzeri* KC (Witt *et al.*, 1998). Although the majority of the added cells colonized aquifer sediments to create a stationary biocurtain, a fraction of the added strain KC cells were apparently motile and capable of CT transformation. Although bromide tracer and KC cells were injected simultaneously, KC cells were detected in samples where bromide had yet to arrive. A possible explanation is chemotaxis, the movement of bacteria in response to chemoattractant gradients. In the case of strain KC these chemoattractants could include nitrate. Widman (1997) demonstrated that strain KC was chemotactic towards nitrate. Therefore, strain KC would be expected to show a chemotactical response towards regions where the concentration of nitrate was relatively higher. The present study confirms this hypothesis and establishes chemotaxis toward nitrate as the underlying mechanism for motility.

The movement of bacteria through porous media is of great interest for *in-situ* bioremediation. The transport of bacteria through porous media has been studied in laboratory-scale column systems (Jenkins *et al.*, 1993; Weiss *et al.*, 1995; Rijnaarts *et al.*, 1996; and Widman, 1997). Researchers have documented bacterial movement through soil and sediment at pore velocities of up to 30 cm/day in both the laboratory studies

(Wollum and Cassel, 1978; Smith *et al.*, 1985; and Fontes *et al.*, 1991) and in the field studies (Harvey *et al.*, 1989; and Martin *et al.*, 1991). Reynolds *et al.* (1989) concluded that motile and chemotactic strains of bacteria had higher penetration rates than non-motile and non-chemotactic mutants. They noted that chemotaxis was not required for transport through sand under nutrient-saturated conditions. Chemotactic strains had lower penetration rates than non-chemotactic mutants. A possible explanation is that chemotactic strains were able to sense nutrient gradients in three dimensions and migrate throughout the entire pore volume of porous media. The non-chemotactic strains did not sense these nutrient gradients and were thus more likely to move through higher-velocity macropores. In an aquifer, however, the distribution of nutrients is not uniform as a result of physical heterogeneity and variable temporal and spatial inputs. Therefore, uniform removal of contaminant may depend upon the existence of cell transport mechanisms such as chemotaxis, which enable bacterial populations to move towards regions of higher nutrient (or contaminant) concentration.

Chemotaxis can greatly enhance the rate of microbial dissemination. The spreading rate of chemotactic cells in swarm plates can be several times greater than that of non-chemotactic mutants that move only via random motility (Emerson *et al.*, 1994; Widman *et al.*, 1997). However, the spreading rate is a function of the bulk chemoattractant concentration; excessively high chemoattractant concentrations reduce chemotactic migration rates by saturating receptors (Widman *et al.*, 1997). Strain KC has been shown to be strongly chemotactic to a variety of organic compounds, including acetate, both under aerobic and denitrifying conditions (Widman, 1997). Evidence for chemotaxis included the formation of one or more rapidly migrating chemotactic bands in

swarm plates or a diffusion gradient chamber (DGC). Adler (1966) demonstrated that a chemotactic band is associated with a sharp chemoattractant concentration gradient that arises from cellular consumption of the chemoattractant. Widman *et al.* (1997) showed that cellular metabolism can result in coupled gradients in both the electron donor and the electron acceptor, and that chemotaxis in response to each of these gradients can be significant.

In the laboratory-scale studies described in this paper, strain KC was injected into columns packed with CT-contaminated Schoolcraft aquifer material. One model column, operated at a groundwater flow velocity of 10 cm/day, was inoculated with strain KC in the slug injection zone and the resulting mobile biocurtain was studied. The second column was operated as a static batch microcosm with no advective flow. This column was inoculated at its midpoint and migration of strain KC was monitored. The results suggest that chemotaxis plays an important role in maximizing the efficiency of CT transformation.

4.3 Materials and methods

Capillary assay experiments

Capillary assays (Adler, 1973) were performed to screen strain KC cells for chemotaxis toward nitrate and oxygen. The cells were grown to late exponential phase in 100 mL of liquid medium in 250 mL shake flasks with 150 rpm shaking in a Lab Line Orbit shaker. The liquid medium consisted of Medium D (Tatara *et al.*, 1993) without vanadium and cobalt trace minerals. Two hours before the capillary assay was performed, the culture was diluted to an OD_{590} of 0.4 with fresh liquid medium. For each

assay, 1.0 mL of culture was centrifuged at room temperature for 10 minutes and then washed twice with 1.0 mL of buffer. The buffer consisted of 2.0 g of KH_2PO_4 and 3.5 g of K_2HPO_4 per liter of deionized water, titrated to a pH of 8.2. After washing, the cells were re-suspended in 4 mL of buffer in a 10 mL test tube.

Glass capillaries (9.5 cm long with an inner diameter of 0.16 cm) were filled with one of the following test solutions: 0.5 g/L sodium nitrate in anaerobic buffer, 5.0 g/L sodium nitrate in anaerobic buffer, 50 g/L sodium nitrate in anaerobic buffer, buffer equilibrated with pure oxygen gas, buffer equilibrated with air, or anaerobic buffer. Each capillary was mounted in one of the test tubes so that open end of the capillary was immersed in the cell suspension. After a two-hour incubation period at room temperature, the capillaries were removed from the test tubes, and the contents of each capillary were diluted by a factor of 500 with sterile buffer. Five-microliter aliquots of each diluted cell suspensions was spread onto sterile LB agar plates. The plates were incubated aerobically at 20°C for two days, and the resulting colonies were counted.

To adjust the oxygen concentration in the buffer solution prior to use, filter-sterilized oxygen, air or nitrogen gas was bubbled through 25 mL of buffer in a 75 mL test tube for 30 minutes. An oxygen electrode was used to confirm that the oxygen concentrations in the gas and liquid phases were essentially at equilibrium after 30 minutes of sparging.

All glassware and buffer solutions were autoclaved at 121°C for 25 minutes prior to use. The cell suspensions in the test tubes were examined under 400X magnification for degree of motility both at the beginning and end of the two-hour incubation period.

Construction of mobile biocurtain column

One laboratory-scale model aquifer column was used to investigate the role of bacterial motility in the transformation of CT by *Pseudomonas stutzeri* KC. A diagram of the two-meter long model aquifer column is provided in Figure 4.1. This column consisted of a section of clear polycarbonate pipe, 5.2 cm in diameter (i.d.) and outfitted with 25 sampling ports spaced at 7.6 cm intervals along the pipe. Both columns were wet-packed with aquifer material obtained from soil borings MLS2 and MLS3 (see Dybas *et al.*, 1998) at a CT-contaminated aquifer in Schoolcraft, Michigan.

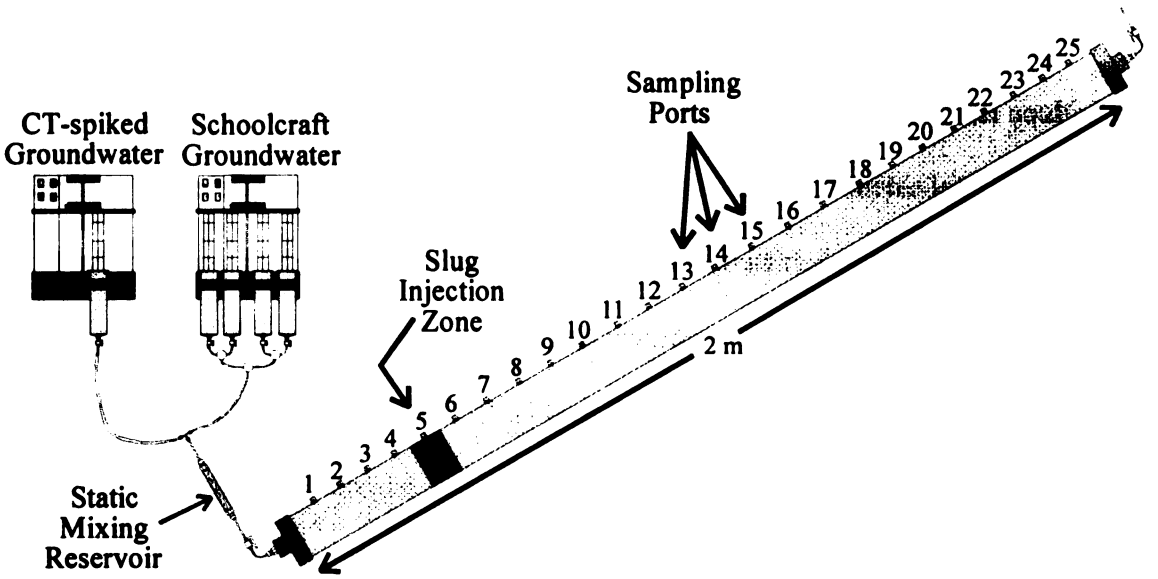

Figure 4.1. Diagram of model aquifer column with a flow velocity of 10 cm/day.

Two Harvard Apparatus syringe pumps (model 22) were used to pump Schoolcraft groundwater through the column at rate yielding an average linear flow velocity of 10 cm/day, which is near the flow velocity in the Schoolcraft aquifer. One

pump was used to deliver filter-sterilized groundwater spiked with CT. The second pump was used to deliver non-filtered, CT-free groundwater. The flows from both syringe pumps were combined in a 1:10 ratio of CT-spiked to CT-free groundwater, yielding an influent CT concentration of 130 μg/L. The column and both syringe pumps were incubated in a constant temperature room at the temperature of the Schoolcraft aquifer (12°C).

Construction of static column

An additional laboratory-scale model aquifer column was used to investigate the role of chemotaxis in the transformation of CT by *Pseudomonas stutzeri* KC under conditions of zero groundwater flow. A diagram of the one-meter long model aquifer column is provided in Figure 4.2. This column consisted of a one-meter-long section of clear polycarbonate tubing, 5.2 cm in diameter (i.d.) and outfitted with 10 sampling ports spaced at 7.6 cm intervals along the pipe. This column was wet-packed with aquifer material obtained from soil borings MLS7 (see Dybas *et al.*, 1998) at a CT-contaminated aquifer in Schoolcraft, Michigan.

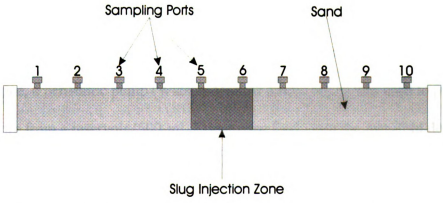

Figure 4.2. Diagram on model aquifer column with no groundwater flow.

Carbon tetrachloride-spiked Schoolcraft groundwater was pumped through the column to saturate the aquifer solids with CT. Pumping continued until the CT concentration in samples taken from all ten sampling ports were 100 ± 5 µg/L. Once this was achieved, the influent and effluent valves were closed and groundwater pumping was discontinued. The model column was incubated in the same constant temperature room as the mobile biocurtain column at a temperature of 12°C.

Construction of slug injection zone

Each model column was outfitted with a manifold for delivery of organisms and nutrients into a section of each column designated the "slug injection zone." The delivery manifold (see photograph in Figure 4.3) consisted of four 8-inch stainless steel pipes (3/16-inch o.d.). Each of these pipes passed through one side of the polycarbonate pipe, through the center of the column, and out the opposite side of the polycarbonate pipe. Sections of manifold located on the inside the polycarbonate pipe (within the column interior) were slotted to create well screens, allowing for free flow of water into and out of the pipe while preventing plugging by sand grains. Sections of the manifold located on the outside the polycarbonate pipe (external to the column) were connected together to create injection and extraction lines. For chemical and organism delivery into the slug injection zone, a peristaltic pump (Watson-Marlow model 502E) was used to pump fluid at 20 mL/min from a reservoir (500-mL Erlenmeyer flask) into the manifold delivery lines.

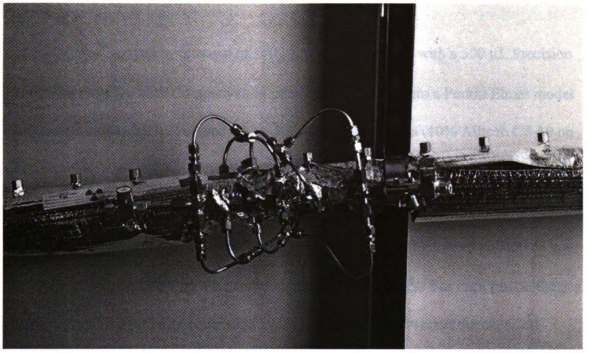

Figure 4.3. Photograph of the delivery manifold on a model aquifer column.

Groundwater

Groundwater from a CT-contaminated aquifer in Schoolcraft, Michigan, was used in these column studies. Groundwater was obtained from a two-inch well screened 46 feet below the water table by using a Grundfus groundwater collection device. Groundwater was transported to the laboratory in pre-sterilized sealed Nalgene carboys. Once in the laboratory, samples were stripped to remove volatiles, transferred to 1 L Wheaton bottles, and sealed with Teflon™-lined caps. Samples were stripped by bubbling a N_2-CO_2 gas mix rapidly through each bottle for a period of 45 minutes. N_2 was used to strip volatiles and displace oxygen, while CO_2 was used to maintain the pH of the groundwater at the background level observed in the field (pH 7.1).

Carbon tetrachloride analysis

CT was assayed by removal of 100 µL of headspace gas with a 500 µL Precision gas-tight syringe (Alltech Company) and injecting the sample into a Perkin Elmer model 8500 gas chromatograph equipped with a 100/120-mesh column (10% Alltech CS-10 on Chromsorb W-AW) and an electron capture detector with nitrogen carrier (40 mL/min).

External standard calibration curves were prepared by addition of a primary standard (8.22 ng of CT per µL of methanol) to secondary solutions having identical gas-to-water ratios and incubation temperatures as the assay samples. For each run on the gas chromatograph, a four point calibration curve was prepared to bracket the expected concentration range of the samples.

Two-hundred microliter samples were obtained from the column sampling ports on alternate days for analysis of volatile organics. Aqueous samples were withdrawn using a 500 µL Pressure-Lok™ gas-tight syringe (Alltech Associates) equipped with a 1.5-inch sideport sampling needle. Both the syringe needle and sampling port septum were pre-sterilized with an ethanol-soaked cotton swab. Each 200 µL sample was dispensed into a 1.5 mL glass vial (Sun Brokers, Inc.) sealed with Teflon™-lined crimp tops (Sun Brokers, Inc.). Between sampling events, the interior of the gas-tight syringe was rinsed internally with 0.5 mL methanol, followed by 0.5 mL autoclaved DI water.

Anions analysis

Anions were assayed by ion chromatography with suppressed conductivity detection on a Dionex model 2000i/SP ion chromatograph equipped with a Dionex AS4A

IonPac™ column and utilizing a 1.8 mM bicarbonate-1.7 mM carbonate mobile phase (3 mL/min). Chromatograms were recorded and data integrated with a Spectra Physics model SP 4270 integrator. Five-point calibration curves were prepared by diluting primary anion standards into secondary DI water standards. Two-hundred microliter samples were obtained from sampling ports on alternate days for analysis on the ion chromatograph. Each sample was diluted into 400 µL of DI water, filtered through a 0.22 µm nylon filter (Scientific Resources Inc.), and dispensed into a polypropylene sample vial (Alcott Chromatography). Each sample was analyzed for acetate, bromide, nitrate, nitrite, phosphate, and sulfate.

Inoculation using Pseudomonas stutzeri KC

Pseudomonas stutzeri KC (DSM deposit number 7136, ATCC deposit number 55595), derived originally from aquifer solids from Seal Beach, California, is routinely maintained in our laboratory on R2A agar plates. To determine the appropriate growth conditions for the inoculum, a series of laboratory experiments were conducted to evaluate the effects of media composition on the ability of strain KC to compete with native microflora and to maximize expression of CT degradation activity (Dybas *et al.*, 1998). The results indicated good growth and transformation activity in an inoculum grown with 1600 mg/L acetate and 10 mg/L phosphate in groundwater adjusted to a pH of 8.2.

A liquid KC culture was initiated by removing one colony from an R2A agar plate and placing it in an Erlenmeyer flask containing 25 mL of sterile nutrient broth. After shaking overnight, 4 mL of the resulting starter culture was transferred to 400 mL of

filter-sterilized Schoolcraft groundwater. Acetate and phosphate were added at concentrations indicated above, pH was adjusted to 8.2, and the flask was shaken overnight. Cell growth was monitored by measuring the OD_{660} of 5 mL samples using a Shimadzu UV-160 spectrophotometer. Final cell concentrations in the inoculum were determined by spreading 100 µL samples on sterile R2A agar plates and counting colonies after incubating at room temperature for five days.

Inoculation with strain KC was performed a single time in each column. The mobile biocurtain column was inoculated in the slug injection zone using a 320 mL volume of an aqueous strain KC ($7.1 \pm 1.3 \times 10^7$ cells/mL) culture grown for 24 hours in filter-sterilized Schoolcraft groundwater. The inoculum was augmented with CT, additional acetate, nitrate, and a conservative tracer (bromide). The concentrations of acetate, bromide, CT, and nitrate in the slug injection zone were 1650 mg/L, 264 mg/L, 100 µg/L, and 47 mg/L, respectively. Equal concentrations of CT and nitrate were present throughout the column.

Before injecting inoculum into the mobile biocurtain column, the ability of the inoculum to transform CT was confirmed. Two sealed test tubes containing 5 mL of inoculum were spiked with 82 µg/L CT. After one hour, 88% of the CT was removed in the inoculated tubes, with no removal in uninoculated control tubes.

Samples of the inoculum used in the mobile biocurtain column were diluted and spread on sterile R2A agar plates. The plates were incubated at room temperature for five days and the strain KC cell concentration was determined to be $7.1 \pm 1.3 \times 10^7$ CFU/mL.

The procedure for inoculating the static column was similar to that of the mobile biocurtain column. This column was inoculated in the slug injection zone using a 320 mL volume of an aqueous strain KC culture grown for 25 hours in filter-sterilized Schoolcraft groundwater. The inoculum was augmented with CT, acetate, nitrate, and a conservative tracer (bromide). The concentrations of acetate, bromide, CT, and nitrate in the slug injection zone were 1533 mg/L, 217 mg/L, 100 μg/L, and 25 mg/L, respectively. Again, equal concentrations of CT and nitrate were present throughout the column immediately after inoculation. Plate count analyses on the inoculum for the static column indicated a KC cell density of $1.2\pm0.1 \times 10^8$ CFU/mL.

A duplicate experiment using the static column was performed similarly to the first experiment with one exception. One-micron-diameter microspheres (Polysciences, Inc.) were added to the inoculum prior to injection into the slug injection zone. These microspheres are neutrally-charged latex beads that fluoresced under UV light. By adding these beads to the inoculum, the goal was to assess the transport properties of 1-μm sized spheres under conditions of zero advective flow. Comparison of the movement of one micron-sized bacteria to these spheres led to estimates of cell migration velocities due to chemotaxis.

Enumeration of planktonic and attached bacteria

For enumeration of planktonic bacteria, 200 microliter aqueous samples were obtained from all sampling ports every third or fourth day and dispensed into sterile culture tubes containing 1.8 mL of 50 mM phosphate buffer (pH 8.0). Serial dilutions were performed as follows: 200 μL were withdrawn from the first dilution and mixed on

a vortex mixer for five seconds with 1.8 mL phosphate buffer in a second culture tube, another 200 µL portion was transferred from the second dilution to the third and mixed as before, and subsequent dilutions were performed in the same manner for a total of six dilutions. A 100 µL subsample of each dilution was spread aseptically in a sterile petri dish containing R2A agar, plates were incubated at room temperature for five days, and plates were then scored for growth of strain KC and indigenous microflora. Strain KC was differentiated from Schoolcraft flora by the unique "fried-egg" appearance of strain KC colonies after five days of incubation (Sneathen, 1996). Results were compiled as colony forming units (CFU) per mL of fluid.

Attached bacteria were enumerated by removing 200 to 700 milligrams of aquifer material from each sampling port. The samples were placed in sterile Eppendorf tubes and weighed. One mL of cell extraction buffer was added to each Eppendorf tube, and the tubes were capped and shaken vigorously for 45 minutes. Two-hundred microliter samples were then removed from each tube and serially diluted six times. Samples were then spread on R2A agar, the plates were incubated for five days, and colonies were counted. The dry weight of soil was determined by drying each sample in a 105°C oven for 24 hours and weighing the mass of dry soil remaining. Results were compiled as colony forming units (CFU) per gram of dry solids.

Cell extraction buffer

Cell extraction buffer (Warren *et al.*, 1992) was used to remove bacterial cells from aquifer solids. This buffer was prepared by adding the following compounds to a 100 mL volume of 20 mM phosphate buffer adjusted to pH 8.0: 38 mg ethylene glycol

Bis (β-aminoethyl ether) N,N,N′,N′-tetraacetic acid (EGTA), 100 μL of 400 mg/L Tween solution, 10 mg peptone, and 7 mg yeast extract. This solution was mixed and autoclaved.

DNA probe specific to strain KC

Three sets of primers of 20-22 base pairs (bp) were selected and tested against aquifer isolates and aquifer groundwater DNA and found to be specific for strain KC. One set of primers JMT 166 (21 bp) and JMT 219 (21 bp) was further optimized for use. The primary structure is 5' TGGCATGGGTCTGGGCTCTAT and 5' CCTGATGACCGATTACGACCA. These amplify a 787 bp strain KC-specific DNA fragment. Polymerase chain reactions (PCR) were carried out in 50 μL volume containing 50 pmol each of two primers, 0.2 mM deoxynucleoside triphosphates and 3 μL of AmpliTaq DNA polymerase (Perkin Elmer) in a buffer containing 50 mM KCl, 10 mM Tris-HCl (pH 8.3), and 1.5 mM MgCl. For selected primers, the cycles used were as follows: 1 cycle at 94°C for 2 minutes, 35 cycles at 94°C for 1 minute, at 64°C for 2 minutes, and at 72°C for 3 minutes, with a 7-minute extension at 72°C in the last cycle. The amplifications were performed with a DNA thermal cycler (Perkin Elmer). Amplification products were separated in 1.5% agarose gel in TAE buffer with ethidium bromide.

Fluorescent microbead assay

Fluoresbrite PC Red microspheres (Polysciences, Inc.), 0.952 μm in diameter and dyed with phycoerythrin, were assayed using a Perkin Elmer model LS 50 luminescence

spectrometer. A five-point calibration curve, bracketing the anticipated sample concentrations, was constructed prior to sample analysis. Calibration standards and samples were analyzed in the LS 50 using a 1.4-mL semi-micro fluorimeter (Buck Scientific) at an excitation maximum of 591 nm and an emission maximum of 657 nm.

Establishment of conditions similar to Schoolcraft aquifer

After construction of the mobile biocurtain column was complete, denitrifying conditions were obtained by pumping oxygen-free Schoolcraft groundwater through the column for a period of four weeks. After this time period, random samples collected from various ports on the column contained no detectable concentrations of dissolved oxygen (less than 0.1 mg/L).

Prior to inoculation, a conservative tracer study was performed in each column to measure the porosity of the aquifer solids. Tritiated water (^3H_2O) was used as the conservative tracer in each column. Porosity determined in this manner was 0.27 for the mobile biocurtain column and 0.32 for the static column.

4.4 Results and discussion

Capillary assay experiments

The results of the capillary assay experiments are given in Table 4.1. The number of colony-forming units (CFU) obtained in the presence of 5 and 50 g/L nitrate was approximately an order of magnitude higher than the control (buffer sparged with nitrogen gas). These results provide strong evidence that strain KC is chemotactic toward nitrate.

An alternative explanation for increased CFU counts is that nitrate may enhance cell motility, and that random motility, rather than chemotaxis, drives accumulation of cells in the capillary. Direct microscopic examination of cells taken from the test tube confirmed a high degree of cell motility both at the beginning and end of the two-hour incubation period. Because no external energy source was supplied, endogenous energy reserves are believed to provide the energy for motility during the incubation (Adler, 1973).

Table 4.1. Number of strain KC colony-forming units (CFU) measured on agar plates during a capillary tube assay experiment.

Test Solution	Average CFU	Standard Deviation
Buffer sparged with nitrogen	26	4
Buffer sparged with air	18	7
Buffer sparged with pure oxygen	22	16
Buffer containing 0.5 g/L nitrate	50	47
Buffer containing 5 g/L nitrate	287	146
Buffer containing 50 g/L nitrate	308	59

Strain KC cells can use either oxygen or nitrate as an electron acceptor. As shown in Table 4.1, capillary experiments performed using oxygen in place of nitrate showed no increase in CFU relative to the control. This result suggests that oxygen is not a chemoattractant for strain KC, and that the higher CFU values observed for nitrate are due to chemotaxis rather than the presence of an electron acceptor. The oxygen concentrations tested were less than the nitrate concentrations due to the limited aqueous solubility of oxygen. However, Adler (1966) has shown that the oxygen concentration in equilibrium with air is sufficient to sustain a strong chemotactic response by *E. coli* in a

capillary, and more than six hours were required for the cells to consume all the oxygen in the capillary.

Mobile biocurtain column

Bromide was included in the initial slug injection to serve as a conservative tracer. Figure 4.4 shows the bromide concentration profile in the model column on days 1, 4, 8, 13 and 18. The successful use of bromide as a conservative tracer has been shown in previous studies (Dybas *et al.*, 1998; and Witt *et al.*, 1998) using Schoolcraft groundwater and aquifer solids. The detection of bromide served as a marker for the location of the inoculum slug in the model aquifer column. The total mass of bromide (19.6 ± 1.3 mg) detected in the migrating slug was unchanged throughout the duration of the experiment.

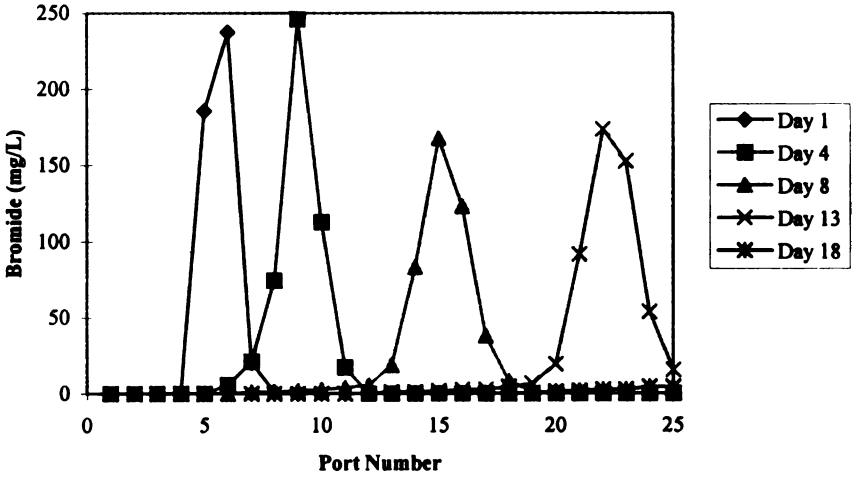

Figure 4.4. Bromide concentration profile in the mobile biocurtain model column on days 1, 4, 8, 13 and 18.

The concentration profile of acetate on days 1, 4, 8, 13 and 18 is shown in Figure 4.5. There was no distinguishable difference in the rate of movement of acetate to that of bromide. The total mass of acetate added with the inoculum was ~137 mg. Over 27 mg of the added acetate was consumed the first day, and an additional 8 mg/day were consumed through day 4. After day 4, however, the rate of acetate consumption in the column was much lower. From day 4 until the end of the experiment, the daily acetate consumption rate varied between 3 and 5 mg/day. It is interesting to note that most of the acetate consumption occurred early in the experiment when strain KC and nitrate (a suitable electron acceptor) was presumably present in the vicinity of the acetate slug. As the electron acceptor (nitrate) became limiting, KC cells no longer had the means to produce energy in the absence of an electron acceptor. Thus, minimal acetate consumption was observed after nitrate concentrations dropped to near zero.

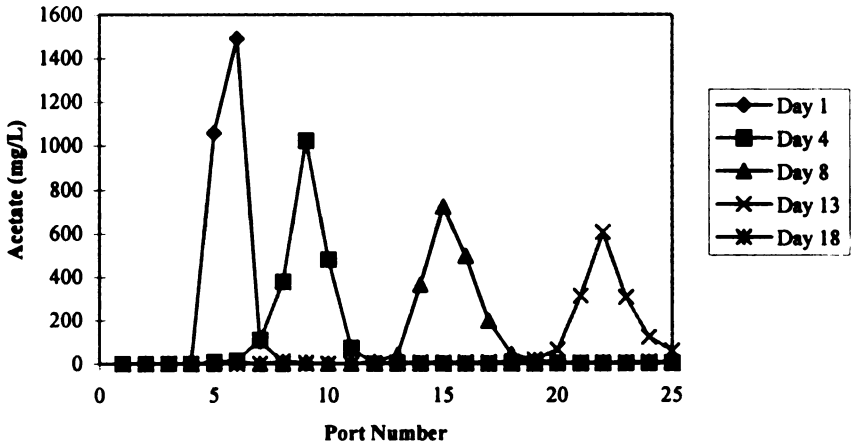

Figure 4.5. Acetate concentration profile in mobile biocurtain model column on days 1, 4, 8, 13, and 18.

In order for the mobile wave of strain KC to reduce nitrate, a carbon source other than acetate must have been present in the downstream region of the column where there was evidence of nitrate reduction without detectable concentrations of acetate. It was possible that strain KC bacteria stored carbon in the form of PHB granules, then migrated downstream in response to an appreciable nitrate gradient, where nitrate was used as an electron acceptor.

Figure 4.6 shows the nitrate concentration profile in the mobile biocurtain column on days 1, 4, 8, 13, and 18. Background concentrations of nitrate prior to inoculation are shown for comparison. On the day after inoculation (day 1), evidence of denitrification is shown by the dramatic drop in nitrate concentration in samples taken from ports 5 and 6. By day 4 the region devoid of nitrate had widened to the area between ports 6 and 12. On day 8, most of the nitrate downgradient from port 6 had been reduced. In fact, the only detectable amount downstream from port 10 was in port 20 (3 mg/L). Considering where the bromide tracer front had traveled by day 8 (center of mass near port 15), evidence that actively denitrifying populations were present downgradient to port 25 was shown by the nitrate concentration profile. A plausible explanation for this loss of nitrate is that strain KC responded chemotactically and accelerated its migration through the column in response to nitrate gradients.

Also, evidence that nitrate had "broken through" the stationary biocurtain (formed upon slug injection of inoculum) became evident on day 8 and continued through the duration of the experiment. Weekly addition of 100 mg/L acetate would most certainly have been sufficient to sustain active removal of both nitrate and CT by attached strain KC in the region of ports 5 and 6 (Witt *et al.*, 1998).

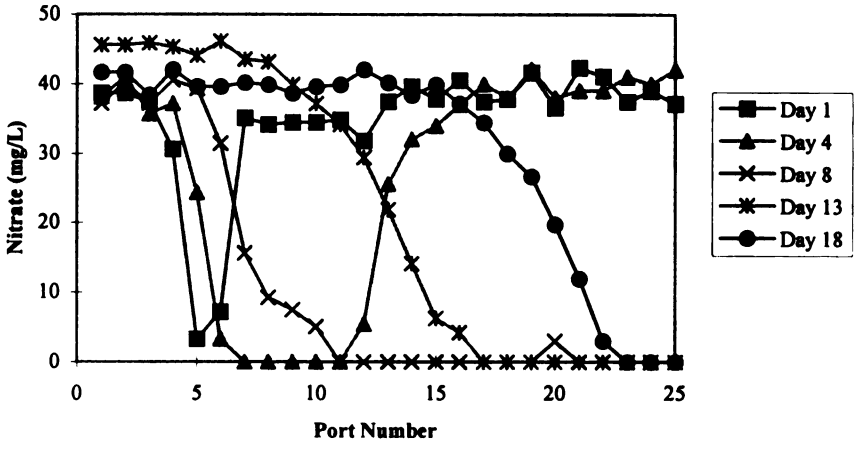

Figure 4.6. Nitrate concentration profile in mobile biocurtain column on days 1, 4, 8, 13, and 18.

The results of the liquid phase strain KC analyses show that KC initially moved with the conservative tracer through the porous media. However, as time elapsed, the rate of movement of strain KC was higher than that of the conservative tracer. Figure 4.7 shows that on day 3, detectable concentrations of strain KC were evident in samples obtained from ports 5, 7 and 9. On day 4, the center-of-mass of the bromide slug was located near sampling port 9. By day 7 there was evidence that strain KC had migrated downstream as far as port number 23. The distance traveled the first seven days by the mobile strain KC biocurtain was approximately 114 cm, which was much longer than the distance traveled by the conservative tracer (~70 cm) over that same time interval. It was likely that strain KC accelerated its migration through the porous media in response to nitrate gradients. This added influence of chemotaxis on the rate of migration of KC cells was approximately 5 cm/day faster than the groundwater flow velocity (10 cm/day). For further evidence of the presence of strain KC, aqueous samples obtained from ports 11 through 25 did not contain any detectable concentrations of nitrate (see Figure 4.6)

indicating the presence of actively denitrifying bacterial population(s), presumably strain KC.

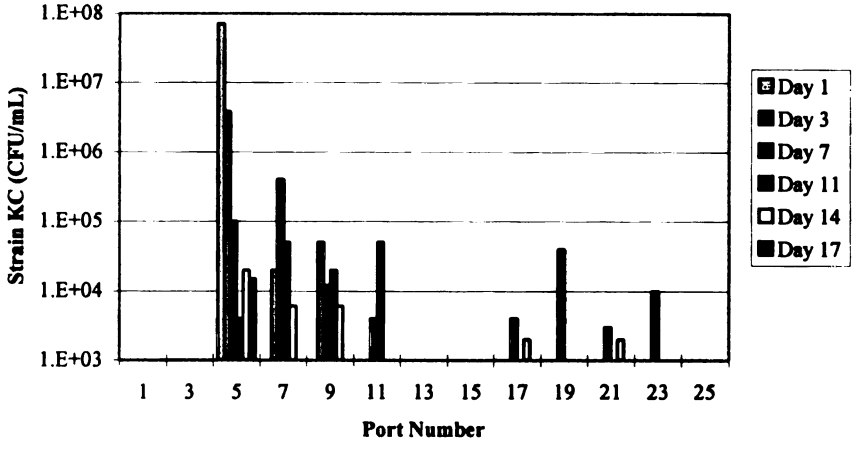

Figure 4.7. Strain KC cell concentrations in aqueous samples obtained from the mobile biocurtain column. Strain KC was not detected in samples obtained from port number locations where bars are not shown.

While the mobility of the strain KC biocurtain has been shown, the ability of the biocurtain to degrade CT can only be evaluated by examining CT concentrations in the entire column. The concentration profiles for CT on days 0 (background), 4, 8, 13 and 18 are shown in Figure 4.8. In addition to the previously mentioned phenomena, results of CT analyses also indicated the presence of strain KC in downstream ports well ahead of the tracer front. This was manifest by the observation of active CT transformation near port 21 by day 8. Further evidence of CT transformation in the liquid phase was evident on days 13 and 18. An overall mass balance on CT in the model aquifer column showed that approximately 55% of the CT in the aqueous phase was transformed by the mobile reaction curtain.

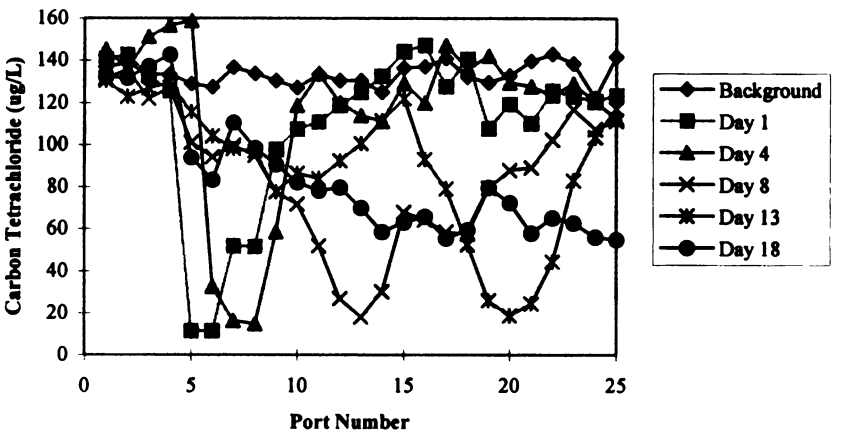

Figure 4.8. Carbon tetrachloride concentration profile in mobile biocurtain column on days 1, 4, 8, 13, and 18.

After the mobile reaction curtain exited the model column, aquifer solids were obtained from all sampling ports on day 20 and analyzed for solid-phase CT and attached strain KC concentrations. Prior to inoculation, the equilibrium CT concentration on the solid phase was approximately 39.5±1.1 μg CT/gram dry solids throughout the column. After the mobile reaction curtain exited the column, approximately 29% of the CT on the solids had been removed downgradient from the slug injection zone.

There was no evidence of the presence of strain KC in soil samples obtained prior to inoculation. After the mobile curtain exited the column, the only detectable concentrations of attached strain KC in the column were found in samples obtained from port 5 (1×10^7 CFU/mL) and port 7 (1×10^5 CFU/mL). The attached strain KC cells, measured 20 days after the single inoculation event, apparently colonized the soil grains in the vicinity of the slug injection zone and were able to withstand the input of pH 7.1 groundwater over that time period. The fact that KC was able to survive in that

environment for 20 days without feeding indicates an ability to endure non-pH-adjusted environments for a prolonged period of time.

The results from the mobile biocurtain column indicate that strain KC cells are indeed motile and are capable of migrating through aquifer material at a rate that exceeds groundwater flow. It was hypothesized that this accelerated movement of cells was due to chemotaxis towards nitrate gradients forming in the column due to rapid nitrate consumption by strain KC bacteria. Research has shown that it is possible for bacteria and bacteria-sized particles to migrate through porous media faster than a conservative tracer such as bromide (Harvey *et al.*, 1989). In this study, evidence was shown that suggests that larger microorganisms transport faster through aquifer material than smaller microorganisms. This observation is supported by colloid filtration theory (Yao *et al.*, 1971), which states that colloids within the bacterial-sized range should sorb to solid surfaces with greater frequency because of their higher rates of diffusion and Brownian motion. Also, colloids in the one micron-size range may transport more rapidly than bromide because of size exclusion. In this case, large cells travel through porous media faster because they only travel through larger pores, whereas smaller molecules travel through all pores. In order to identify the mechanism responsible for the accelerated migration of cells, we proposed an experiment whereby KC cells would be used to inoculate a column where the groundwater flow velocity was zero.

Static column

Strain KC bioaugmentation in the static model column was evaluated using an inoculum cell age of 25 hours. Inoculation was performed by injecting a 320-mL slug of

Schoolcraft groundwater containing $1.2 \pm 0.1 \times 10^8$ KC cells/mL. Figure 4.9 shows the concentration of bromide, a conservative tracer, in the column on days 1, 5, 7, and 26. Minimal diffusion of the bromide from the slug injection zone was observed during the first seven days. Only after 26 days was there evidence of diffusion from the slug injection zone to ports 3 and 8.

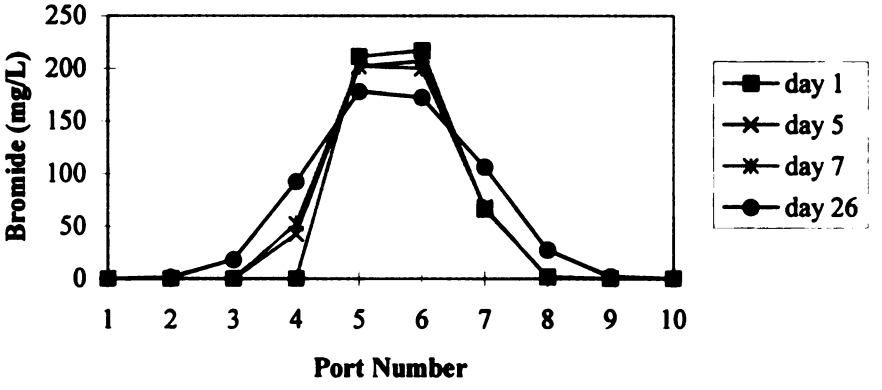

Figure 4.9. Bromide concentrations in the static model column 1 on days 1, 5, 7, and 26.

Figure 4.10 shows the acetate concentration profile in samples obtained on days 1, 5, 7, and 26. The observed behavior of acetate was similar to bromide, with the only difference being acetate was consumed over the duration of the experiment as it served as the electron donor for strain KC. Of the ~151 mg of acetate that was injected into the slug injection zone with the inoculum, 16 mg was consumed over the first two days. After day 2 no significant acetate consumption was measured in the column, presumably due to the absence of nitrate in the vicinity of the acetate slug.

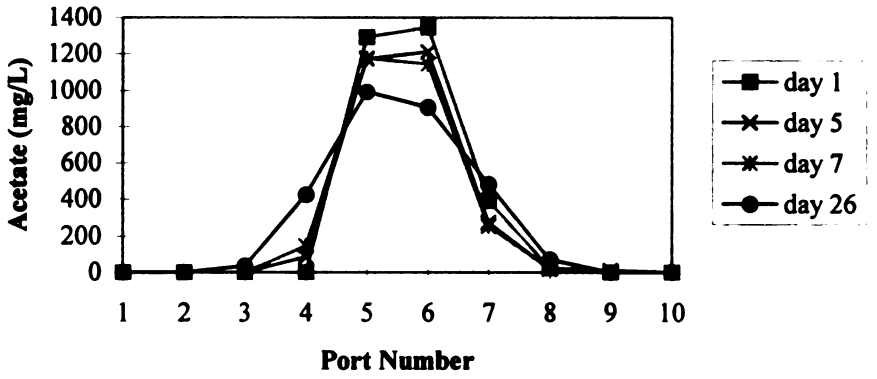

Figure 4.10. Acetate concentrations in the static model column 1 on days 1, 5, 7, and 26.

Figure 4.11 shows the nitrate concentration profile in the static column. The initial concentration of nitrate throughout the column prior to inoculation was near 25 mg/L. One day after inoculation, there was evidence of nitrate depletion in samples obtained from ports 4 through 7, with no detectable concentrations in samples obtained from ports 5 and 6. By day 5, most of the nitrate had been consumed throughout the column. Exceptions were in samples obtained from ports 3 and 9 where concentrations of 12 mg/L and 3 mg/L, respectively, were measured (port 10 sample was destroyed by analytical equipment). After 26 days, the only detectable nitrate concentrations were in samples from ports 9 and 10. It is apparent from these data that an actively denitrifying population(s) migrated from the slug injection zone towards both ends of the column. It was unlikely that the observed nitrate reduction was due to indigenous populations since no carbon source was present near the ends of the column. The results of previous experiments using batch microcosms showed that indigenous populations were unable to reduce nitrate without the addition of an electron donor (data not shown). Strain KC,

however, was likely utilizing endogenous reserves as a source of electrons to complete the reduction of nitrate.

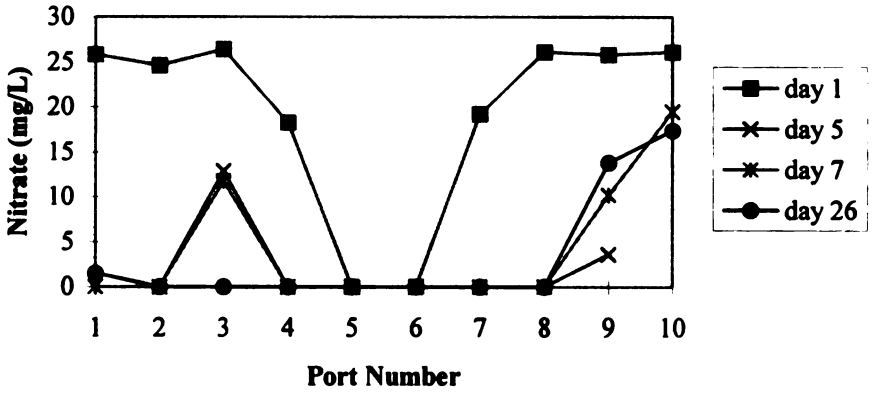

Figure 4.11. Nitrate concentrations in the static model column 1 on days 1, 5, 7, and 26.

Strain KC cells were enumerated in aqueous samples obtained on days 2 and 5. Figure 4.12 shows the results of these enumeration assays. On day two, evidence of high concentrations of KC cells (~10^5 CFU/mL) were observed in ports 3 through 8. By day 5, evidence of detectable concentrations of strain KC were observed in samples from all column ports. Verification of the presence of strain KC throughout the column was measured by using a strain KC-specific DNA probe and performing a PCR assay on samples taken from all sampling ports on day 26. Results of this assay confirmed the presence of strain KC in samples obtained from all sampling ports (1-10). The distance traveled by bacteria to either end of the column from the centrally-located slug injection zone was a minimum of 30 cm. Therefore, the mean velocity of KC cells due to chemotactic movement towards increasing concentrations of nitrate was 5 cm/day. This rate compares favorably with the chemotactic velocity calculated for KC cells in the

mobile biocurtain column (5 cm/day). It is likely that the swimming speed of the cells was faster than 5 cm/day due to the tortuous path that must be taken by each cell to migrate through the porous media.

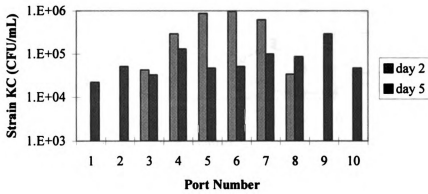

Figure 4.12. Strain KC concentrations in the liquid phase in the static model column 1 on days 2 and 5.

The success of bioremediation using chemotaxis as a tool for cleanup was evaluated by measuring the CT concentration in the static column over the duration of the experiment. Figure 4.13 shows the carbon tetrachloride concentration profile in the column on days 0, 2, 5, 7, and 26. From an initial concentration of ~100 µg/L, CT is rapidly removed in the slug injection zone after two days. Subsequent days (5 and 7) show an increased drop in the CT concentrations measured in all column ports. By day 7, over 70% of the CT in the column had been degraded. Further CT transformation occurred over the following 19 days with concentrations ranging from less than 1 µg/L to a high of 13 µg/L. Therefore, a single inoculation event using strain KC was capable of

removing over 94% of the CT in a one-meter long model column in the absence of advective flow.

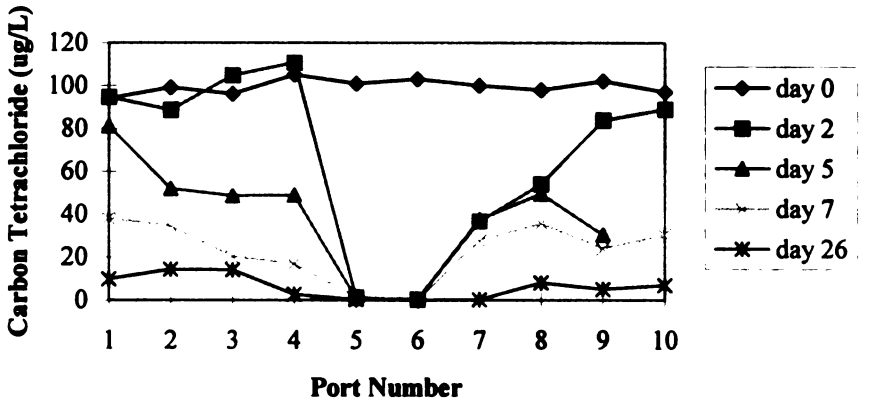

Figure 4.13. Carbon tetrachloride concentrations in the static model column 1 on days 0, 2, 5, 7, and 26.

A second static column was wet-packed and prepared similar to the first static column. Strain KC was injected into the slug injection zone of the column with 3.4±0.4 x 10^7 CFU/mL. Added to the inoculum was 1500 mg/L of one micron fluorescent microspheres. Similar results with respect to acetate and bromide diffusion, CT and nitrate removal, and KC cell migration were observed in the second static column. The purpose of performing this experiment was to verify the experimental results of the first static column and to evaluate the movement, if any, of the one micron-sized spheres relative to bromide and KC cells. The diffusion of the microspheres was similar to that of bromide. Figure 4.14 shows the microsphere concentration profile in the column over a five day period. Therefore, it is evident that strain KC cells have the ability to accelerate their migration through porous media by a chemotactic mechanism. Strain KC cells,

known to be chemotactic towards nitrate, migrated through the static column without the influence of advective flow. It was shown that KC cells migrated in response to the formation of nitrate gradients, and this migration resulted in the movement of KC cells and subsequent CT removal throughout the column.

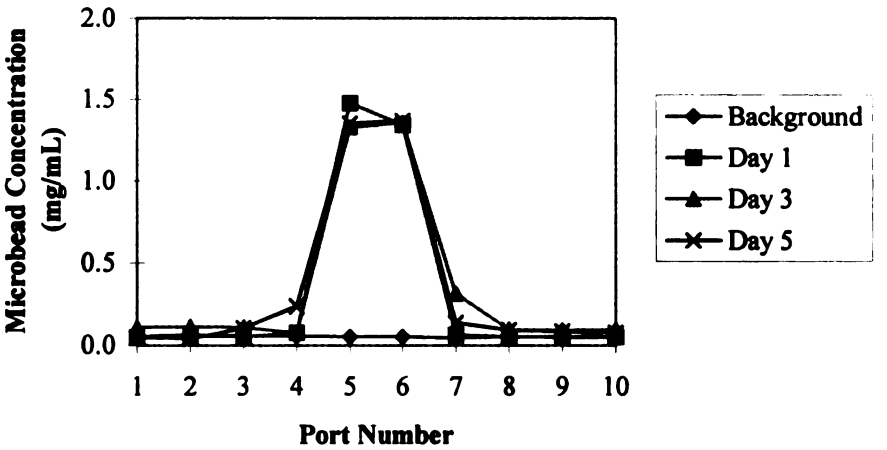

Figure 4.14. Microbead concentration profile in the static model column 2 on days 0, 1, 3 and 5.

We conclude that bioaugmentation using *Pseudomonas stutzeri* KC can be used to establish a mobile biocurtain that migrates through aquifer solids at a rate greater than groundwater flow. In addition, the active biocurtain sustains CT transformation capabilities for extended periods of time. The results of this study indicate that chemotaxis plays an important role in efficient CT transformation by strain KC in saturated porous media.

4.5 Acknowledgments

I gratefully acknowledge the contributions to this chapter by Dr. R. Mark Worden of the Chemical Engineering Department at Michigan State University. His capillary assay experimental results were critical in identifying that strain KC exhibits chemotaxis towards nitrate. Funding for this research was provided by the State of Michigan, Department of Environmental Quality.

4.6 Literature cited

Adler, J. 1966. Chemotaxis in bacteria: motile *Escherichia coli* migrate in bands that are influenced by oxygen and organic nutrients. *Science*. **153**:708-716.

Adler, J. 1973. A method for measuring chemotaxis and use of the method to determine optimum conditions for chemotaxis by *Escherichia coli*. *J. Gen. Microbiol.* **74**:77-91.

Dybas, M.J., M. Barcelona, S. Bezborodnikov, S. Davies, L. Forney, O. Kawka, T. Mayotte, L. Sepulveda-Torres, K. Smalla, M. Sneathen, J. Tiedje, T. Voice, D.C. Wiggert, M.E. Witt, and C.S. Criddle. 1998. Pilot-Scale Evaluation of Bioaugmentation for In-situ Remediation of a Carbon Tetrachloride-Contaminated Aquifer. Submitted for publication to *Environ. Sci. Technol.*

Emerson, D., R.M. Worden, and J.A. Breznak. 1994. A diffusion gradient chamber for studying microbial behavior and deparating microorganisms. *Appl. Environ. Microbiol.* **60**:1269-1278.

Fontes, D.E., A.L. Mills, G.M. Hornberger, and J.S. Herman. 1991. Physical and chemical factors influencing transport of microorganisms through porous media. *Appl. Environ. Microbiol.* **57**:2473-2481.

Harvey, R.W., L.H. George, R.L. Smith, and D.R. LeBlanc. 1989. Transport of microspheres and indigenous bacteria through a sandy aquifer: Results of natural and forced-gradient tracer experiments. *Environ. Sci. Technol.* **23**:51-56.

Jenkins, M.B. and L.W. Lion. 1993. Mobile bacteria and transport of polynuclear aromatic hydrocarbons in porous media. *Appl. Environ. Microbiol.* **59**:3306-3313.

Martin, R.E., L.M. Hanna, and E.J. Bouwer. 1991. Determination of bacteria collision efficiencies in a rotating disk system. *Environ. Sci. Technol.* **25**:2075-2082.

Reynolds, P.J., P. Sharma, G.E. Jenneman, and M.J. McInerney. 1989. Mechanisms of microbial movement in subsurface materials. *Appl. Environ. Microbiol.* **55**:2280-2286.

Rijnaarts, H.H.M., W. Norde, E.J. Bouwer, J.Lyklema, and A.J.B. Zehnder. 1996. Bacterial deposition in porous media related to the clean bed collision efficiency and to substratum blocking by attached cells. *Environ. Sci. Technol.* **30**:2869-2876.

Smith, M.S., G.W. Thomas and R.E. White. 1985. Transport of *Escherichia coli* through intact and disturbed soil columns. *J. Environ. Qual.* **7**:487-494.

Sneathen, M.L. 1996. Theoretical and experimental competitiveness of *Pseudomonas stutzeri* KC. Master's thesis, Department of Civil and Environmental Engineering, Michigan State University, East Lansing, Michigan.

Tatara, G.M., M.J. Dybas, and C.S. Criddle. 1993. Effects of medium and trace metals on kinetics of carbon tetrachloride transformation by *Pseudomonas* sp. strain KC. *Appl. Environ. Microbiol.* **59**:2126-2131.

Yao, K.M., M.T. Habibian, and C.R. O'Melia. 1971. Water and wastewater filtration: concepts and application. *Environ. Sci. Technol.* **5**:1102-1112.

Warren, T.M., V. Williams, and M. Fletcher. 1992. Influence of solid surface, adhesive ability, and inoculum size on bacterial colonization in microcosm studies. *Appl. Environ. Microbiol.* **58**:2954-2959.

Weiss, T.H., A.L. Mills, G.M. Hornberger, and J.S. Herman. 1995. Effect of bacterial cell shape on transport of bacteria in porous media. *Environ. Sci. Technol.* **29**:1737-1740.

Widman, M.T., D. Emerson, C.C. Chiu, and R.M. Worden. 1997. Modeling microbial chemotaxis in a diffusion gradient chamber. *Biotechnol. Bioeng.* **55**:191-205.

Widman, M.T. 1997. Engineering applications of microbial chemotaxis. Doctoral dissertation, Deparment of Chemical Engineering, Michigan State University, East Lansing, Michigan.

Witt, M.E., M.J. Dybas, D.C. Wiggert, and C.S. Criddle. 1998. Use of bioaugmentation to create a biocurtain capable of long-term, continuous removal of carbon tetrachloride in model aquifer columns. Submitted for publication to *Environ. Sci. Technol.*

Wollum, A.G.I. and D.K. Cassel. 1978. Transport of microorganisms in sand columns. *Soil Sci. Am. J.* **42**:72-76.

Chapter 5

NUMERICAL SIMULATION OF CHEMOTAXIS AND CARBON TETRACHLORIDE TRANSFORMATION IN A STATIC MODEL AQUIFER COLUMN

5.1 Abstract

Pseudomonas stutzeri KC is a natural aquifer isolate that rapidly transforms carbon tetrachloride to carbon dioxide and nonvolatile end products without the production of chloroform. Laboratory experiments were performed in a model aquifer column to characterize the enhanced motility of strain KC in aquifer sediments. After inoculation with strain KC and addition of nutrients, carbon tetrachloride (CT) was transformed in an 85 cm-long column operated in the absence of groundwater flow. A carbon tetrachloride removal efficiency of 94% was achieved after 26 days without the production of chloroform.

A computer model was developed from a system of six one-dimensional mass balance equations to simulate KC migration and CT transformation in a model aquifer column. The model was developed to predict liquid and solid-phase concentrations of CT, attached and planktonic strain KC, acetate, and nitrate as functions of time in the model column. The computer model accurately predicted strain KC migration, CT degradation, and acetate and nitrate utilization.

5.2 Introduction

Carbon tetrachloride (CT), once widely used as a solvent and degreasing agent, is a common groundwater contaminant found throughout the world. Significant amounts of

money have been invested in remediating CT-contaminated groundwater by conventional means. This has been achieved by pumping the contaminated groundwater to the surface and stripping CT into the air, a method that is costly and time-consuming because large amounts of groundwater must be extracted to achieve the desired removal efficiency from the solids and the groundwater.

A potentially less costly alternative to extraction and air-stripping is *in-situ* bioremediation (Quinton *et al.*, 1997). Bioremediation involves transformation of target compound(s) by stimulating indigenous microbes (biostimulation) or by adding non-indigenous microbes (bioaugmentation). Biostimulation is usually preferred because it does not require transport of non-indigenous organisms and avoids the ecological challenges associated with addition of non-native organisms. However, biostimulation does not always have a favorable result. For CT transformation, chloroform is a common endproduct of biostimulation under anoxic conditions (Criddle *et al.*, 1990; Egli *et al.* 1987 and 1988; and Semprini *et al.*, 1992). A potential advantage of bioaugmentation is that the introduced organism and the transformation it mediates can be studied and optimized in the laboratory. This can facilitate pathway control, ensuring detoxification of the target contaminant. A potential drawback of bioaugmentation is competition between indigenous microflora and the added microorganisms. A method of overcoming this obstacle is to create conditions that favor the added organism. This method of habitat or "niche" adjustment provides conditions that favor the growth of the non-indigenous microbe. A niche is defined as "the combined description of the physical habitat, functional role, and interactions of the microorganisms occurring at a given location" (Atlas and Bartha, 1993). For *Pseudomonas stutzeri* KC, a specialized functional role

that can be exploited to ensure survival of strain KC is its capacity for iron-scavenging. This role becomes more important at slightly elevated pH (8.0 to 8.3). Adjustment of pH to 8.0-8.3 therefore provides a competitive advantage for organisms that possess efficient iron-scavenging systems and can occupy the iron-scavenging niche.

Numerous experiments have evaluated the mechanism by which strain KC transforms CT (Tatara *et al.*, 1993, and Dybas *et al.*, 1995). These experiments indicate that CT transformation is controlled by the availability of iron. Even in iron-rich groundwater and soils inoculated with strain KC, CT transformation can be achieved by raising the pH of the groundwater and soil materials to 8.0-8.3 (Tatara *et al.*, 1993), a range where ferric iron solubility is lowest (Stumm and Morgan, 1981). Dybas *et al.* (1995) investigated the complex mechanism responsible for CT transformation and determined that a plausible model involves: (1) production and export of a CT-transforming factor(s) from the KC cell in response to iron limitation, (2) deactivation of the factor(s) upon transformation of CT, and (3) reactivation of the factor(s) at the cell membrane. Evidence suggests that production and export of this CT-transforming factor from the cell in response to iron-limitation, along with reactivation of the factor by viable cells after transformation of CT, is the mechanism that enables strain KC to degrade CT. The secreted factor is produced during periods of rapid-growth and is re-activated by a wide variety of organism types (Tatara, 1996).

The maximum specific growth rate for strain KC at pH 8.2 is approximately 3.12 day^{-1} compared to 0.81 day^{-1} for indigenous flora (Knoll, 1994). However, in the conversion of nitrite to gaseous endproducts, indigenous Schoolcraft flora have a maximum specific growth rate approximately three times that of strain KC at pH 8.2

(0.67 day^{-1} and 0.23 day^{-1}, respectively). Therefore, the overall conversion of nitrate to gaseous endproducts during the denitrification process is likely a two-step process with strain KC responsible for nitrate reduction and indigenous flora for nitrite reduction.

In the static model aquifer column described in Chapter 4, a zone of CT transformation formed near the slug injection zone immediately after inoculation. In this chapter, a computer model is presented which simulates the numerous processes occurring in the model column after inoculation. This one-dimensional numerical model simulates substrate use, cell growth and motility, and CT degradation in the absence of advective flow. A FORTRAN computer program was written to simultaneously solve a system of six mass-balance convective-dispersion-motility equations for concentrations of acetate, nitrate, CT (in both the liquid and solid phases), and strain KC (in both the liquid and solid phases). A comparison of the results of the computer model with experimental data suggests that cell chemotaxis may play an important role in ensuring a more uniform cell distribution and higher CT removal efficiencies.

5.3 Development of an energy model

In order to accurately describe the effects of motility on growth and maintenance of bacterial cells, a model was developed in which energy production from catabolism and endogenous respiration is consumed by energy requirements for cell growth, maintenance, and motility. The model presented here expands on a model developed by Beeftink *et al.* (1990). Figure 5.1 illustrates the various rates of production and consumption of ATP as they influence the growth and maintenance of motile and non-motile cells. Symbols for this model are defined in Table 5.1.

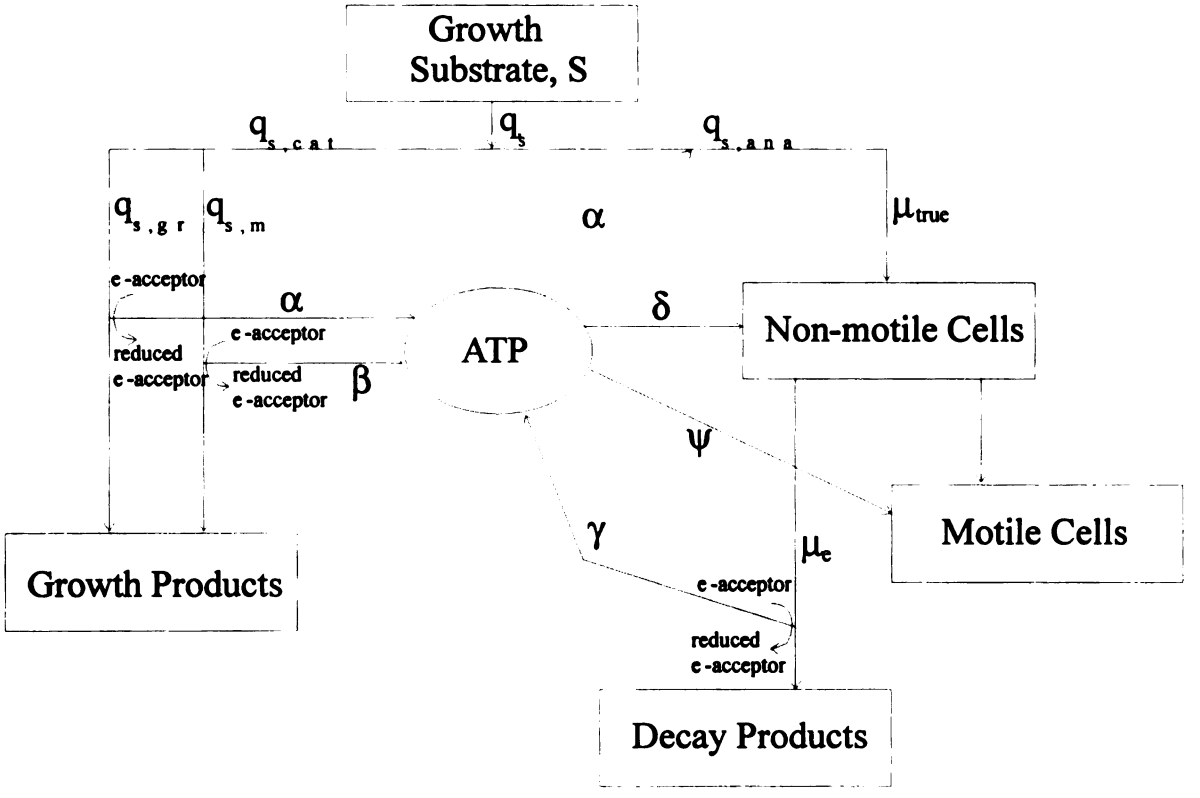

Figure 5.1. Energy model diagram.

In the proposed model, the observed specific growth rate of KC cells associated with substrate utilization (μ_{obs}) is equal to the true specific growth rate (μ_{true}) minus the specific endogenous decay rate (μ_e):

$$\mu_{obs} = \mu_{true} - \mu_e \tag{5.1}$$

Table 5.1. Definitions of symbols used in the development of an energy model.

Symbol	Definition	Units
q_s	specific substrate utilization rate	mg substrate/mg cell-day
$q_{s,\,cat}$	specific substrate utilization rate for catabolism	mg substrate/mg cell-day
$q_{s,\,ana}$	specific substrate utilization rate for anabolism	mg substrate/mg cell-day
$q_{s,\,gr}$	specific substrate utilization rate for growth	mg substrate/mg cell-day
$q_{s,\,m}$	specific substrate utilization rate for catabolic maintenance	mg substrate/mg cell-day
μ_e	specific endogenous decay rate	mg cell/mg cell-day
μ_{obs}	observed specific growth rate	mg cell/mg cell-day
μ_{true}	true specific growth rate	mg cell/mg cell-day
α	growth-related specific ATP production rate	moles ATP/mg cell-day
β	maintenance-related specific ATP production rate from substrate degradation	moles ATP/mg cell-day
δ	maintenance-related specific ATP consumption rate	moles ATP/mg cell-day
γ	specific ATP production rate from biomass decay	moles ATP/mg cell-day
ψ	motility-related specific ATP consumption rate	moles ATP/mg cell-day

The specific rate of substrate utilization, q_s, is equal to the specific rate of substrate utilization for energy production, $q_{s,cat}$, plus the specific rate of substrate utilization for cell synthesis, $q_{s,\,ana}$. The specific rate of substrate utilization for energy production, $q_{s,cat}$, is further defined as the sum of the specific utilization rates for growth and maintenance, $q_{s,gr}$ and $q_{s,m}$. Therefore, the specific substrate utilization rate is given by:

$$q_s = q_{s,gr} + q_{s,m} + q_{s,ana} \tag{5.2}$$

The sum of the specific rates of substrate utilization for growth ($q_{s,gr}$) and anabolism ($q_{s,ana}$) is equal to the true specific growth rate (μ_{true}) divided by the yield of cells on substrate ($Y_{s,x}$).

$$q_{s,gr} + q_{s,ana} = \frac{\mu_{true}}{Y_{s,x}} \tag{5.3}$$

Substituting 5.3 into 5.2 gives:

$$q_s = \frac{\mu_{true}}{Y_{s,x}} + q_{s,m} \tag{5.4}$$

Both $q_{s,gr}$ and $q_{s,m}$ generate ATP, resulting in specific rates of ATP production α and β, respectively, where:

$$\alpha = Y_{cat,ATP} \cdot q_{s,gr} \tag{5.5}$$

$$\beta = Y_{cat,ATP} \cdot q_{s,m} \tag{5.6}$$

where $Y_{cat,ATP}$ is the moles of ATP produced per unit mass of substrate oxidized for energy. ATP produced by growth-associated catabolism at a specific rate of α is used in the production of biomass at a specific rate of μ_{true}, as suggested by Eq. 5.3.

The proposed model also includes terms for ATP consumption for maintenance (δ), ATP consumption for cell motility (ψ), and ATP production from endogenous respiration (γ). A balance on maintenance energy supply and demand yields:

$$\delta + \psi = \beta + \gamma \tag{5.7}$$

where the left side of the equation is the energy demanded or consumed, and the right side is energy supplied or generated. A central assumption is that at high concentrations of substrate, the energy for maintenance and cell motility is obtained by substrate oxidation alone, and not by oxidative decay of biomass (endogenous respiration). Mathematically, this assumption can be expressed as:

$$\beta = (\delta + \psi) M \tag{5.8}$$

where M is a saturation term such as the saturation term of the Monod equation:

$$M = \frac{S}{K_s + S} \tag{5.9}$$

Here, K_s is equal to the half-saturation coefficient. Rearranging Eq. 5.7 and substituting Eq. 5.8 for β yields:

$$\gamma = (\delta + \psi)(1 - M) \tag{5.10}$$

The specific rate of ATP production from endogenous decay, γ, is equal to the product of the moles of ATP produced by cell oxidation, $Y_{x,ATP}$, and μ_e. Therefore, an expression for μ_e can be written as:

$$\mu_e = \frac{\gamma}{Y_{x,ATP}} = \frac{(\delta + \psi)(1 - M)}{Y_{x,ATP}} \tag{5.11}$$

Since μ_{true} includes substrate effects on μ but neglects the effects of decay, it is equal to:

$$\mu_{true} = \mu_{max} M \tag{5.12}$$

Another expression for μ_{true} can be derived for a dual-substrate limitation by performing a balance on the growth-related specific ATP production rate. From Figure 5.1, ATP used for cell synthesis is equal to:

$$\alpha = \mu_{true} Y_{x,ATP} \tag{5.13}$$

and the ATP produced is equal to:

$$\alpha = Y_{cat,ATP} q_{s,gr} M_n \tag{5.14}$$

where M_n is saturation term for the electron acceptor (in this case, nitrate) shown as:

$$M_n = \frac{C_n}{K_{s,n} + C_n} \tag{5.15}$$

Combining Eqs. 5.13 and 5.14 gives the following expression for μ_{true}:

$$\mu_{true} = \frac{Y_{cat,ATP}}{Y_{x,ATP}} q_{s,gr} M_n \tag{5.16}$$

Defining μ_{max} as a function of $Y_{cat,ATP}$, $Y_{x,ATP}$, and k (substrate utilization rate):

$$\mu_{\max} = \frac{Y_{cat,ATP}}{Y_{x,ATP}} k \tag{5.17}$$

and $q_{s,gr}$ as the product of k and M_s, where M_s is a saturation term for the growth substrate (in this case, acetate) results in the following equation for μ_{true}:

$$\mu_{true} = \mu_{max} M_n M_s \tag{5.18}$$

Equation 5.18 defines the true specific growth rate of bacterial cells under conditions of multiple substrate limitation. An expression for μ_{obs} is then obtained by combining Eqs. 5.11 and 5.18:

$$\mu_{obs} = \mu_{\max} M_n M_s - \frac{\delta}{Y_{x,ATP}}(1 - M_s) - \frac{\psi}{Y_{x,ATP}}(1 - M_s) \qquad (5.19)$$

The specific rate of endogenous decay, b, is given by δ divided by $Y_{x,ATP}$. In addition, ψ can be defined as the product of $Y_{mot,ATP}$ (moles of ATP required for cell motility) and V, the swimming speed of the cells. These simplifications can be applied to equation 5.13 to give the following equation for μ_{obs}:

$$\mu_{obs} = \mu_{\max} M_n M_s - b\,(1 - M_s) - \frac{Y_{mot,ATP} V}{Y_{x,ATP}}(1 - M_s) \qquad (5.20)$$

Equation 5.20 describes the specific growth rate of cells as a function of the growth substrate concentration, electron acceptor concentration, maximum specific growth rate, the rate of endogenous decay, and the velocity of motile cells. These terms were incorporated into mass-balance equations describing temporal changes in planktonic strain KC, acetate, and nitrate. Description of the six equation model is provided in the following section. Derivation of the reaction terms in each of models are shown in Appendix G.

5.4 Development of mass balance equations

Mass balance equations were derived to describe the change in concentration of each of the variables involved with CT transformation by strain KC, including the concentrations of acetate, nitrate, CT and strain KC. The equations presented in this chapter are based on mass-balance equations previously developed by Witt *et al.* (1995). It was assumed that CT is transformed by both mobile and stationary cells, and that CT transformation is first order with respect to concentration of cells and first order with respect to CT concentration. It was also assumed that a partial equilibrium exists between the CT concentration in the liquid phase and the solid phase, with desorption limitations on the remaining sorbed CT (Zhao *et al.*, 1998). Utilization kinetics for acetate, the electron donor, are assumed to obey Monod saturation kinetics. Finally, specific rates of attachment and detachment are described by first order rate expressions, with the assumption that detachment increases for fast-growing cells.

$$\frac{\partial C_{CT}}{\partial t} = \frac{D_{CT}}{R_{CT}}\frac{\partial^2 C_{CT}}{\partial x^2} - \frac{k' C_{CT}}{R_{CT}}\left(X_{KC} + \overline{X}_{KC}\right) - \frac{\rho_b \kappa}{n R_{CT}}\left[(1-f)K_d C_{CT} - S_{CT}\right] \quad (5.21)$$

$$\frac{\partial X_{KC}}{\partial t} = \omega_{eff} M_n \frac{\partial^2 X_{KC}}{\partial x^2} - \left(\chi_{o,eff}\frac{k_{rc}}{\left(k_{rc}+C_n\right)^2}\frac{\partial C_n}{\partial x}\right)\frac{\partial X_{KC}}{\partial x} + K_{de} M_s \overline{X}_{KC} \quad (5.22)$$
$$+\left[\mu_{\max} M_n M_s - b_{KC}(1-M_s) - Z_{KC}\left(V_{\max} M_s'\right)(1-M_s) - K_{at}\right]X_{KC}$$

$$\frac{\partial C_a}{\partial t} = \frac{D_a}{R_a}\frac{\partial^2 C_a}{\partial x^2} - \frac{\mu_{\max} M_n M_s}{Y_a R_a}\left(X_{KC} + \overline{X}_{KC}\right) - Z_{ac,1} M_s\left(X_{KC} + \overline{X}_{KC}\right) \quad (5.23)$$
$$- Z_{ac,2}\left(V_{\max} M_s'\right)(1-M_s)X_{KC}$$

$$\frac{\partial \overline{X}_{KC}}{\partial t} = \left[\mu_{\max} M_n M_s - b_{KC}(1 - M_s) - K_{de} M_s\right]\overline{X}_{KC} + K_{at} X_{KC} \tag{5.24}$$

$$\frac{\partial C_n}{\partial t} = \frac{D_n}{R_n}\frac{\partial^2 C_n}{\partial x^2} - \frac{\mu_{\max} M_n M_s}{Y_n R_n}\left(X_{KC} + \overline{X}_{KC}\right) - \frac{b_{KC}}{Y_{nb} R_n}(1 - M_s)\left(X_{KC} + \overline{X}_{KC}\right) - Z_{nit}\left(V_{\max} M_s'\right)(1 - M_s) X_{KC} \tag{5.25}$$

$$\frac{\partial S_{CT}}{\partial t} = \kappa\left[(1 - f) K_d C_{CT} - S_{CT}\right] \tag{5.26}$$

In the above expressions, C_{CT} and S_{CT} are the carbon tetrachloride concentrations in the aqueous and solid phases, respectively; X_{KC} and $\overline{X}_{KC}$ are the concentrations of strain KC in the aqueous and solid phases, respectively; C_a is the concentration of acetate in the aqueous phase; and C_n is the concentration of nitrate in the aqueous phase. V_{max} is the maximum one-dimensional cell swimming speed and M_s' is the Monod saturation term for growth substrate. This term, M_s', is assumed to be equal to one since it was likely that sufficient electron donor was available to the KC cells in the absence of acetate. Stored cell carbon and soil organic carbon would likely have been a source for electrons in the experimental system.

The second-order spatial derivatives in Eqs. 5.21, 5.22, 5.23, and 5.25 describe the diffusion of liquid-phase CT, mobile cells, acetate, and nitrate, respectively. The first-order spatial derivative in Eq. 5.22 describes the advective movement of strain KC cells due to bacterial chemotaxis. This expression is discussed in section 1.6 of this dissertation. The remaining terms in these four equations are reaction terms.

Equation 5.24 does not contain an advection or dispersion term because it describes attached cells. The only terms required for this case are for growth, decay, detachment, and attachment of planktonic cells.

The first reaction term in Eq. 5.21 describes the degradation of CT, which is assumed to be first-order with respect to CT concentration and first-order with respect to the concentration of strain KC (Tatara *et al.*, 1993). The second reaction term describes sorption of CT onto the solid phase and desorption of CT into the liquid phase (Zhao *et al.*, 1998).

In Eq. 5.22, terms are included for detachment of attached cells, growth and decay of planktonic cells (including "decay" caused by cell motility), and attachment of planktonic cells. For Eq. 5.23, the reaction terms include utilization of the electron donor for growth, maintenance, and motility. Equation 5.25 includes terms for utilization of the electron acceptor for growth, endogenous decay, and motility. The only term in Eq. 5.26 is a term describing sorption of aqueous-phase CT and desorption of solid-phase CT. Other input parameters used in the system of mass-balance equations are defined in Table 5.2, along with their input values and source.

5.5 Numerical simulation

The six mass balance equations were solved numerically using the Quickest finite-difference spatial discretization form combined with an Euler approximation in the time domain (Leonard, 1979; and Chapra and Canale, 1988). The Quickest formulation is detailed in Appendix H. Because the computer simulation used a forward-stepping

Table 5.2. Input variable values used in the numerical simulation.

Input Parameters	Definition	Value	Procedure	Source
b_{KC}	Decay rate, day^{-1}	0.1	estimated	Tchobanoglous and Burton (1991)
χ_o	Chemotactic sensitivity coefficient, cm^2/day	6.0	estimated	Widman (1997)
D	Dispersion, cm^2/day	0.075	measured	Witt
f	Fraction of exchange sites at equilibrium	0.12	measured	Zhao *et al.* (1998)
K_{at}	Attachment rate, day^{-1}	0.9	measured	Radabaugh (1998)
K_d	Distribution coefficient, L/mg	2.6×10^{-7}	measured	Zhao *et al.* (1998)
K_{de}	Detachment rate, day^{-1}	0.018	measured	Radabaugh (1998)
K_s	Half-saturation coefficient, mg/L			
	Acetate, $K_{s,a}$	1.0	estimated	
	Nitrate, $K_{s,n}$	12.0	measured	Knoll (1994)
k'	Second order rate coefficient, L/mg-day	2.7	measured	Tatara (1996)
k_{rc}	Dissociation constant for the chemoattractant-receptor complex, mg/L	1.0	estimated	Ford and Lauffenburger (1991)
κ	First-order kinetic rate coefficient for desorption, day^{-1}	0.6	measured	Zhao *et al.* (1998)
μ_{max}	Maximum specific growth rate, day^{-1}	2.0	measured	Sneathen (1996)
n	Sediment porosity	0.32	measured	Witt
ω	Random motility coefficient, cm^2/day	60	estimated	Schmidt *et al.* (1996)
R	Retardation coefficient			
	Carbon tetrachloride	2.3	measured	Zhao *et al.* (1998)
	Acetate	1.0	measured	Witt
	Nitrate	1.0	measured	Witt
ρ_b	Soil bulk density, mg/L	1.59×10^6	measured	Zhao *et al.* (1998)
τ	Tortuosity	2.0	estimated	Duffy *et al.* (1995)
V_{max}	Maximum cell swimming speed, cm/day	3.5	estimated	Ford
Y	Yield, mg cells/mg substrate			
	Acetate, Y_a	0.4	measured	Knoll (1994)
	Nitrate, Y_n	0.25	measured	Knoll (1994)
	Biomass, Y_{nb}	0.46	estimated	stoichiometry
Z_{KC}	Decay coefficient related to motility, day^{-1}	0.13	estimated	see Appendix G
$Z_{ac,1}$	Maintenance coefficient for acetate, day^{-1}	0.99	estimated	see Appendix G
$Z_{ac,2}$	Motility coefficient for acetate, mg acetate/mg cell-day	0.23	estimated	see Appendix G
Z_{nit}	Motility coefficient for nitrate, mg nitrate/mg cell-day	0.32×10^5	estimated	see Appendix G

numerical scheme, the model assumed that the static column was half its actual length, and that the injection zone (for strain KC and acetate) was at one end of the column. The response for the entire column was then obtained by symmetry.

The numerical solution incorporated initial and boundary conditions for each of the mass balance equations. The initial conditions specified that the concentration of each of the parameters along the length of the column was equal to the concentration measured in the laboratory-scale model aquifer column. Boundary conditions were also specified. Neumann boundary conditions were specified at both the proximal and distal ends of the column. This type of boundary condition essentially assumes that the gradient across the boundary is zero.

The system of six mass-balance equations together with the initial and boundary conditions comprised the numerical model used to predict the six model variable concentrations. The code was written in FORTRAN language and executed using Microsoft FORTRAN PowerStation 4.0. The time step, Δt, for the time derivative and the distance step, Δx, for the spatial derivatives were 0.001 day and 1 cm, respectively. The numerical results predicted by the model were based on explicit numerical formulations. The computer program simulated processes in the static model aquifer column for 26 days and predicted concentrations along one-half the length of the column (43 cm). Since predictions were only calculated for one-half of the model column, predicted concentrations were plotted and a mirror-image was constructed to compare with experimental results for the entire length of the model column.

5.6 Results and discussion

The computer model simulated strain KC growth and chemotaxis, acetate and nitrate utilization, and CT degradation within the static model aquifer column. The model included initial injection concentrations of strain KC and acetate of 20 and 1533 mg/L, respectively. Experimental data were obtained from the model aquifer column at position numbers 8, 16, 24, 32, 40, 46, 54, 62, 70, and 78. The numerical results predicted by the computer model compared well with experimental data.

The numerical predictions of planktonic strain KC are close to the experimental values measured in the laboratory. Figure 5.2 shows the predicted and experimental values for static column 1 on day 2. The model prediction is shown by the solid line and the experimental data are shown by the squares. On day 2, the model slightly over-predicted the measured strain KC concentration in the column (between positions 15 and 70), however the general trend of the KC concentration profile was captured by the numerical prediction. Strain KC was not detected in samples from positions 8, 16, 70, and 78.

Experimental and predicted strain KC concentrations on day 5 are shown in Figure 5.3. The model accurately predicted strain KC concentration throughout the length of the column. The two "shoulders" of strain KC concentration, as predicted by the model near positions 10 and 75, represent the bulk of the mobile wave of strain KC migrating through the column presumably in response to the nitrate gradient. The high concentration of planktonic KC cells predicted between position numbers 35 and 50 is likely due to the detachment of attached KC cells in the region where the KC cells were introduced.

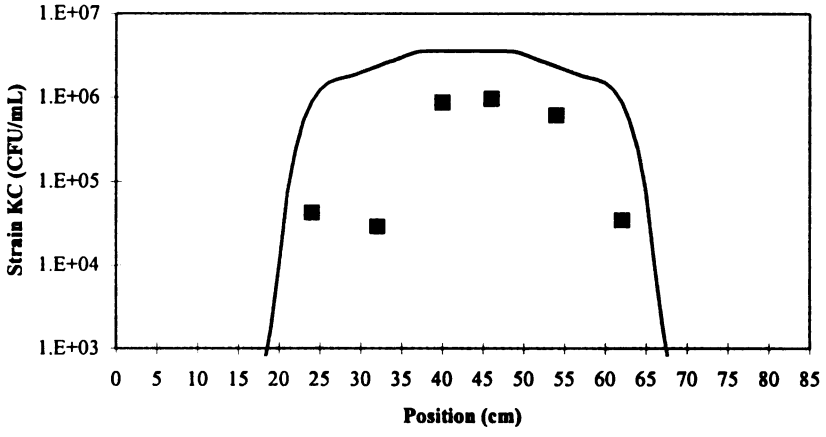

Figure 5.2. Predicted vs. measured planktonic strain KC concentrations in the static model aquifer column on day 2. No strain KC was detected in samples from positions 8, 16, 70, and 78.

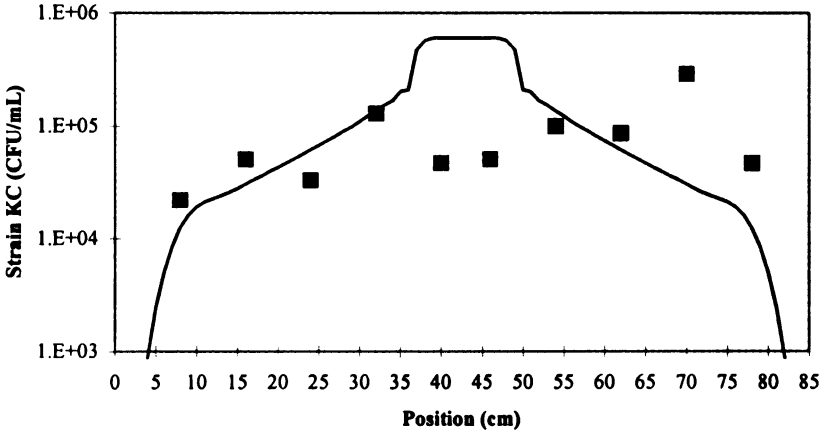

Figure 5.3. Predicted vs. measured planktonic strain KC concentrations in the static model aquifer column on day 5.

Figures 5.4 through 5.6 show the predicted and experimental nitrate concentrations on days 2, 5, and 7, respectively. On day 2, the model over-predicts nitrate consumption, likely a result of the over-prediction of planktonic strain KC

concentrations (see Figure 5.2). On day 5 the model predicted that the nitrate concentration throughout the length of the column was zero, indicating that strain KC had migrated to both ends of the column and consumed all of the nitrate in five days. However, detectable concentrations of nitrate were measured near position numbers 24 and 70 (ports 3 and 9). The existence of "dead zones", or regions where strain KC was not physically able to migrate into, may explain this experimental observation. In fact, on day 7, samples obtained from the sampling ports 3 and 9 still contained nitrate at concentrations near 10 mg/L. Measured values of nitrate on day 26 throughout the length of the column were at or near zero.

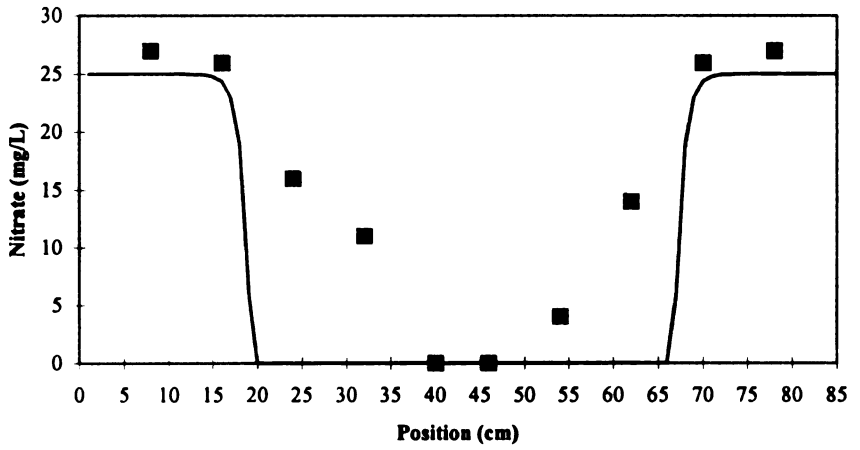

Figure 5.4. Predicted vs. measured nitrate concentrations in the static model aquifer column on day 2.

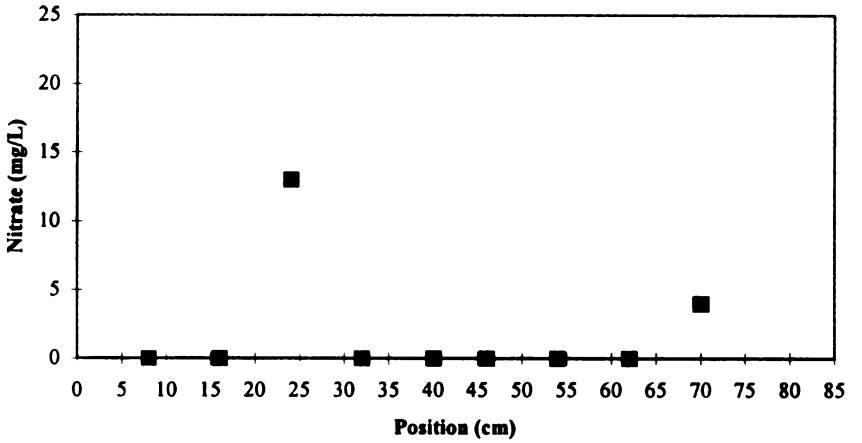

Figure 5.5. Predicted vs. measured nitrate concentrations in the static model aquifer column on day 5. The model predicts that the nitrate concentration throughout the length of the column is zero.

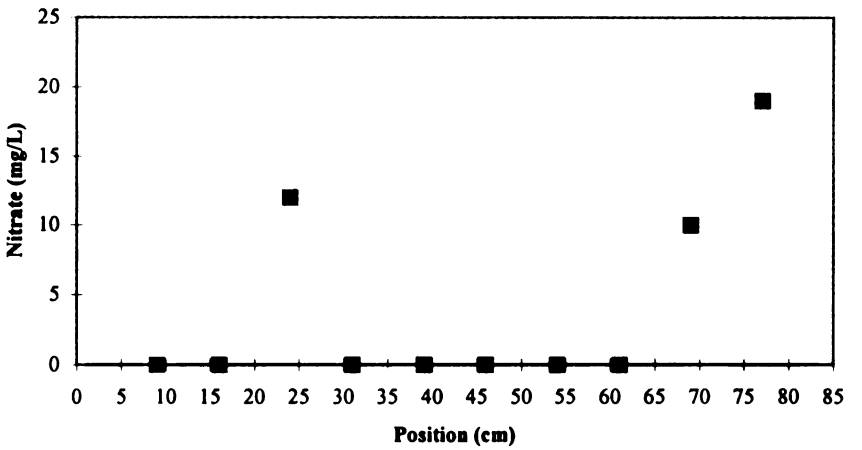

Figure 5.6. Predicted vs. measured nitrate concentrations in the static model aquifer column on day 7. The model predicts that the nitrate concentration throughout the length of the column is zero.

Figures 5.7 through 5.10 show numerical predictions and experimental values for aqueous-phase CT in the model column on days 2, 5, 7, and 26, respectively. On day 2,

the predicted CT concentration profile was similar to the measured values. The measured CT concentrations in one end of the column, near positions 60 through 80, were slightly lower than the model predictions. It is possible that low concentrations of strain KC migrated to this end of the column by preferential flow paths (i.e. macropores), thus resulting in a low level of CT degradation.

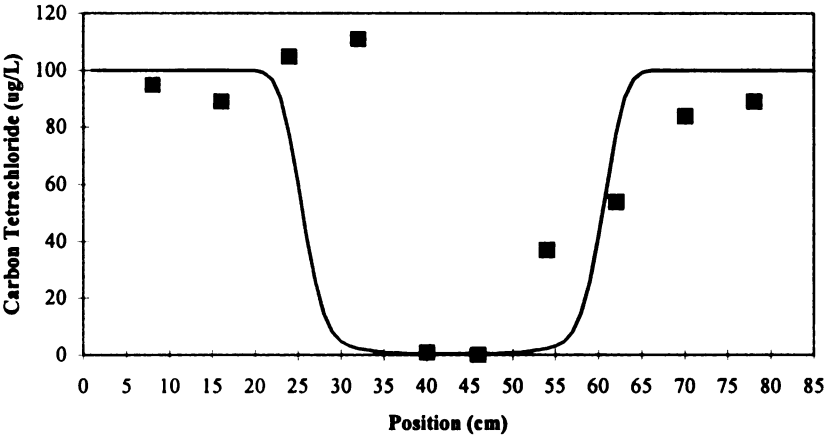

Figure 5.7. Predicted vs. measured carbon tetrachloride concentrations in the static model aquifer column on day 2.

On day 5, the experimental and predicted values for CT concentration do not compare well (see Figure 5.8). The model predicted that the CT concentration in the region between positions 25 and 60 was near zero, while some experimentally measured values were in excess of 40 µg/L. Heterogeneity within the model aquifer column could explain less efficient CT removal in some regions compared to others. Slow desorption of CT from the solid phase may also have elevated the concentration of CT in the liquid phase after the mobile wave of strain KC moved through. As the mobile wave of strain

KC migrated away from the slug injection zone, it may have moved at a rate that was too fast for desorption and transformation of sorbed CT.

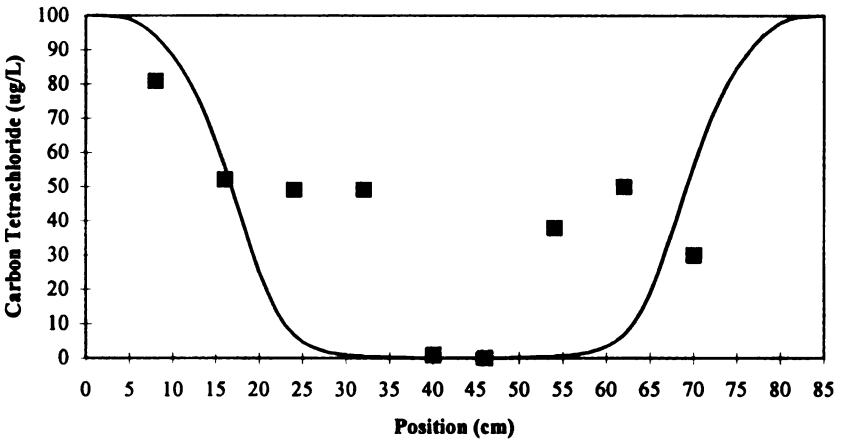

Figure 5.8. Predicted vs. measured carbon tetrachloride concentrations in the static model aquifer column on day 5.

Figure 5.9 shows the predicted and experimental CT concentrations in the model aquifer column on day 7. As observed on day 5, elevated CT concentrations were measured between positions 25 and 60, a region in which the model predicted CT concentrations near zero. In addition, measured CT concentrations at the extreme ends of the column were much lower than predicted. Again, heterogeneity may play a role in explaining these observations. Low concentrations of strain KC at the extreme ends of the column might result in CT transformation at positions 8 and 78 (ports 1 and 10). The elevated concentrations of CT in the central portion of the column may have resulted from desorption of CT from the solid phase into the liquid phase. Also, in the absence of actively growing KC cells (no electron acceptor was present), CT transformation rates would be lower than the rates observed for growing cells.

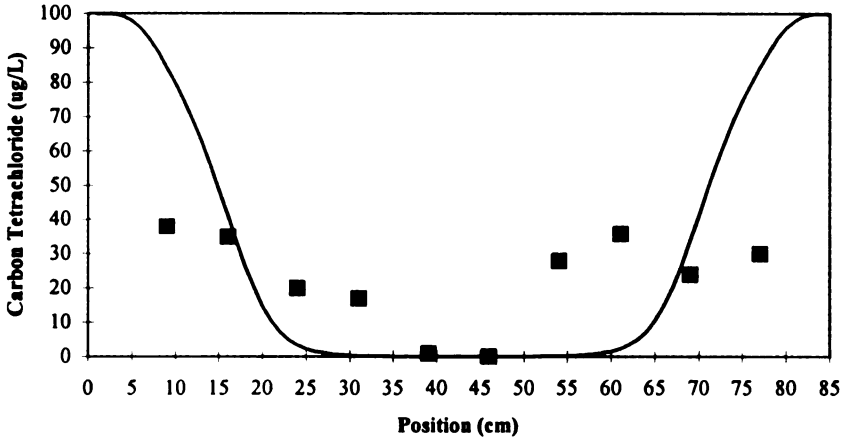

Figure 5.9. Predicted vs. measured carbon tetrachloride concentrations in the static model aquifer column on day 7.

Figure 5.10 shows the measured values of CT in the model column on day 26. The computer model predicted that CT concentrations throughout the length of the model column were zero after 26 days. The measured CT remaining in the column was a result of the inefficiency of strain KC at completely removing all CT. Nevertheless, between the date of inoculation and day 26, strain KC degraded over 94% of the CT that was originally present within the column.

Figures 5.11 through 5.14 show the predicted and measured acetate concentration profiles in the model aquifer column on days 2, 5, 7, and 26, respectively. Comparison of the predicted and measured values shows that the numerical model was quite accurate at predicting the diffusion and consumption of acetate during the static column experiment. However, on day 2, the experimentally measured values were slightly higher than predicted values near positions 32 and 54. It was likely that during each sampling event, groundwater containing acetate from the slug injection zone was drawn closer to sampling ports 4 and 7 (positions 32 and 54, respectively) by the removal of an analytical

sample. This may explain why the observed diffusion of acetate was greater than what the numerical model predicted for days 2, 5, 7, and 26.

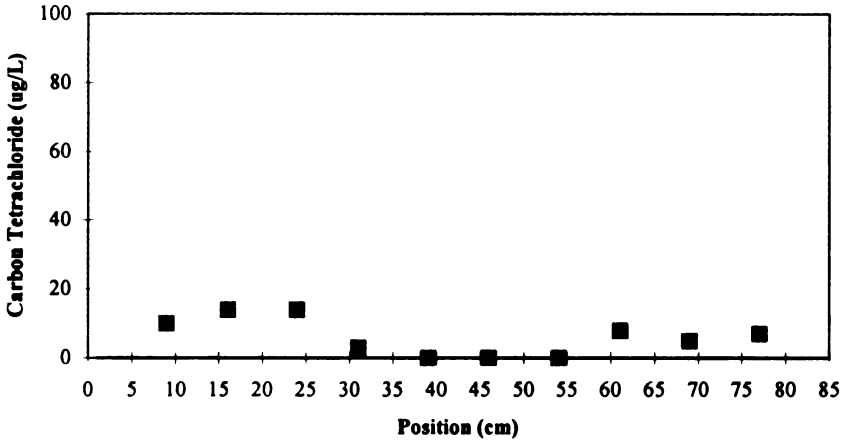

Figure 5.10. Predicted vs. measured aqueous-phase carbon tetrachloride concentrations in the static model aquifer column on day 26.

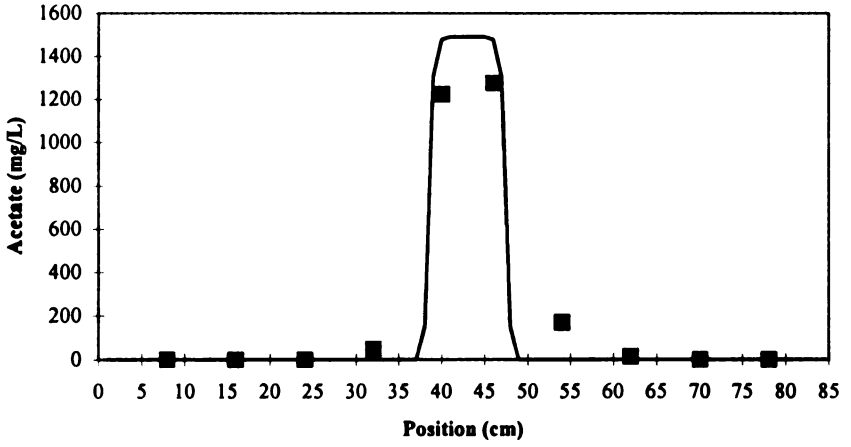

Figure 5.11. Predicted vs. measured acetate concentrations in the static model aquifer column on day 2.

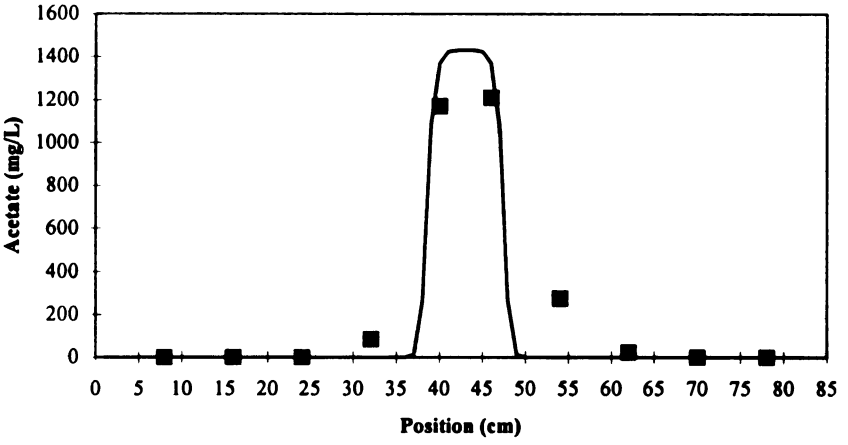

Figure 5.12. Predicted vs. measured acetate concentrations in the static model aquifer column on day 5.

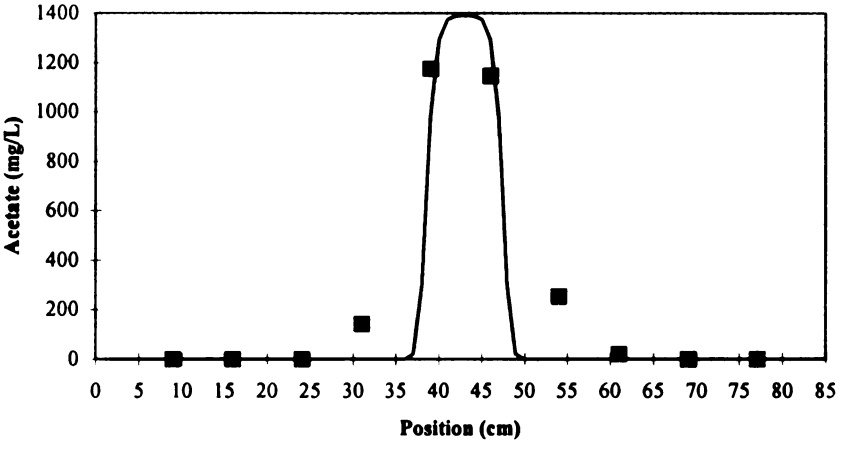

Figure 5.13. Predicted vs. measured acetate concentrations in the static model aquifer column on day 7.

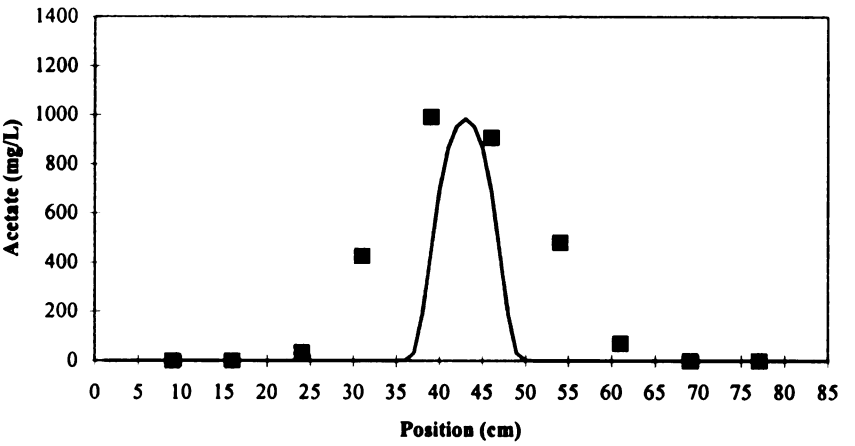

Figure 5.14. Predicted vs. measured acetate concentrations in the static model aquifer column on day 26.

The computer model developed in this work was used to predict the concentrations of six parameters in the model aquifer column. Two of these parameters, attached strain KC and sorbed CT, were not measured but predictions for the other four parameters matched reasonably well with measured values. These predictions are important in gaining an understanding of metabolism, cometabolism, and chemotaxis of strain KC in an aquifer environment.

5.7 Sensitivity analysis

A sensitivity analysis was performed on six of the key parameters used in the six equation computer model. Sensitivity analyses were performed on the bacterial decay coefficient (b), chemotactic sensitivity coefficient (χ_o), second-order rate coefficient for CT transformation (k'), random motility coefficient (ω), maximum cell growth rate (μ_{max}), and cell yields (Y_a, Y_n, and Y_{nb}). The bacterial decay coefficient was chosen due to

its inclusion in the planktonic KC, attached KC, and nitrate mass-balance equations. The chemotactic sensitivity and random motility coefficients were chosen because these two terms are used to describe chemotaxis. The second-order rate coefficient for CT transformation was chosen because it governs the degradation of CT in the CT mass-balance equation. The maximum cell growth rate was chosen because it is used to describe planktonic and attached KC growth, and acetate and nitrate consumption. And the yield coefficients were chosen due to their anticipated effect on the consumption of acetate and nitrate.

The sensitivity analysis was performed by increasing the value of one parameter by 50%, executing the computer model, and comparing the new output with the original prediction. A variation coefficient, φ, was then calculated for each model variable according to the following equation:

$$\varphi = \frac{\Delta W / W}{\Delta P / P} \tag{5.21}$$

where P is a parameter (b, χ_o, k', ω, μ_{max}, or Y) and W is a variable (C_{CT}, X_{KC}, C_a, or C_n). The variation coefficient was calculated by identifying the largest change in W over the length of the column, and dividing it by the original variable value as calculated when the parameter was not increased. This number was then divided by the value of change in P divided by P. Since all parameters were increased by 50%, the value of the denominator in Eq. 5.21 is 0.50.

Table 5.3 provides the values of the variation coefficient for all four variables when each parameter was increased. The results show that predictions for C_{CT}, X_{KC}, C_a, and C_n are insensitive to changes in the decay coefficient. The chemotactic sensitivity coefficient is sensitive to changes when predicting the planktonic strain KC and CT concentrations. The second-order rate coefficient is only sensitive with respect to C_{CT} since k' only appears in the mass-balance equation for C_{CT}. Variation of the random motility coefficient has an impact on the prediction for planktonic strain KC. A 50% increase of μ_{max} has a minimal impact on predictions of the four model variables tested. The variation coefficients calculated for an increase in Y, which included simultaneous 50% increases in Y_a, Y_n, and Y_{nb}, show that model predictions are not very sensitive to changes in Y.

Table 5.3. Variation coefficients for model parameters b, χ_o, k', ω, μ_{max}, and Y on day 5.

	b	χ_o	k'	ω	μ_{max}	Y
C_{CT}	0.48	1.68	0.94	0.04	0.02	0
X_{KC}	0.36	1.44	0	0.90	0.20	0
C_a	0.66	0.16	0	0.02	0.08	0
C_n	0	0	0	0	0	0

An additional sensitivity analysis was performed by neglecting certain terms that appear in the six mass balance equations. By doing this, it is possible to identify those terms that most affect the predictions for the model variables. Figures 5.15 through 5.17 show the predictions of C_{CT}, X_{KC}, and C_n on day 5 when the effects of chemotaxis were

neglected. To achieve this, the values for the random motility (ω) and chemotactic sensitivity (χ_o) coefficients were set equal to zero.

The resulting prediction of the acetate concentration in the column on day 5 is unchanged by the exclusion of the chemotaxis terms in the model. When the effects of chemotaxis are neglected, the model drastically under-predicts the measured strain KC migration from the slug injection zone, which results in under-predictions of both CT transformation and nitrate consumption. Therefore, the inclusion of the chemotaxis terms to describe the movement of strain KC is critical to achieving an accurate prediction of the static column.

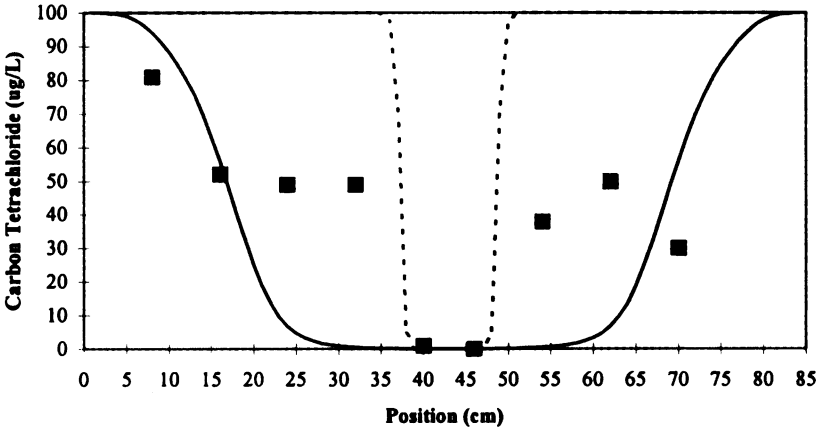

Figure 5.15. Predicted vs. measured carbon tetrachloride concentrations in the static model aquifer column on day 5. The solid line represents the prediction including the effects of chemotaxis and the dashed line represents the prediction neglecting the effects of chemotaxis.

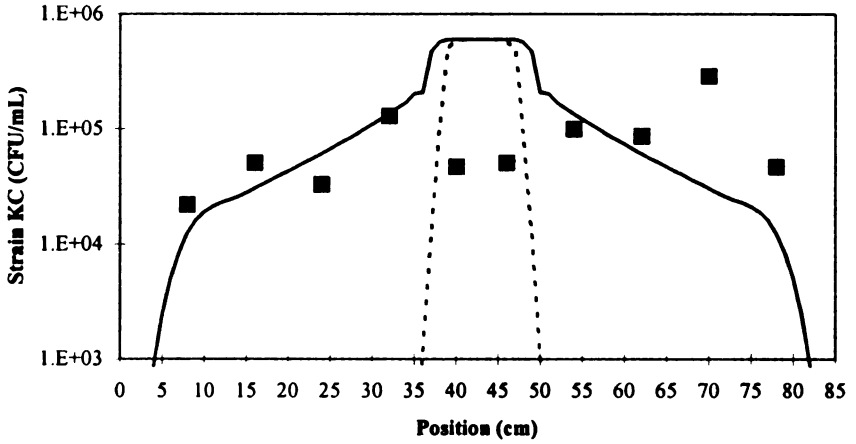

Figure 5.16. Predicted vs. measured planktonic strain KC concentrations in the static model aquifer column on day 5. The solid line represents the prediction including the effects of chemotaxis and the dashed line represents the prediction neglecting the effects of chemotaxis.

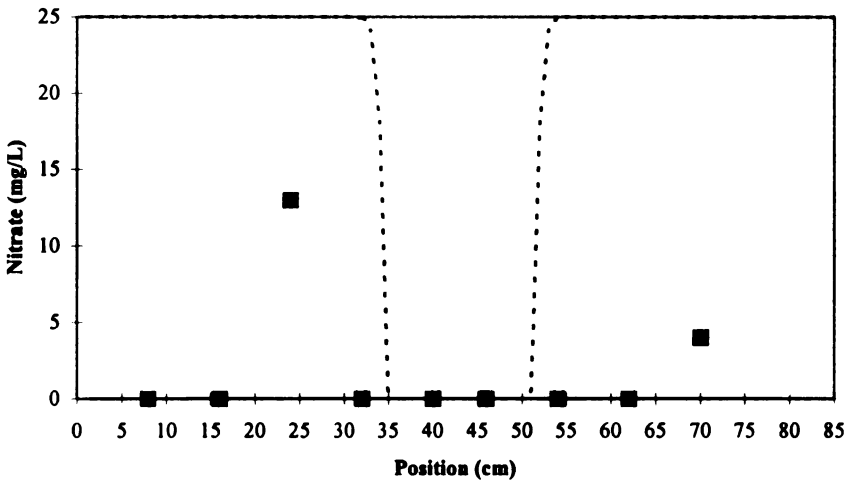

Figure 5.17. Predicted vs. measured nitrate concentrations in the static model aquifer column on day 5. The solid line represents the prediction including the effects of chemotaxis and the dashed line represents the prediction neglecting the effects of chemotaxis.

The omission of the energy terms (represented as reaction terms containing the "*Z*" coefficients in Eqs. 5.21 through 5.26) had a major effect on the model predictions

for C_{CT}, X_{KC}, C_a, and C_n. Figures 5.18 through 5.20 show the predicted vs. measured concentrations of C_{CT}, X_{KC}, and C_n, respectively, for the prediction containing the energy coefficients (represented by solid lines) and the prediction neglecting the energy coefficients (represented by dashed lines). By neglecting the energy terms, the model under-predicts CT transformation. More importantly, the model is unable to account for nitrate depletion due to reduction by motile strain KC cells. Therefore, the energy terms are essential in providing accurate predictions for planktonic strain KC and the resulting CT degradation and nitrate utilization.

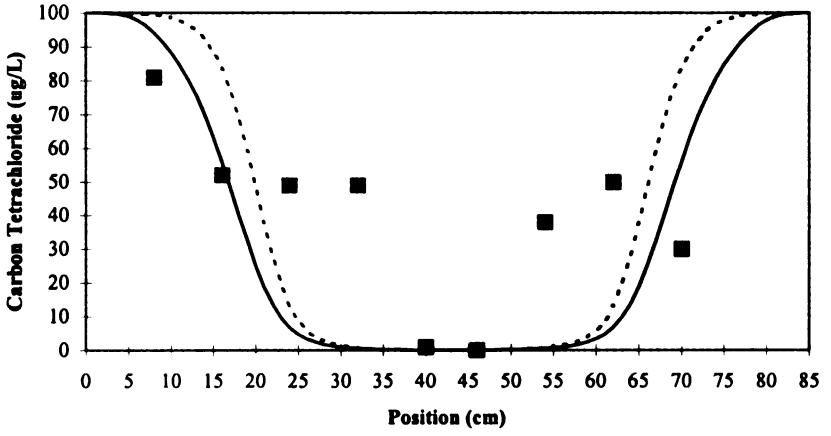

Figure 5.18. Predicted vs. measured carbon tetrachloride concentrations in the static model aquifer column on day 5. The solid line represents the prediction including the energy terms and the dashed line represents the prediction neglecting the energy terms.

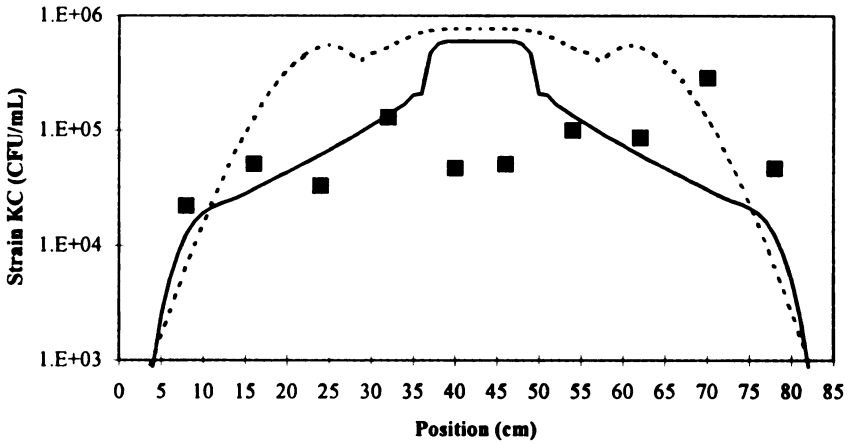

Figure 5.19. Predicted vs. measured planktonic strain KC concentrations in the static model aquifer column on day 5. The solid line represents the prediction including the energy terms and the dashed line represents the prediction neglecting the energy terms.

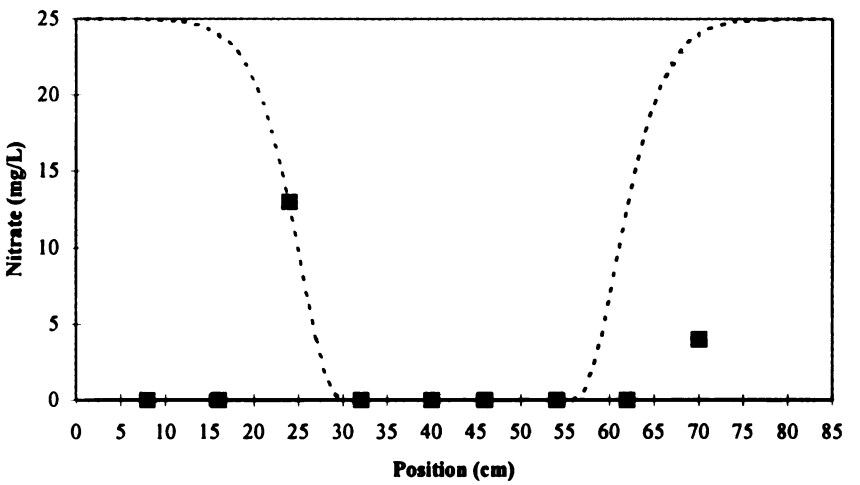

Figure 5.20. Predicted vs. measured nitrate concentrations in the static model aquifer column on day 5. The solid line represents the prediction including the energy terms and the dashed line represents the prediction neglecting the energy terms.

A final prediction was executed assuming that the growth rate was not variable, rather equal to the maximum growth rate of the strain KC cells. This assumption had a

large impact on the resulting predictions for C_{CT}, X_{KC}, C_a, and C_n. Figure 5.21 shows the predicted versus measured concentrations of planktonic strain KC on day 5. The dashed lines represent the predictions assuming μ is equal to μ_{max}. Figures are not shown for acetate, CT, and nitrate because the new predictions calculate the resulting concentrations of all three variables to be zero throughout the column. Therefore, assuming a maximum growth rate throughout the experiment will yield results that greatly over-predict the growth of strain KC and subsequent consumption of acetate and nitrate and the resulting CT degradation.

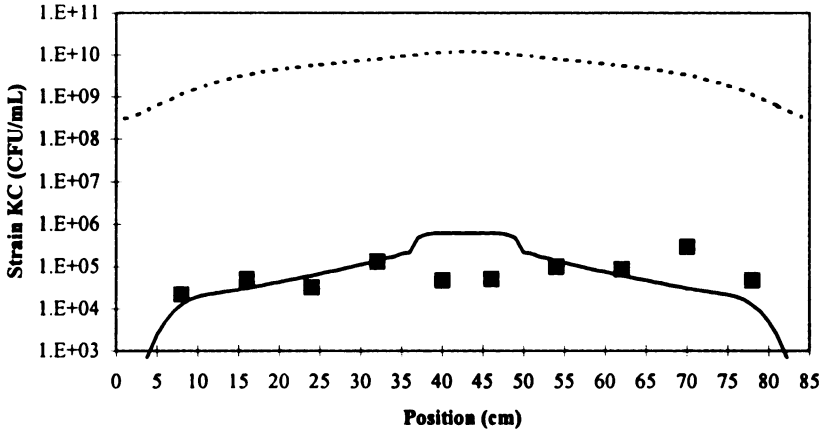

Figure 5.21. Predicted vs. measured planktonic strain KC concentrations in the static model aquifer column on day 5. The solid line represents the prediction including the effects of a variable growth rate and the dashed line represents the prediction assuming μ is equal to μ_{max}.

The goal of the preceding analysis was to identify which variables are most sensitive to changes in the input parameters. The results of these sensitivity analyses show that, in general, the model is insensitive to changes in b, k', μ_{max}, and Y. In addition,

exclusion of the energy coefficients has little affect on the resulting predictions. On the other hand, the model proves to be sensitive to changes in χ_o and ω, as is evidenced by marked changes in the numerical predictions when changes in these parameters are incorporated. Neglecting the chemotaxis terms all together results in a prediction that does not accurately match the observed migration of strain KC, and the resulting nitrate consumption and CT transformation.

5.8 Acknowledgments

I gratefully acknowledge the contributions to the development of this computer model by Kelly C. Kelly, Sashi Nair, and Dr. David C. Wiggert. Funding for this work was provided by the State of Michigan, Department of Environmental Quality.

5.9 Literature cited

Atlas, R.M. and R. Bartha. 1993. *Microbial Ecology: Fundamentals and Applications.* The Benjamin/Cummings Publishing Company, Inc., New York, New York.

Beeftink, H.H., R.T.J.M. van der Heijden, and J.J. Heijnen. 1990. Maintenance requirements: energy supply from simulateous endogenous respiration and substrate consumption. *FEMS Microbiol. Ecol.* **73**:203-210.

Chapra, S.C. and R. P. Canale. 1988. *Numerical Methods for Engineers.* Second edition. McGraw-Hill, Inc., New York, New York.

Criddle, C.S., J.T. DeWitt, D. Grbic-Galic, and P.L. McCarty. 1990. Transformation of carbon tetrachloride by *Pseudomonas* sp. strain KC under denitrification conditions. *Appl. Environ. Microbiol.* **56**:3240-3246.

Duffy, K.J., P.T. Cummings, and R.M. Ford. 1995. Random walk calculations for bacterial migration in porous media. *Biophys. J.* **68**:800-806.

Dybas, M.J., G.M. Tatara, and C.S. Criddle. 1995. Localization and characterization of the carbon tetrachloride transforming activity of *Pseudomonas* sp. strain KC. *Appl. Environ. Microbiol.* **61**:758-762.

Egli, C., R. Scholtz, A.M. Cook, and T. Leisinger. 1987. Anaerobic dechlorination of tetrachloromethane and 1,2-dichloromethane to degradable products by pure cultures of *Desulfobacterium* sp. and *Methanobacterium* sp. *FEMS Microbiol. Lett.* **43**:257-261.

Egli, C., T. Tschan, R. Scholtz, A.M. Cook, and T. Leisinger. 1988. Transformation of tetrachloromethane to dichloromethane and carbon dioxide by *Acetobacterium woodii*. *Appl. Environ. Microbiol.* **54**:2819-2823.

Ford, R.M. and D.A. Lauffenburger. 1991. Analysis of chemotactic bacterial distributions in population migration assays using a mathematical model applicable to steep or shallow attractant gradients.

Knoll, W.H. 1994. Factors influencing the competitive advantage of *Pseudomonas* sp. strain kC for subsequent remediation of a carbon tetrachloride impacted aquifer. Master's Thesis, Department of Civil and Environmental Engineering, Michigan State University, East Lansing, Michigan.

Leonard, B.P. 1979. A stable accurate convective modeling procedure based on quadratic upstream interpolation. *Comp. Meth. Appl. Mech. Engr.* **19**:59-98.

Tchobanoglous, G. and F.L. Burton. 1991. *Wastewater Engineering: Treatment, Disposal, and Reuse*. McGraw-Hill, Inc. New York, New York.

Quinton, G.E., R.J. Buchanan, Jr., D.E. Ellis, and S.H. Shoemaker. 1997. A method to compare groundwater cleanup technologies. *Remediation*. Autumn 1997.

Radabaugh, P.D. 1998. Factors affecting transport of *Pseudomonas stutzeri* KC. Master's Thesis, Department of Civil and Environmental Engineering, Michigan State University, East Lansing, Michigan.

Schmidt, S., M.T. Widman, and R.M. Worden. 1996. A laser-diffraction capillary assay to measure random motility. *Biotech. Bioeng.*

Semprini, L., G.D. Hopkins, P.L. McCarty, and P.V. Roberts. 1992. In-situ transformation of carbon tetrachloride and other halogenated compounds resulting from biostimulation under anoxic conditions. *Environ. Sci. Technol.* **26**:2454-2461.

Sneathen, M.A. 1996. Theoretical and experimental competitiveness of *Pseudomonas stutzeri* KC. Master's thesis. Department of Civil and Environmental Engineering, Michigan State University, East Lansing, Michigan.

Stumm, W. and J.J. Morgan. 1981. *Aquatic Chemistry*, 2nd edition. John Wiley & Sons. New York, New York.

Tatara, G.M., M.J. Dybas, and C.S. Criddle. 1993. Effects of medium and trace metals on kinetics of carbon tetrachloride transformation by *Pseudomonas* sp. strain KC. *Appl. Environ. Microbiol.* **59**:2126-2131.

Tatara, G.M. 1996. Physiology of carbon tetrachloride transformation by *Pseudomonas stutzeri* strain KC. Doctoral Dissertation, Department of Microbiology, Michigan State University, East Lansing, Michigan.

Widman, M.T. 1997. Engineering applications of microbial chemotaxis. Doctoral Dissertation, Department of Chemical Engineering, Michigan State University, East Lansing, Michigan.

Witt, M.E., M.J. Dybas, R.L. Heine, S. Nair, D.C. Wiggert, and C.S. Criddle. 1995. Development of a model aquifer column to monitor the transformation of carbon tetrachloride by *Pseudomonas* sp. strain KC. *Bioaugmentation for Site Remediation*. Battelle Press, Columbus, Ohio.

Zhao, X., M.J. Szafranski, M.A. Maraqa, and T.C. Voice. 1998. Desorption and bioavailability of carbon tetrachloride in a low organic content sandy soil. Submitted for publication to *Environ. Tox. Chem.*

Chapter 6

ENGINEERING APPLICATION OF BIOAUGMENTATION USING *PSEUDOMONAS STUTZERI* KC

6.1 Historical groundwater remediation methods

A variety of methods can be used to contain CT-contaminated groundwater and prevent off-site migration. One of the more widely used methods involves hydraulic containment coupled with product recovery, i.e. pump and treat systems. Migration of contaminants is controlled by intercepting groundwater using one or more recovery wells. Since this process relies on pumping groundwater to achieve hydraulic containment, it requires that considerable volumes of groundwater be treated on the surface. This method of pumping and treating the contaminated groundwater *ex-situ* is both expensive and labor-intensive. Physical barriers, such as slurry walls, have also been used to contain subsurface contamination. However, to maximize efficiency, pumping wells must also be installed inside the barrier wall to insure the direction of groundwater flow is into, rather than out of, the region. This process also requires the *ex-situ* treatment of large quantities of water.

6.2 *In-situ* bioremediation

In-situ bioremediation is an alternative approach to these more traditional methods. The major advantage of employing such a method to control off-site migration is that bioremediation attenuates the contaminant *in-situ*. The physical removal of contaminated sediments and pollutants is eliminated. Because this approach relies on

groundwater flow to deliver the contaminants to the zone of remediation, there is a reduced pumping requirement. In addition, *in-situ* bioremediation doesn't generate waste solids for disposal. Use of strain KC to transform CT in groundwater is potentially useful because of these attractive advantages that *in-situ* bioremediation offers.

The formation of a biologically-active zone, or biocurtain, may be accomplished in many ways. Microorganisms capable of degrading target contaminants can be delivered into the subsurface by suspending the cells in an aqueous medium and pumping the cells into the contaminated aquifer via injection wells. Figure 6.1 illustrates this concept of biocurtain formation using an injection well to deliver bacteria and/or nutrients to the subsurface. If suitable conditions exist for the microorganisms, colonization and subsequent degradation of the contaminants will occur.

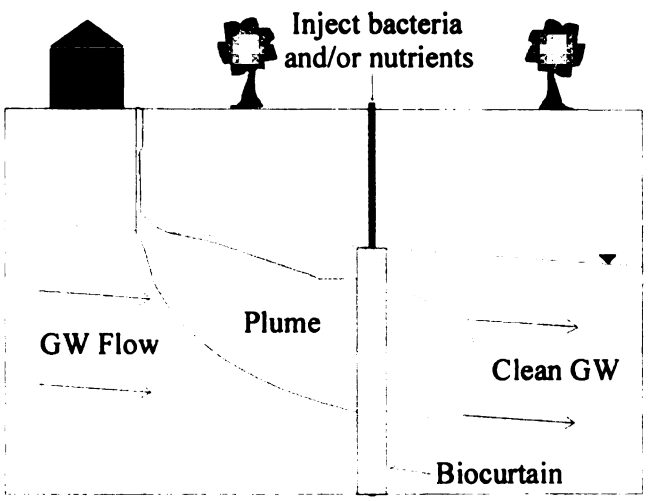

Figure 6.1. Profile view of the biocurtain concept for *in-situ* bioremediation.

In cases of extremely low hydraulic conductivity (e.g. clayey sediments), hydraulic fracturing may be required to provide an area of coverage large enough to

intercept the flowing contaminated groundwater. This method is achieved by pumping cells and nutrients into the subsurface at an extremely high flow rate and pressure (Murdoch *et al.*, 1991). The high pressure actually "fractures" the porous media and provides flow paths for the cells and nutrients. Conversely, in situations where the groundwater velocities are high, the cells and nutrients must be injected at high flow rates to ensure adequate coverage between each injection well.

The funnel and gate system proposed by Starr and Cherry (1994) is another method which utilizes the capability of microorganisms to degrade groundwater contaminants. This method proposes the use of low hydraulic conductivity walls to direct contaminated groundwater through biologically-active zones where contaminant degradation occurs. These low hydraulic conductivity cutoff walls may consist of frozen ground barriers, sheet piling, or slurry walls.

The process of bioremediation within an active biozone has many applications. It has been demonstrated that this type of remedial activity is successful in treating spills consisting of spent halogenated solvents and compounds from the manufacture of chlorinated aliphatic hydrocarbons; wastes from the use and manufacture of chlorinated phenols, benzenes, and their derivatives; spent non-halogenated solvents; metal plating and cleaning wastes; and petrochemical products and wastes (Bourquin, 1989).

The applicability of using *in-situ* bioremediation as a means of degrading CT in contaminated groundwater and sediment may be widespread. Only under certain conditions, however, can this transformation proceed in such a way that undesirable endproducts are avoided. Degradation of CT by numerous types of bacteria have been studied. CT has been shown to be degraded under denitrifying, sulfate-reducing, and

methanogenic conditions. In these cases, bacteria derive energy from fermentative processes using nitrate, sulfate, carbon dioxide, or other compounds as electron acceptors. *Desulfobacterium autotrophicum* is a marine bacterium capable of dechlorinating CT to chloroform and dichloromethane (Egli *et al.*, 1987). *Acetobacterium woodii* is an acetogenic anaerobe that converts CT to dichloromethane and chloromethane (Egli *et al.*, 1988). Bouwer and McCarty (1983) observed CT transformation to CO_2 and other metabolites under denitrifying conditions. The disadvantage of employing these types of bacteria to degrade CT *in-situ* is that most transform CT via pathways where chloroform and/or dichloromethane accumulate. These undesirable endproducts can be more harmful and more persistent in the environment than CT. Therefore, the use of a bacterium that mediates the transformation of CT to non-harmful endproducts must be employed.

6.3 The use of *Pseudomonas stutzeri* KC for bioremediation

The ability of *Pseudomonas stutzeri* KC to degrade CT in an aquifer environment has been shown, both in this dissertation and by others (Dybas *et al.*, 1998, and Tatara *et al.*, 1993). The advantage of using strain KC to mediate this degradation *in-situ* is that chloroform is not produced during the transformation. Strain KC was used to remediate a portion of a CT-contaminated aquifer near Schoolcraft, Michigan (Dybas *et al.*, 1998). In this field experiment, bioaugmentation using strain KC was successful at degrading almost 80% of CT in the liquid phase and 65% on the solid phase. A larger-scale remediation effort is currently underway at the Schoolcraft site, and preliminary results indicate that strain KC is capable of degrading approximately 98% of the CT in the liquid phase.

The applicability of using strain KC to remediate aquifers contaminated with CT may be limited. The sensitivity of KC toward metal ions in solution may limit the applicability unless low metal concentrations are present at the target site. Strain KC optimally transforms CT under denitrifying conditions but will mediate the transformation under low-oxygen conditions (Lewis and Crawford, 1993). However, the efficiency of this transformation is much lower than under denitrifying conditions. At sites where there is not sufficient nitrate to sustain nitrate-reducing populations, additional nitrate could be intermittently injected into the aquifer. Nitrate addition, however, may not be approved by state and/or federal regulatory agencies.

Overall, *in-situ* bioremediation using strain KC to remove CT is a remediation approach that shows promise for cleaning up contaminated groundwater and sediments. The appeal of such a technology to remove CT from the groundwater is the reduced cost at which a remediation may be completed. The high costs associated with traditional cleanup methods stem from the prolonged operational periods needed to adequately detoxify the target medium. Bioaugmentation using *Pseudomonas stutzeri* KC shows promise for cleaning up CT-contaminated aquifers in a cost-effective manner.

6.4 Literature cited

Bourquin, A.W. 1989. Bioremediation of hazardous waste. *Haz. Mat. Cont.* **2**:16-59.

Bouwer, E.J. and P.L. McCarty. 1983. Transformations of halogenated organic compounds under denitrification conditions. *Appl. Environ. Microbiol.* **45**:1295-1299.

Dybas, M.J., M. Barcelona, S. Bezborodnikov, S. Davies, L. Forney, H. Heuer, O. Kawka, T. Mayotte, L. Sepulveda-Torres, K. Smalla, M. Sneathen, J. Tiedje, T. Voice, D.C. Wiggert, M.E. Witt, and C.S. Criddle. Pilot-scale evaluation of bioaugmentation for in-situ remediation of a carbon tetrachloride-contaminated aquifer. 1998. Submitted for publication to *Environ. Sci. Technol.*

Egli, C., R. Scholtz, A.M. Cook, and T. Leisinger. 1987. Anaerobic dechlorination of tetrachloromethane and 1,2-dichloromethane to degradable products by pure cultures of *Desulfobacterium* sp. And *Methanobacterium* sp. *FEMS Microbiol. Lett.* **43**:257-261.

Egli, C. T. Tschan, R. Scholtz, A.M. Cook, and T. Leisinger. 1988. Transformation of tetrachloromethane to dichloromethane and carbon dioxide by *Acetobacterium woodii*. *Appl. Environ. Microbiol.* **54**:2819-2824.

Lewis, T.A. and R.L. Crawford. 1993. Physiological factors affecting carbon tetrachloride dehalogenation by the denitrifying bacterium *Pseudomonas* sp. strain KC. *Appl. Environ. Microbiol.* **59**:1635-1641.

Murdoch, L.C., G. Losonsky, P. Cluxton, B. Patterson, I. Klich, and B. Braswell. 1991. Feasibility of hydraulic fracturing of soil to improve remedial actions. USEPA Project Summary 600-S2-91-012.

Starr, R.C. and J.A. Cherry. 1994. In situ remediation of contaminated groundwater: the funnel-and-gate system. *Ground Water*. **32**:465-476.

Tatara, G.M., M.J. Dybas, and C.S. Criddle. 1993. Effects of medium and trace metals on kinetics of carbon tetrachloride transformation by *Pseudomonas* sp. Strain KC. *Appl. Environ. Microbiol.* **59**:2126-2131.

Chapter 7

CONCLUSIONS AND FUTURE INVESTIGATIONS

7.1 Conclusions

1. Bioaugmentation of aquifer sediments using *Pseudomonas stutzeri* KC leads to efficient carbon tetrachloride removal over extended periods of time without chloroform production.
2. After inoculation using *Pseudomonas stutzeri* KC, frequent base additions may select for indigenous microflora capable of transforming carbon tetrachloride to chloroform. Microbial populations indigenous to the Schoolcraft aquifer can convert carbon tetrachloride to chloroform, and such populations can be selected by twice-weekly base additions.
3. A mobile biocurtain of *Pseudomonas stutzeri* KC activity is capable of migrating through porous media at a rate that exceeds groundwater flow, while simultaneously degrading carbon tetrachloride in the groundwater and on aquifer sediments. The mechanism for the accelerated migration is chemotaxis of *Pseudomonas stutzeri* KC towards nitrate.
4. *Pseudomonas stutzeri* KC has the ability to remediate carbon tetrachloride-contaminated groundwater and aquifer sediments in the absence of advective flow. The mechanism for migration of *Pseudomonas stutzeri* KC in the absence of flow is chemotaxis towards nitrate.
5. A six-equation computer model was developed to simulate the inter-related processes that occur in the transformation of carbon tetrachloride. This model predicts

Pseudomonas stutzeri KC migration, acetate and nitrate consumption, and the resulting CT transformation in a static model aquifer column.

7.2 Future Investigations

1. Duplicate the static column experiment using a non-motile *Pseudomonas stutzeri* KC mutant to assess the effect of motility and chemotaxis on the migration of strain KC through porous media.
2. Identify the extent to which chemotaxis plays a role in the field-scale remediation of carbon tetrachloride-contaminated groundwater and sediments.
3. Modify the computer model to account for *Pseudomonas stutzeri* KC activity as a function of groundwater pH.
4. Modify the computer model to account for acetate and nitrate utilization by indigenous microbes, and the resulting carbon tetrachloride transformation to chloroform.
5. Modify the computer model to account for carbon tetrachloride degradation by indigenous microflora using the biomolecule secreted from strain KC.

APPENDICES

APPENDIX A

Evaluation of Prototype Model Aquifer Column

A.1 Evaluation of Prototype Model Aquifer Column

An experiment was performed to examine the extent of adsorption of carbon tetrachloride (CT) on the sidewall and endcaps of two-inch diameter polycarbonate piping. All connections were completed as they would have been for an actual column experiment, except the column was not packed with aquifer material. Instead, the internal contents of a model aquifer column were filled with Schoolcraft groundwater containing 100 µg/L CT. Care was taken to make sure that no air bubbles were trapped in the column prior to the first sampling event. Triplicate samples were removed from the center point of the column daily for a period of two weeks and were analyzed for CT immediately after sample acquisition. Figure A.1 shows the resulting CT concentrations measured in port 5 (center-point of the column) over the two week period. Based on the results of this experiment, it was apparent that the model aquifer column was a good candidate for the proposed studies. Only 5% of the original CT in solution was lost over the duration of the experiment.

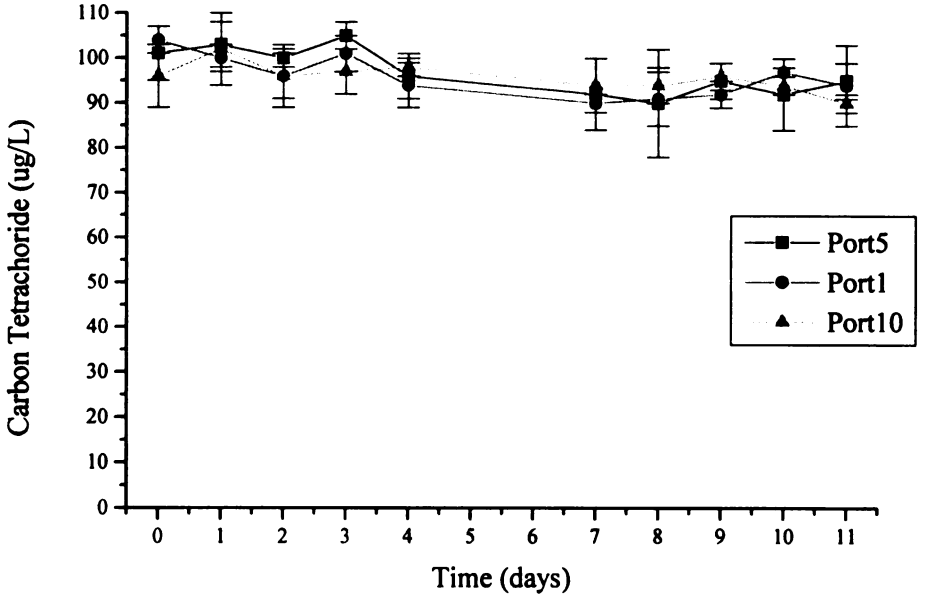

Figure A.1. Carbon tetrachloride concentration in model column during the polycarbonate adsorption experiment.

APPENDIX B

Experimental Data from Model Aquifer Column 1

B.1 Experimental Data from Model Aquifer Column 1

Table B.1. Carbon tetrachloride data from model aquifer column 1. CT concentrations are in units of μg/L (or ppb).

Port	Day 0	Day 1	Day 3	Day 5	Day 11	Day 19	Day 34	Day 63	Day 83	Day 89
1	101	111	102	113	103	99	100	107	101	109
2	99	102	108	108	97	98	98	107	101	107
3	103	101	98	108	97	102	98	102	96	114
4	102	103	100	96	97	97	76	96	105	103
5	106	87	104	106	98	97	78	108	82	101
6	104	89	112	101	99	100	82	63	45	86
7	97	26	105	98	93	83	66	56	30	111
8	108	86	81	100	94	83	43	39	26	83
9	113	85	37	88	94	91	58	49	42	63
10	101	89	32	41	81	37	26	22	23	36
11	110	90	44	37	96	33	20	13	20	32
12	107	97	88	25	112	29	12	8	13	28
13	112	106	80	50	89	18	11	11	12	54
14	101	112	84	90	43	25	9	7	9	31
15	100	105	108	108	47	52	15	10	14	83
16	101	101	106	109	26	41	14	10	16	44
17	93	108	116	107	30	35	15	12	12	55
18	97	92	113	110	30	42	12	11	9	56
19	91	101	110	119	16	30	10	10	9	39
20	107	109	112	110	23	63	13	6	8	40
21	97	86	106	108	20	63	8	6	12	28
22	92	92	88	110	32	72	8	5	8	39
23	97	103	79	113	35	43	9	7	8	18
24	100	105	68	116	58	22	7	3	10	34
25	97	94	77	99	71	47	8	3	10	51

Table B.1. (continued) Carbon tetrachloride data from model aquifer column 1. CT concentrations are in units of µg/L (or ppb).

Port	Day 96	Day 103	Day 111	Day 117	Day 124	Day 145
1	105	101	109	97	107	89
2	56	113	105	98	111	104
3	112	96	101	89	88	104
4	60	118	79	30	87	66
5	120	111	94	93	95	99
6	72	112	91	80	50	69
7	47	111	86	78	47	43
8	64	100	93	63	67	35
9	49	104	81	70	98	40
10	35	63	61	32	47	33
11	43	59	52	49	43	35
12	28	46	61	37	28	29
13	45	85	16	23	24	42
14	42	60	26	45	23	22
15	23	52	28	59	41	38
16	19	48	59	33	35	25
17	21	37	26	31	33	40
18	29	46	29	42	29	31
19	21	35	24	41	41	26
20	24	23	27	35	35	37
21	17	23	13	21	21	20
22	16	40	27	25	21	17
23	17	34	15	37	33	26
24	15	36	27	34	39	29
25	16	51	28	24	49	67

Table B.2. Indigenous microflora enumeration data from liquid samples obtained from model aquifer column 1. Cell concentrations are in units of CFU/mL.

Port	Day 85	Day 155
1	2.0E+05	6.0E+04
3	1.0E+05	1.0E+05
5	2.0E+05	2.0E+04
7	3.0E+06	1.0E+04
9	1.0E+05	1.0E+04
11	1.0E+05	1.8E+04
13	5.0E+05	2.0E+04
15	6.0E+05	5.0E+04
17	4.0E+05	4.0E+04
19	1.2E+05	1.0E+04
21	5.0E+05	2.3E+04
23	2.0E+05	1.1E+04
25	4.0E+04	3.0E+04

Table B.3. Indigenous microflora enumeration data from solid samples obtained from model aquifer column 1. Cell concentrations are in units of CFU/mL.

Port	Day 85	Day 155
1	1.50E+05	3.40E+06
3	1.40E+05	3.10E+04
5	8.30E+05	8.70E+05
7	1.70E+06	5.00E+05
9	5.30E+05	1.20E+05
11	1.40E+06	3.40E+05
13	6.60E+05	7.10E+05
15	8.10E+05	3.80E+05
17	6.00E+06	3.40E+05
19	6.10E+06	2.60E+06
21	5.80E+05	6.20E+06
23	1.50E+05	3.00E+06
25	1.60E+05	6.70E+05

Table B.4. *Pseudomonas stutzeri* KC enumeration data from liquid samples obtained from model aquifer column 1. Cell concentrations are in units of CFU/mL.

Port	Day 0	Day 85	Day 155
1	NS	ND	ND
3	NS	ND	1.0E+03
5	1.0E+07	3.0E+03	5.0E+03
7	NS	ND	ND
9	NS	ND	ND
11	NS	ND	ND
13	NS	ND	ND
15	NS	ND	6.0E+03
17	NS	ND	1.0E+03
19	NS	ND	ND
21	NS	ND	1.0E+03
23	NS	ND	ND
25	NS	ND	ND

ND = Not Detected
NS = No Sample Obtained

Table B.5. *Pseudomonas stutzeri* KC enumeration data from solid samples obtained from model aquifer column 1. Cell concentrations are in units of CFU/mL.

Port	Day 85	Day 155
1	ND	ND
3	ND	ND
5	1.7E+05	2.6E+04
7	2.6E+04	4.0E+04
9	5.3E+03	2.4E+04
11	6.9E+03	1.0E+04
13	6.6E+03	7.1E+03
15	8.1E+03	ND
17	ND	ND
19	ND	ND
21	ND	ND
23	ND	ND
25	ND	ND

ND = Not Detected
NS = No Sample Obtained

APPENDIX C

Experimental Data From Model Aquifer Column 2

C.1 Experimental Data From Model Aquifer Column 2

Table C.1. Carbon tetrachloride data from liquid samples obtained from model aquifer column 2. CT concentrations are in units of μg/L (or ppb).

Port	Day 0	Day 1	Day 3	Day 4	Day 5	Day 6	Day 9	Day 12	Day 14	Day 17
1	101	101	109	98	100	98	97	111	105	104
2	100	101	91	99	94	105	103	105	100	105
3	97	100	105	97	97	96	98	106	99	94
4	95	100	102	67	106	99	100	109	107	91
5	96	35	90	35	22	106	86	99	38	41
6	87	40	89	34	48	49	74	32	21	30
7	96	24	70	25	43	47	42	44	21	25
8	86	38	34	27	18	46	37	32	26	22
9	92	78	45	27	29	37	38	38	44	25
10	100	92	44	35	32	24	23	35	40	18
11	100	93	77	38	32	35	38	35	31	23
12	108	102	81	34	32	32	38	29	33	28
13	99	99	73	47	33	20	39	31	36	29
14	103	101	51	62	37	26	30	25	37	26
15	102	97	84	54	51	32	29	22	31	27
16	99	98	94	59	51	36	21	22	26	25
17	105	100	99	90	88	61	19	23	29	20
18	106	95	98	86	88	53	34	22	25	29
19	98	96	102	101	101	71	49	28	28	24
20	93	100	100	103	107	99	31	27	22	31
21	87	98	103	112	103	105	88	54	39	34
22	92	98	99	104	100	104	103	40	47	41
23	87	97	101	103	105	102	114	30	41	41
24	97	94	94	104	107	110	95	48	49	46
25	91	101	104	103	102	109	107	72	64	68

Table C.1. (continued) Carbon tetrachloride data from liquid samples obtained from model aquifer column 2. CT concentrations are in units of μg/L (or ppb).

Port	Day 21	Day 24	Day 27	Day 31	Day 34	Day 38	Day 41	Day 45	Day 48	Day 55
1	100	101	102	102	103	99	104	108	106	98
2	101	100	99	102	97	95	104	99	110	88
3	102	105	102	102	101	101	109	97	103	109
4	100	104	104	100	102	99	102	105	111	107
5	32	36	3	42	39	63	98	82	105	112
6	10	26	10	25	22	30	42	37	37	58
7	18	20	21	20	21	20	32	22	25	39
8	11	12	20	16	16	13	19	21	16	21
9	20	15	18	15	22	16	25	16	21	36
10	16	12	18	12	13	9	21	13	22	23
11	14	11	18	13	11	11	16	15	22	22
12	16	17	16	14	12	13	14	14	18	19
13	15	19	15	17	13	13	14	14	16	16
14	17	13	14	16	12	12	12	11	13	11
15	20	16	15	17	14	11	11	12	15	14
16	17	17	19	12	14	10	12	10	13	12
17	20	15	16	12	13	10	12	9	12	12
18	21	15	15	16	17	12	16	11	13	12
19	24	17	18	15	17	7	17	10	14	11
20	25	25	22	17	18	9	16	12	12	10
21	25	27	15	24	21	11	14	9	12	8
22	29	25	26	28	23	10	13	14	11	9
23	29	27	25	22	24	8	12	14	12	9
24	34	26	26	31	26	10	11	13	10	7
25	36	35	28	37	29	12	9	12	9	7

Table C.1. (continued) Carbon tetrachloride data from liquid samples obtained from model aquifer column 2. CT concentrations are in units of µg/L (or ppb).

Port	Day 62	Day 69	Day 78	Day 86	Day 93	Day 100	Day 114
1	110	114	108	100	102	81	105
2	108	108	82	102	106	94	103
3	101	105	104	94	97	89	103
4	106	108	90	93	106	94	101
5	101	106	103	37	94	98	96
6	82	78	92	112	99	89	75
7	59	53	82	105	108	101	79
8	30	53	90	78	101	67	63
9	39	42	84	57	100	82	98
10	37	37	48	27	45	62	98
11	34	23	42	33	71	56	91
12	27	27	25	36	82	66	67
13	28	27	32	37	46	60	75
14	19	25	11	49	67	49	57
15	24	32	20	32	41	61	68
16	23	25	25	26	40	40	58
17	18	22	22	35	32	42	60
18	19	23	24	27	29	36	43
19	16	22	13	16	21	34	47
20	14	20	15	10	18	33	43
21	13	24	15	18	21	28	49
22	14	17	20	25	20	34	52
23	12	15	21	27	26	35	50
24	11	13	19	26	28	31	45
25	10	9	13	14	22	31	47

Table C.2. Indigenous microflora enumeration data from liquid samples obtained from model aquifer column 2. Cell concentrations are in units of CFU/mL.

Port	Day 69	Day 140
1	1.0E+05	8.0E+03
3	1.0E+05	6.0E+03
5	1.7E+05	1.6E+04
7	1.9E+05	1.7E+05
9	8.0E+04	4.0E+04
11	1.0E+06	7.0E+04
13	1.0E+05	2.0E+04
15	8.0E+04	5.0E+05
17	2.0E+05	2.0E+04
19	6.0E+04	3.0E+04
21	1.0E+05	1.1E+05
23	2.1E+05	6.0E+03
25	4.0E+06	2.0E+04

Table C.3. Indigenous microflora enumeration data from solid samples obtained from model aquifer column 2. Cell concentrations are in units of CFU/mL.

Port	Day 69	Day 140
1	2.2E+05	7.9E+05
3	6.7E+05	4.3E+05
5	6.7E+05	1.1E+06
7	1.0E+07	3.5E+06
9	4.8E+06	6.3E+05
11	3.7E+05	9.1E+05
13	1.2E+07	8.8E+05
15	1.3E+06	1.1E+06
17	5.2E+06	1.4E+06
19	5.2E+06	2.2E+06
21	5.6E+07	1.0E+06
23	4.8E+06	8.1E+04
25	1.0E+06	1.8E+06

Table C.4. *Pseudomonas stutzeri* KC enumeration data from liquid samples obtained from model aquifer column 2. Cell concentrations are in units of CFU/mL.

Port	Day 0	Day 10	Day 20	Day 69
1	NS	ND	ND	ND
3	NS	ND	ND	ND
5	1.0E+07	3.0E+06	1.0E+05	2.0E+03
7	NS	4.0E+05	8.0E+04	1.0E+04
9	NS	8.0E+05	7.0E+04	ND
11	NS	1.0E+06	2.0E+05	1.0E+04
13	NS	8.0E+05	9.0E+04	3.0E+03
15	NS	3.0E+05	9.0E+04	2.0E+03
17	NS	7.0E+05	6.0E+04	ND
19	NS	1.0E+06	4.0E+04	ND
21	NS	1.0E+06	5.0E+04	ND
23	NS	5.0E+05	6.0E+04	1.0E+04
25	NS	3.0E+05	4.0E+04	ND

ND = Not Detected
NS = No Sample Obtained

Table C.5. *Pseudomonas stutzeri* KC enumeration data from solid samples obtained from model aquifer column 2. Cell concentrations are in units of CFU/mL.

Port	Day 69	Day 140
1	ND	ND
3	ND	ND
5	ND	2.2E+06
7	5.2E+05	2.0E+04
9	4.8E+04	7.0E+03
11	3.7E+04	ND
13	1.2E+04	ND
15	6.5E+04	7.1E+03
17	5.2E+05	ND
19	ND	ND
21	1.9E+05	ND
23	ND	ND
25	ND	ND

ND = Not Detected
NS = No Sample Obtained

APPENDIX D

Experimental Data From Mobile Biocurtain Column

D.1 Experimental Data From Mobile Biocurtain Column

Table D.1. Carbon tetrachloride data from liquid samples obtained from mobile biocurtain column. CT concentrations are in units of µg/L (or ppb).

Port	Background	Day 1	Day 4	Day 8	Day 13	Day 18
1	137	141	145	132	130	132
2	139	143	136	136	123	132
3	133	133	151	122	127	137
4	134	126	157	127	129	143
5	129	11	159	101	116	94
6	127	11	32	94	104	83
7	137	52	16	100	98	111
8	134	52	15	95	97	98
9	130	98	58	78	78	91
10	127	107	119	72	86	82
11	133	111	134	52	84	78
12	130	119	120	27	92	80
13	130	125	114	18	100	70
14	125	133	111	30	112	59
15	136	144	129	68	122	63
16	137	147	120	64	93	66
17	141	128	147	59	79	56
18	132	141	136	58	53	59
19	129	108	142	79	26	80
20	133	119	129	88	19	72
21	140	110	128	89	24	58
22	143	126	124	102	44	65
23	139	123	129	117	83	63
24	122	121	120	108	104	56
25	142	124	113	112	117	55

Table D.2. Bromide data from liquid samples obtained from mobile biocurtain column. Bromide concentrations are in units of mg/L (or ppm).

Port	Day 1	Day 4	Day 8	Day 13	Day 18
1	0	0	0	0	0
2	0	0	0	0	0
3	0	0	0	0	0
4	0	0	0	0	0
5	186	0	0	0	0
6	238	6	0	0	0
7	20	21	1	0	0
8	2	74	2	0	0
9	0	246	2	0	0
10	0	113	3	0	0
11	0	17	4	0	0
12	0	0	6	0	0
13	0	0	19	2	0
14	0	0	83	2	0
15	0	0	168	2	0
16	0	0	123	2	0
17	0	0	38	3	0
18	0	0	8	4	0
19	0	0	2	6	0
20	0	0	0	20	2
21	0	0	0	92	2
22	0	0	0	174	2
23	0	0	0	153	3
24	0	0	0	54	4
25	0	0	0	15	4

Table D.3. Acetate data from liquid samples obtained from mobile biocurtain column. Acetate concentrations are in units of mg/L (or ppm).

Port	Day 1	Day 4	Day 8	Day 13	Day 18
1	0	0	0	0	0
2	0	0	0	0	0
3	0	0	0	0	0
4	0	0	0	0	0
5	1060	10	0	0	0
6	1490	15	8	0	0
7	104	110	0	0	0
8	10	377	0	12	0
9	0	1025	7	5	0
10	0	481	0	0	0
11	0	73	0	0	0
12	0	0	9	0	5
13	0	0	38	6	0
14	0	0	362	5	0
15	0	0	722	5	0
16	0	0	496	6	0
17	0	0	195	7	0
18	0	0	42	10	0
19	0	0	15	20	0
20	0	0	3	65	2
21	0	0	3	311	2
22	0	0	4	604	2
23	0	0	3	306	3
24	0	0	3	122	7
25	0	0	7	59	2

Table D.4. Nitrate data from liquid samples obtained from mobile biocurtain column. Nitrate concentrations are in units of mg/L (or ppm).

Port	Background	Day 1	Day 4	Day 8	Day 13	Day 18
1	43	39	38	37	46	42
2	38	39	41	40	46	42
3	35	38	36	37	46	38
4	40	31	37	41	45	42
5	40	3	24	39	44	40
6	36	7	3	32	46	40
7	37	35	0	16	44	40
8	34	34	0	9	43	40
9	32	35	0	8	40	39
10	39	35	0	5	37	40
11	37	35	0	0	34	40
12	38	32	5	0	29	42
13	41	38	26	0	22	40
14	35	40	32	0	14	38
15	33	38	34	0	6	40
16	36	41	37	0	4	37
17	38	38	40	0	0	35
18	39	38	38	0	0	30
19	38	42	42	0	0	27
20	42	37	38	3	0	20
21	42	42	39	0	0	12
22	40	41	39	0	0	3
23	41	38	41	0	0	0
24	40	39	40	0	0	0
25	41	37	42	0	0	0

Table D.5. *Pseudomonas stutzeri* KC enumeration data from liquid samples obtained from mobile biocurtain column. Cell concentrations are in units of CFU/mL.

Port	Day 1	Day 3	Day 7	Day 11	Day 14	Day 17
1	NS	ND	ND	ND	ND	ND
3	NS	ND	ND	ND	ND	ND
5	7.1E+07	3.8E+06	1.0E+05	4.0E+03	2.0E+04	1.5E+04
7	NS	2.0E+04	4.0E+05	5.0E+04	6.0E+03	1.0E+03
9	NS	5.0E+04	1.2E+04	2.0E+04	6.0E+03	ND
11	NS	ND	4.0E+03	5.0E+04	ND	ND
13	NS	ND	ND	ND	ND	ND
15	NS	ND	ND	ND	ND	ND
17	NS	ND	4.0E+03	ND	2.0E+03	ND
19	NS	ND	4.0E+04	ND	ND	ND
21	NS	ND	3.0E+03	1.0E+03	2.0E+03	ND
23	NS	ND	1.0E+04	ND	ND	ND
25	NS	ND	ND	1.0E+03	ND	ND

ND = Not Detected
NS = No Sample Obtained

Table D.6. *Pseudomonas stutzeri* KC enumeration data from solid samples obtained from mobile biocurtain column. Cell concentrations are in units of CFU/mL.

Port	Pre-Experiment	Post-Experiment
1	ND	ND
3	ND	ND
5	ND	9.8E+06
7	ND	9.4E+04
9	ND	ND
11	ND	ND
13	ND	ND
15	ND	ND
17	ND	ND
19	ND	ND
21	ND	ND
23	ND	ND
25	ND	ND

ND = Not Detected

APPENDIX E

Experimental Data From Static Column 1

E.1 Experimental Data From Static Column 1

Table E.1. Carbon tetrachloride data from liquid samples obtained from static column 1. CT concentrations are in units of μg/L (or ppb).

Port	Day 0	Day 2	Day 5	Day 7	Day 26
1	94	95	81	38	10
2	99	89	52	35	14
3	96	105	49	20	14
4	105	111	49	17	3
5	101	1	1	1	0
6	103	0	0	0	0
7	100	37	38	28	0
8	98	54	50	36	8
9	102	84	30	24	5
10	97	89	NS	30	7

NS = No Sample Obtained

Table E.2. Bromide data from liquid samples obtained from static column 1. Bromide concentrations are in units of mg/L (or ppm).

Port	Day 0	Day 1	Day 2	Day 5	Day 7	Day 26
1	0	0	0	0	0	0
2	0	0	0	0	0	1
3	0	0	0	0	0	18
4	0	0	11	42	53	92
5	217	211	204	202	202	178
6	217	217	214	207	200	172
7	0	66	49	68	68	106
8	0	2	2	2	2	27
9	0	0	0	0	0	2
10	0	0	0	NS	0	0

NS = No Sample Obtained

Table E.3. Acetate data from liquid samples obtained from static column 1. Acetate concentrations are in units of mg/L (or ppm).

Port	Day 0	Day 1	Day 2	Day 5	Day 7	Day 26
1	0	0	0	0	0	0
2	0	0	0	0	0	0
3	0	0	0	0	0	35
4	0	0	47	84	144	425
5	1533	1295	1226	1172	1176	992
6	1533	1348	1277	1211	1145	908
7	0	394	169	275	255	482
8	0	0	14	23	20	72
9	0	0	0	0	0	0
10	0	0	0	NS	0	0

NS = No Sample Obtained

Table E.4. Nitrate data from liquid samples obtained from static column 1. Nitrate concentrations are in units of mg/L (or ppm).

Port	Day 0	Day 1	Day 2	Day 5	Day 7	Day 26
1	23	26	27	0	0	2
2	23	25	26	0	0	0
3	23	26	16	13	12	0
4	24	18	11	0	0	0
5	20	0	0	0	0	0
6	26	0	0	0	0	0
7	24	19	4	0	0	0
8	24	26	14	0	0	0
9	25	26	26	4	10	14
10	26	26	27	NS	19	17

NS = No Sample Obtained

Table E.5. *Pseudomonas stutzeri* KC enumeration data from liquid samples obtained from static column 1. Cell concentrations are in units of CFU/mL.

Port	Day 2	Day 5
1	ND	2.2E+04
2	ND	5.1E+04
3	4.2E+04	3.3E+04
4	2.9E+04	1.3E+05
5	8.7E+05	4.7E+04
6	9.7E+05	5.1E+04
7	6.2E+05	1.0E+05
8	3.4E+04	8.7E+04
9	ND	2.9E+05
10	ND	4.7E+04

ND = Not Detected

APPENDIX F

Experimental Data From Static Column 2

F.1 Experimental Data From Static Column 2

Table F.1. Carbon tetrachloride data from liquid samples obtained from static column 2. CT concentrations are in units of µg/L (or ppb).

Port	Background	Day 1	Day 2	Day 3	Day 4	Day 5	Day 6	Day 7
1	100	106	97	80	40	65	12	14
2	105	111	60	67	30	46	14	14
3	105	109	51	31	24	12	8	18
4	96	101	36	10	16	16	15	5
5	107	12	19	12	11	9	9	8
6	97	5	12	11	15	18	9	10
7	99	96	27	12	25	9	12	12
8	96	108	49	41	25	12	24	15
9	100	113	102	56	33	29	19	28
10	105	115	94	92	91	72	49	20

Table F.2. Bromide data from liquid samples obtained from static column 2. Bromide concentrations are in units of mg/L (or ppm).

Port	Background	Day 1	Day 2	Day 3	Day 4	Day 5	Day 6	Day 7
1	0	0	0	0	0	0	0	0
2	0	0	0	0	0	0	0	0
3	0	0	0	0	0	0	0	5
4	0	0	13	77	31	47	61	70
5	0	233	239	226	245	241	246	241
6	0	205	205	191	133	122	119	122
7	0	14	19	5	6	8	11	9
8	0	2	2	14	0	0	0	0
9	0	0	0	0	0	0	0	0
10	0	0	0	0	0	0	0	0

Table F.3. Acetate data from liquid samples obtained from static column 2. Acetate concentrations are in units of mg/L (or ppm).

Port	Background	Day 1	Day 2	Day 3	Day 4	Day 5	Day 6	Day 7
1	0	0	0	0	0	0	0	0
2	0	0	0	0	0	0	0	0
3	0	0	0	0	0	0	0	0
4	0	0	0	0	13	77	122	166
5	0	1631	1439	1342	1476	1439	1457	1415
6	0	925	816	410	406	373	355	374
7	0	85	41	83	30	32	34	38
8	0	0	0	0	16	0	0	0
9	0	0	0	0	0	0	0	0
10	0	0	0	0	0	0	0	0

Table F.4. Nitrate data from liquid samples obtained from static column 2. Nitrate concentrations are in units of mg/L (or ppm).

Port	Background	Day 1	Day 2	Day 3	Day 4	Day 5	Day 6	Day 7
1	74	76	80	69	63	20	16	11
2	77	79	90	74	45	8	7	8
3	65	89	60	44	43	9	8	3
4	77	60	10	31	10	6	4	2
5	80	37	5	7	0	0	0	0
6	79	32	25	0	0	0	0	0
7	73	73	74	12	9	5	6	4
8	77	75	84	47	29	20	7	2
9	74	83	70	77	44	20	6	1
10	72	72	72	74	62	62	42	32

Table F.5. *Pseudomonas stutzeri* KC enumeration data from liquid samples obtained from static column 2. Cell concentrations are in units of CFU/mL.

Port	Background	Day 1	Day 2	Day 3	Day 4	Day 5
1	ND	ND	ND	ND	ND	1.2E+04
2	ND	ND	ND	ND	ND	2.0E+04
3	ND	ND	ND	ND	8.0E+03	9.1E+04
4	ND	ND	ND	1.0E+05	1.0E+05	4.1E+04
5	ND	6.4E+05	3.7E+05	1.9E+05	3.9E+05	3.2E+04
6	ND	6.0E+05	3.4E+06	6.0E+05	4.4E+05	1.1E+05
7	ND	ND	ND	1.4E+05	6.2E+05	6.4E+04
8	ND	ND	ND	ND	1.9E+04	2.8E+04
9	ND	ND	ND	ND	ND	8.9E+04
10	ND	ND	ND	ND	ND	ND

ND = Not Detected

Table F.6. Microbead concentration data from liquid samples obtained from static column 2. Microbead concentrations are in units of g/mL.

Port	Background	Day 1	Day 3	Day 4	Day 5	Day 6
1	0.052	0.050	0.107	0.109	0.048	0.060
2	0.064	0.051	0.111	0.061	0.040	0.079
3	0.058	0.053	0.110	0.056	0.105	0.089
4	0.054	0.078	0.078	0.152	0.236	0.189
5	0.051	1.476	1.327	1.283	1.354	1.354
6	0.051	1.343	1.357	1.349	1.369	1.318
7	0.046	0.064	0.314	0.108	0.138	0.265
8	0.054	0.054	0.095	0.107	0.093	0.093
9	0.048	0.053	0.093	0.104	0.086	0.087
10	0.050	0.052	0.096	0.104	0.078	0.053

APPENDIX G

Development of an Energy Model

G.1 Development of an energy model

The development of an energy model to describe the growth and transport of strain KC is presented in Chapter 5. For completeness, the procedure for estimating some of the important model parameters will be presented here. Specifically, derivation of the specific utilization rate equation, estimation of $Y_{cat,ATP}$, $Y_{mot,ATP}$, $Y_{x,ATP}$, and $Y_{n,x}$, and calculation of the energy coefficients (or Z terms) are presented.

G.2 Derivation of specific utilization rate equation

Equation 5.20 was derived to describe the observed growth rate for motile cells:

$$\mu_{obs} = \mu_{\max} M_n M_s - b\left(1 - M_s\right) - \frac{Y_{mot,ATP} V}{Y_{x,ATP}}\left(1 - M_s\right) \qquad \text{(G.1)}$$

where M_n is defined in Eq. 5.15, and M_s is in terms of the concentration of the growth substrate . The last term in Eq. 5.20 is a term that relates decay to the energy used for motility. An energy coefficient, Z_{KC}, is used to define the ratio of $Y_{mot,ATP}$ to $Y_{x,ATP}$ and the one-dimensional swimming speed of the cells, V, is defined as:

$$V = V_{\max} M_s' \qquad \text{(G.2)}$$

where V_{max} is the maximum cell swimming speed (40 μm/sec or 3.5 cm/day) and M_s' is a growth substrate saturation term. Based on the experimental conditions of the static column experiment, an assumption for this model is that the value of M_s' is equal to one.

This assumption was made to account for a electron availability to the chemotactic cells in the absence of acetate. In this experimental system, it was possible that energy was available to the cells in the form of storage granules. Also, organic carbon content of the Schoolcraft sediments was measured to be 0.03%. A portion of this carbon may have also been available to the chemotactic strain KC cells.

For acetate consumption, Eq. 5.4 describes the specific rate of acetate utilization in terms of μ_{true}, $Y_{s,x}$, and $q_{s,m}$. Eq. 5.18 is the result of a derivation for μ_{true}, and from Eq. 5.6 a relationship for $q_{s,m}$, in terms of β and $Y_{cat,ATP}$, may be substituted to yield the following equation for q_s:

$$q_s = \frac{\mu_{\max} M_n M_s}{Y_{s,x}} + \frac{\delta . M_s}{Y_{cat,ATP}} + \frac{\psi . M_s}{Y_{cat,ATP}} \tag{G.3}$$

where ψ is the product of $Y_{mot,ATP}$ and V. Two additional energy coefficients will be defined to simplify Eq. G.3.

$$Z_{ac,1} = \frac{\delta}{Y_{cat,ATP}} \tag{G.4}$$

$$Z_{ac,2} = \frac{Y_{mot,ATP} V}{Y_{cat,ATP}} \tag{G.5}$$

Therefore, an equation for q_s that accounts for consumption of acetate due to cell growth, cell maintenance, and cell motility may be written as:

$$q_s = \frac{\mu_{\max} M_n M_s}{Y_{s,x}} + Z_{ac,1} M_s + Z_{ac,2} V(1 - M_s) \qquad \text{(G.6)}$$

where V, the swimming speed of the cells is equal to the product of V_{max} and M_s.

G.3 Estimation of $Y_{cat,ATP}$

$Y_{cat,ATP}$ is the term used to describe the ATP yield on the catabolic substrate acetate. Figure G.1 is a diagram showing the metabolic pathway of a carbon substrate (acetate) to 3-phosphoglycerate (PGA), from which all cell components are synthesized. The consumption and generation of ATP is also shown.

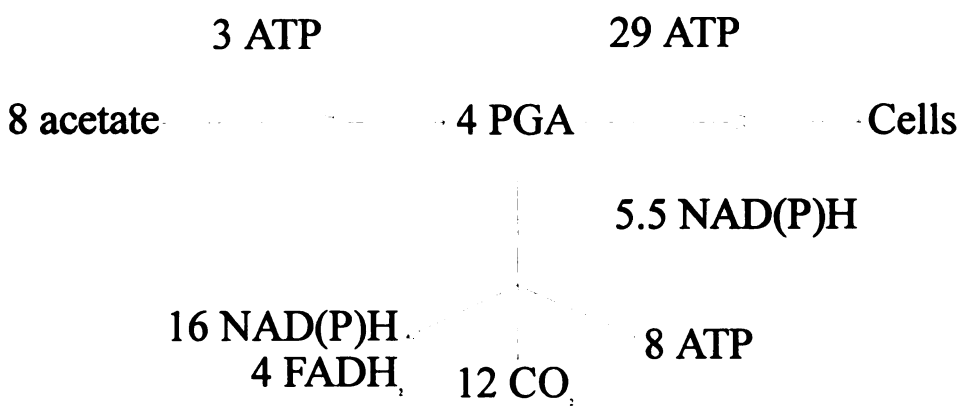

Figure G.1. Synthesis of biomass from acetate (from Babel and Müller, 1985).

The production of cells from 8 moles of acetate requires 32 moles ATP and 5.5 moles NAD(P)H (or an additional 16.5 moles ATP), or a total of 48.5 moles ATP. Therefore, the number of moles of ATP required per mole of acetate is 48.5/8 or 6.06 moles ATP per mole of acetate. Converting this to moles ATP per mg of acetate yields 0.000103 moles ATP per mg of acetate. This is the value used for $Y_{cat,ATP}$ in development of the computer model.

G.4 Estimation of $Y_{mot,ATP}$

The parameter $Y_{mot,ATP}$ is a measure of the number of moles of ATP required for cell motility. In Brock and Madigan (1991), it is shown that it takes ~1000 protons to rotate a flagellum once. During the process of oxidative phosphorylation, it takes 4 protons to produce 1 molecule of ATP. Therefore, a cell requires ~250 molecules of ATP to rotate its flagellum once. If a typical flagellum rotates 200 times per second (Brock and Madigan, 1991), then a total of 50,000 ATPs are required per cell per second to drive motility. Using Avagadro's number (6.02×10^{23} molecules per mole) and assuming that one bacterial cell weighs ~3×10^{-10} mg, the number of moles of ATP required per mg cell per second is ~2.77×10^{-10}. Converting the seconds to days yield a value for $Y_{mot,ATP}$ of 2.4×10^{-5} mole ATP required per mg cell per day.

G.5 Estimation of $Y_{x,ATP}$

A generally accepted value for the yield (in grams dry weight) of cells per mole ATP is 10.5 (Stouthamer and Bettenhaussen, 1973). Assuming that cells are only 50%

efficient at utilizing ATP as an energy source, the value of $Y_{x,ATP}$ is calculated to be 1.9 x 10^{-4} moles ATP required per mg cell (dry weight).

G.6 Calculation of $Y_{n,x}$

The value $Y_{n,x}$ was estimated by stoichiometry according to the following equations:

$$\frac{1}{28}C_5H_7O_2N + \frac{11}{28}H_2O \rightarrow \frac{5}{28}CO_2 + \frac{1}{28}NO_3^- + \frac{29}{28}H^+ + e^-$$

$$\frac{1}{10}\left[2NO_3^- + 12H^+ + 10e^- \rightarrow N_2 + 6H_2O\right]$$

sum: $$\frac{1}{28}C_5H_7O_2N + \left(\frac{1}{5} - \frac{1}{28}\right)NO_3^- + \left(\frac{6}{5} - \frac{29}{28}\right)H^+ \rightarrow \frac{5}{28}CO_2 + \left(\frac{3}{5} - \frac{11}{28}\right)H_2O + \frac{1}{10}N_2$$

$$\frac{massNO_3^-}{massCell} = \frac{\left(\frac{1}{5} - \frac{1}{28}\right)mmoleNO_3^- x62\frac{mg}{mmole}}{\frac{1}{28}mmoleCellx113\frac{mg}{mmole}} = 2.52\frac{mgNO_3^-}{mgCell}$$

G.7 Calculation of Z coefficients

$$Z_{KC} = \frac{Y_{mot,ATP}}{Y_{x,ATP}} = \frac{2.4x10^{-5}\ moleATP/mgCell - day}{1.9x10^{-4}\ moleATP/mgCell} = 0.13day^{-1}$$

$$Z_{ac,1} = \frac{\delta}{Y_{cat,ATP}} = \frac{3.4x10^{-5}\ moleATP/mgAcetate - day}{1.03x10^{-4}\ moleATP/mgAcetate} = 0.33day^{-1}$$

For use in the computer model, the value of $Z_{ac,1}$ was multiplied by three to adequately account for the acetate consumption by the motile strain KC cells.

$$Z_{ac,2} = \frac{Y_{mot,ATP}}{Y_{cat,ATP}} = \frac{2.4x10^{-5}\ moleATP/mgCell-day}{1.03x10^{-4}\ moleATP/mgAcetate} = 0.23\frac{mgAcetate}{mgCell-day}$$

$$Z_{nit} = \frac{Y_{mot,ATP}}{Y_{x,ATP}Y_{n,x}} = \frac{\left(2.4x10^{-5}\ moleATP/mgCell-day\right)\left(2.52\ mgNitrate/mgCell\right)}{\left(1.9x10^{-4}\ moleATP/mgCell\right)} = 0.32\frac{mgNitrate}{mgCell-day}$$

For use in the computer model, the value of Z_{nit} was increased by five orders of magnitude to adequately account for the nitrate consumption by the motile strain KC cells.

G.8 Literature cited

Babel, W. and R.H. Müller. 1985. Mixed substrate utilization in micro-organisms: Biochemical aspects and energetics. *J. Gen. Microbiol.* **131**:39-45.

Brock, T.D. and M.T. Madigan. 1991. *Biology of Microorganisms*. Prentice Hall, Englewood Cliffs, New Jersey.

Knoll, W.H. 1994. Factors influencing the competitive advantage of *Pseudomonas* sp. strain KC for subsequent remediation of a carbon tetrachloride impacted aquifer. Master's Thesis, Department of Civil and Environmental Engineering, Michigan State University, East Lansing, Michigan.

Stouthamer, A.H. and C. Bettenhaussen. 1973. Utilization of energy for growth and maintenance in continuous and batch cultures of microorganisms. *Biochimica et Biophysica Acta.* **301**:53-70.

APPENDIX H

Quickest Formulation for Computer Model

H.1 Quickest solution for dispersion and advective terms

Consider the general form of the one-dimensional advective-dispersive equation for C, with a reaction term Z:

$$\frac{\partial.C}{\partial.t} = D\frac{\partial^2 C}{\partial.x^2} - V\frac{\partial.C}{\partial.x} + Z \tag{H-1}$$

The Quickest formulation for the dispersion term is:

$$D\frac{\partial^2 C_i}{\partial.x^2} \approx \frac{D}{\Delta x^2}\left[\begin{array}{l} C_{i+1} - 2C_i + C_{i-1} - \dfrac{CO}{2}\left(C_{i-1} + C_{i+1} - 2C_i\right) \\ + \dfrac{CO}{2}\left(C_{i-2} + C_i - 2C_{i-1}\right) \end{array}\right] \tag{H-2}$$

and the Quickest formulation for the advective term is:

$$V\frac{\partial^2 C_i}{\partial.x^2} \approx \frac{V}{\Delta x}\left[\begin{array}{l} \dfrac{1}{2}\left(C_{i+1} - C_{i-1}\right) + \dfrac{CO}{2}\left(-C_{i-1} + 2C_i - C_{i-1}\right) \\ + \dfrac{q}{6}\left(C_{i-2} - 3C_{i-1} + 3C_i - C_{i+1}\right) \end{array}\right] \tag{H-3}$$

where V is the linear velocity, i is the node position, CO is the Courant number, and α is the dispersion parameter. CO, α, and q are defined as:

$$CO = \frac{V\Delta t}{\Delta x} \tag{H-4}$$

$$\alpha = \frac{D\Delta t}{\Delta x^2} \tag{H-5}$$

$$q = 1 - CO^2 - 3\alpha \tag{H-6}$$

The Euler approximation for the time derivative is shown in the following equation, where k designates the current time, $t = k\Delta t$:

$$\frac{\partial . C_i}{\partial . t} = \frac{C_i^{k+1} - C_i^k}{\Delta t} \tag{H-7}$$

Table H.1 shows the reaction terms for the six mass-balance equations in the computer model.

Table H.1. Reaction terms for the six mass-balance equations in the model.

Model	C	Z
1	C_{CT}	$-\frac{k'C_{CT}}{R_{CT}}\left(X_{KC}+\bar{X}_{KC}\right)$ $-\frac{\rho_b \kappa}{nR_{CT}}\left[(1-f)K_d C_{CT}-S_{CT}\right]$
2	X_{KC}	$+\left[\mu_{\max} M_n M_s - b_{KC}(1-M_s)\right]X_{KC}$ $-Z_{KC}\left(V_{\max} M_s'\right)(1-M_s)X_{KC}$ $+K_{de} M_s \bar{X}_{KC} - K_{at} X_{KC}$
3	C_a	$-\frac{\mu_{\max} M_n M_s}{Y_a R_a}\left(X_{KC}+\bar{X}_{KC}\right)$ $-Z_{ac,1} M_s\left(X_{KC}+\bar{X}_{KC}\right)$ $-Z_{ac,2}\left(V_{\max} M_s'\right)(1-M_s)X_{KC}$
4	$\bar{X}_{KC}$	$+\left[\mu_{\max} M_n M_s - b_{KC}(1-M_s)\right]\bar{X}_{KC}$ $+K_{at} X_{KC} - K_{de} M_s \bar{X}_{KC}$
5	C_n	$-\frac{\mu_{\max} M_n M_s}{Y_n R_n}\left(X_{KC}+\bar{X}_{KC}\right)$ $-\frac{b_{KC}}{Y_{nb} R_n}(1-M_s)\left(X_{KC}+\bar{X}_{KC}\right)$ $-Z_{nit}\left(V_{\max} M_s'\right)(1-M_s)X_{KC}$
6	S_{CT}	$\kappa\left[(1-f)K_d C_{CT}-S_{CT}\right]$

The Quickest solution can be written for each of the six mass-balance equations in the computer model:

Carbon tetrachloride in liquid phase

$$C_{CT_i}^{k+1} = \left[\frac{CO}{R_{CT}}\left(\alpha - \frac{1}{6} + \frac{CO^2}{6}\right)\right] C_{CT_{i-2}}^{k} + \left[\frac{1}{R_{CT}}\left(\alpha - 2\alpha CO + \frac{2}{3}CO + \frac{CO^2}{2} - \frac{CO^3}{6}\right)\right] C_{CT_{i-1}}^{k}$$
$$+ \left[\begin{array}{l} \frac{1}{R_{CT}}\left(R_{CT} + 3\alpha CO - 2\alpha - CO^2 - \frac{CO}{2} + \frac{CO^3}{2}\right) \\ -\frac{k'\Delta t}{R_{CT}}\left(X_{KC_i}^{k} + \overline{X}_{KC_i}^{k}\right) - \frac{\rho_b \kappa}{nR_{CT}}(1-f)K_d \Delta t \end{array}\right] C_{CT_i}^{k} \qquad \text{(H-8)}$$
$$+ \left[\frac{1}{R_{CT}}\left(\alpha - CO\alpha - \frac{1}{3}CO + \frac{CO^2}{2} - \frac{CO^3}{6}\right)\right] C_{CT_{i+1}}^{k} + \frac{\rho_b \kappa}{nR_{CT}} \Delta t S_{CT_i}^{k}$$

Planktonic Pseudomonas stutzeri KC

$$X_{KC_i}^{k+1} = \left[CO\left(\alpha - \frac{1}{6} + \frac{CO^2}{6}\right)\right] X_{KC_{i-2}}^{k} + \left(\alpha - 2\alpha CO + \frac{2}{3}CO + \frac{CO^2}{2} - \frac{CO^3}{6}\right) X_{KC_{i-1}}^{k}$$
$$+ \left[\begin{array}{l} \left(R_{KC} + 3\alpha CO - 2\alpha - CO^2 - \frac{CO}{2} + \frac{CO^3}{2}\right) \\ +\left(\mu_{\max} M_n M_s - b_{KC}(1-M_s) - Z_{KC}\left(V_{\max} M_s'\right)(1-M_s) - K_{at}\right)\Delta t \end{array}\right] X_{CT_i}^{k} \qquad \text{(H-9)}$$
$$+ \left(\alpha - CO\alpha - \frac{1}{3}CO + \frac{CO^2}{2} - \frac{CO^3}{6}\right) X_{KC_{i+1}}^{k} + K_{de} M_s \Delta t \, \overline{X}_{KC_i}^{k}$$

Acetate

$$C_{ai}^{k+1} = \left[\frac{CO}{R_a}\left(\alpha - \frac{1}{6} + \frac{CO^2}{6}\right)\right] C_{ai-2}^{k} + \left[\frac{1}{R_a}\left(\alpha - 2\alpha CO + \frac{2}{3}CO + \frac{CO^2}{2} - \frac{CO^3}{6}\right)\right] C_{ai-1}^{k}$$
$$+ \left[\frac{1}{R_a}\left(R_a + 3\alpha CO - 2\alpha - CO^2 - \frac{CO}{2} + \frac{CO^3}{2}\right) C_{ai}^{k}\right.$$
$$+ \left[\frac{1}{R_a}\left(\alpha - CO\alpha - \frac{1}{3}CO + \frac{CO^2}{2} - \frac{CO^3}{6}\right)\right] C_{ai+1}^{k} - \left(\frac{\mu_{max} M_n M_s}{Y_a R_a} + Z_{ac,1} M_s\right) \Delta t \left(X_{KCi}^{k} + \bar{X}_{KCi}^{k}\right) \quad \text{(H-10)}$$
$$- Z_{ac,2}\left(V_{max} M_s'\right)\left(1 - M_s\right) \Delta t X_{KCi}^{k}$$

Attached Pseudomonas stutzeri KC

$$\bar{X}_{KCi}^{k+1} = \left[\left(\mu_{max} M_n M_s - b_{KC}\left(1 - M_s\right) - K_{de} M_s\right)\right] \Delta t \bar{X}_{KCi}^{k} + K_{at} \Delta t X_{KCi}^{k} \quad \text{(H-11)}$$

Nitrate

$$C_{ni}^{k+1} = \left[\frac{CO}{R_n}\left(\alpha - \frac{1}{6} + \frac{CO^2}{6}\right)\right] C_{ni-2}^{k} + \left[\frac{1}{R_n}\left(\alpha - 2\alpha CO + \frac{2}{3}CO + \frac{CO^2}{2} - \frac{CO^3}{6}\right)\right] C_{ni-1}^{k}$$
$$+ \left[\frac{1}{R_n}\left(R_n + 3\alpha CO - 2\alpha - CO^2 - \frac{CO}{2} + \frac{CO^3}{2}\right) C_{ni}^{k}\right.$$
$$+ \left[\frac{1}{R_n}\left(\alpha - CO\alpha - \frac{1}{3}CO + \frac{CO^2}{2} - \frac{CO^3}{6}\right)\right] C_{ni+1}^{k} \quad \text{(H-12)}$$
$$- \left[\frac{\mu_{max} M_n M_s}{Y_n R_n} + \frac{b_{KC}}{Y_{nb} R_n}\left(1 - M_s\right)\right] \Delta t \left(X_{KCi}^{k} + \bar{X}_{KCi}^{k}\right)$$
$$- Z_{nit}\left(V_{max} M_s'\right)\left(1 - M_s\right) \Delta t X_{KCi}^{k}$$

Carbon tetrachloride on solid phase

$$S_i^{k+1} = -\beta \Delta t S_{CTi}^{k} + \beta\left(1 - f\right) K_d C_{CTi}^{k} \quad \text{(H-13)}$$

H.2 FORTRAN Code

```
C*************************************************************************
C  Quickest method combined with Euler
C  Static model aquifer column
C  Michael E. Witt, PhD Candidate
C  Department of Civil and Environmental Engineering
C  Michigan State University
C  SOLUTION OF THE 1-D TRANSPORT EQUATION
C    RdC/dt = Dd^2C/dx^2 - vdC/dx
C  1-D  TRANSPORT EQUATIONS FOR 6 MODELS
C    Model 1 is for Carbon Tetrachloride
C      RctdCct/dt=Dctd^2Cct/dx^2 - k'Cct(Xkc + XSkc)
C              -rho*kappa/por[(1-frac)KdCct-Sct]
C    Model 2 is for KC Cells
C      RkcdX/dt=RMCeff(Mn)d^2Xkc/dx^2
C        -[Xo(krc/(krc+Cn)^2)dCn/dx dXkc/dx]
C        -Zkc[vmax(Msprime)(1-Ms)]Xkc
C        +[mumaxMnMs-bkc(1-Ms)-Kat]Xkc+Kde(Ms)XSkc
C    Model 3 is for Acetate
C      RadCa/dt=Dad^2Ca/dx^2-mumaxMnMs/Ya(Xkc+XSkc)-Zacone(Ms)(xkc+xskc)
C        -Zactwo[vmax(Msprime)(1-Ms)]Xkc
C    Model 4 is for KC Cells associated with solid phase
C      RkcdXSkc/dt=[mumaxMnMs-bkc(1-Ms)-Kde(Ms)]XSkc + KatXkc
C    Model 5 is for nitrate
C      RndCn/dt=Dnd^2Cn/dx^2-mumaxMnMs/Yn(Xkc+XSkc)
C        -bkc/Ynb(1-Ms)(Xkc+XSkc)
C        -Znit[vmax(Msprime)(1-Ms)]Xkc
C    Model 6 is for sorption of Carbon Tetrachloride
C      dSct/dt=kappa[(1-frac)KdCct-Sct]
C*************************************************************************
C  Variables Declaration
C*************************************************************************
C
implicit double precision (a-h,o-z)
dimension c(43,6)
double precision Ksa,Ksn,kprime,Kat,Kde,mumax,cour,alpha,
          Kd,por,kappa,frac,rho,Ms,Mn,Msprime
common /cc/ v,d,dx,Ksa,Ksn,mumax,Kat,Kde,kprime,bkc,retard(6)
common /cc/ qest,term1a,term1b,term1c,term2a,term2b,term2c
common /cc/ cour,alpha,Kd,por,tort,rmc,Xo,Kra,kappa,frac,rho
common /cc/ xkccoef,no3t,zkc,zacone,zactwo,znit,vmax
common /c/ nnodes,Ya,Yn,Ynb,Mn,Ms,Msprime
common /counter/kk
open(4,file='alldata',status='unknown')
open(5,file='day1',status='unknown')
open(6,file='day2',status='unknown')
open(7,file='day5',status='unknown')
open(8,file='day7',status='unknown')
open(9,file='day26',status='unknown')
nnodes = 43
C
C*************************************************************************
C                  INITIAL CONDITIONS AT t = 0
```

```
C*************************************************************************
C
mumax = 2.0d0
Ksa = 1.0d0
Ksn = 12.0d0
Ya = 0.4d0
Yn = 0.25d0
Ynb = 0.46d0
kprime = 2.7d0
Kat = 0.9d0
Kde = 0.18d-1
bkc = 0.1d0
zkc = 0.13d0
zacone = 0.99d0
zactwo = 0.23d0
znit = 0.32d5
v = 0.0d0
vmax = 3.5d0
Kd = 2.6d-7
frac = 0.12d0
kappa = 0.6d0
rho = 1.59d6
por = 0.32d0
tort = 2.0d0
rmc = 6.0d1
Xo = 6.0d0
Kra = 1.0d0
retard(1) = 2.3d0
retard(2) = 1.0d0
retard(3) = 1.0d0
retard(4) = 1.0d0
retard(5) = 1.0d0
retard(6) = 1.0d0
d = 0.075d0
dt = 0.001d0
do 150 k = 1,6,1
        do 100 i = 1,nnodes,1
          if (k.eq.1) then
            c(i,k) = 0.1d0
          else if (k.eq.5) then
            c(i,k) = 25.0d0
          else if (k.eq.6) then
            c(i,k) = (1.0-frac)*Kd*c(i,1)
          else
            c(i,k) = 0.0d0
          end if
100     continue
150   continue
C
C*************************************************************************
C       PRINTING SCHEDULE
C*************************************************************************
C
t = 0.0d0
m = 0
```

```
f = 0
n = 0
t0 = 0.5d0
dx = 1.0d0
ntime = 26.0d0/dt
cour = (v*dt)/dx
alpha = (d*dt)/(dx*dx)
C
C*************************************************************************
C       STABILITY TEST CO<1 and alpha<(3-2CO)(1-DO^2)/^(1-2CO)
C*************************************************************************
C
if(cour.lt.1) then
        if (cour.lt.0.5) then
                temp=(3-2*cour)*(1-(cour*cour))/(6*(1-2*cour))
                if (alpha.lt.temp) then
                        write(4,*)' Stability condition satisfied ie. cour<1'
                endif
        else if(cour.gt.0.5) then
                temp=(3-2*cour)*((cour*cour)-1)/(6*(1-2*cour))
                write(4,*)' Stability condition satisfied ie. cour<1'
        end if
else
        write(4,*)' Stability not satisfied'
endif
C
C*************************************************************************
C       BOUNDARY CONDITIONS
C*************************************************************************
C
j1=0
do 200 kk = 1,ntime+1
    j1=j1+1
    if (kk.eq.1) then
          do 250 j=1,5
          c(j,2) = 2.0d1
          c(j,3) = 1.533d3
250         continue
     endif
C
C*************************************************************************
C       SIMULATION
C*************************************************************************
C
      call rungn(c,dt)
      t = t + dt
      m = m + 1
      h = h + 1
      f = f + 1
      if (m.eq.1000) then
        do 300 i = 1,nnodes,1
             dis = (i-1)*dx
         write(4,3) t,dis,c(i,1),c(i,2),c(i,3),c(i,4),c(i,5),c(i,6)
3        format(2x,f6.3,2x,f5.1,2x,6(f18.12,2x))
300       continue
```

```
        m = 0
        n = n+1
      endif
           if (kk.eq.1000) then
                  do 305 i = 1,nnodes
                  dis=(i-1)*dx
                  write(5,9)kk,dis,c(i,1),c(i,2),c(i,3),c(i,4),c(i,5),c(i,6)
9                 format(2x,i7,2x,f5.1,2x,6(f18.12,2x))
305         continue
            else if (kk.eq.2000) then
                  do 306 i = 1,nnodes
                  dis=(i-1)*dx
                  write(6,10)kk,dis,c(i,1),c(i,2),c(i,3),c(i,4),c(i,5),c(i,6)
10                format(2x,i7,2x,f5.1,2x,6(f18.12,2x))
306         continue
            else if (kk.eq.5000) then
                  do 307 i = 1,nnodes
                  dis=(i-1)*dx
                  write(7,11)kk,dis,c(i,1),c(i,2),c(i,3),c(i,4),c(i,5),c(i,6)
11                format(2x,i7,2x,f5.1,2x,6(f18.12,2x))
307         continue
            else if (kk.eq.7000) then
                  do 308 i = 1,nnodes
                  dis=(i-1)*dx
                  write(8,12)kk,dis,c(i,1),c(i,2),c(i,3),c(i,4),c(i,5),c(i,6)
12                format(2x,i7,2x,f5.1,2x,6(f18.12,2x))
308         continue
            else if (kk.eq.26000) then
                  do 309 i = 1,nnodes
                  dis=(i-1)*dx
                  write(9,13)kk,dis,c(i,1),c(i,2),c(i,3),c(i,4),c(i,5),c(i,6)
13                format(2x,i7,2x,f5.1,2x,6(f18.12,2x))
309         continue
            end if
      if (j1.eq.100) then
        write (*,17) kk,t,m,n
17       format(2x,i8,2x,f7.3,2x,i5,2x,i7)
        j1=0
      endif
200    continue
end
C
C*************************************************************************
C                        RUNGE KUTTA
C*************************************************************************
C
subroutine rungn(c,dt)
implicit double precision (a-h,o-z)
dimension c(43,6)
double precision k1(43,6)
double precision Ksa,Ksn,kprime,Kat,Kde,mumax,cour,alpha,
          Kd,por,kappa,frac,rho,Mn,Ms,Msprime
common /cc/ v,d,dx,Ksa,Ksn,mumax,Kat,Kde,kprime,bkc,retard(6)
common /cc/ qest,term1a,term1b,term1c,term2a,term2b,term2c
common /cc/ cour,alpha,Kd,por,tort,rmc,Xo,Kra,kappa,frac,rho
```

```
common /cc/ xkccoef,no3t,zkc,zacone,zactwo,znit,vmax
common /c/ nnodes,Ya,Yn,Ynb,Mn,Ms,Msprime
common /counter/kk
do 50 k = 1,6
      do 100 i = 1,nnodes,1
          cct  = c(i,1)
          cxkc = c(i,2)
          cact = c(i,3)
          cxskc= c(i,4)
          cno3 = c(i,5)
          csct = c(i,6)
          Mn = cno3/(Ksn+cno3)
          Ms = cact/(Ksa+cact)
          Msprime = 1.0d0
          if (i.eq.1) then
               c1 = c(i+1,k)
               c2 = c(i,k)
          else if (i.eq.2) then
               c1 = c(i-1,k)
               c2 = c(i-1,k)
          else
               c1 = c(i-2,k)
               c2 = c(i-1,k)
          endif
          c3 = c(i,k)
          c4 = c(i+1,k)
          k1(i,k) = fxi(c1,c2,c3,c4,cct,cxkc,cxskc,cno3,csct,i,k)*dt
 100    continue
 50   continue
     do 600 k = 1,6
      do 500 i = 1,nnodes
       c(i,k) = c(i,k) + k1(i,k)
            if (c(i,k).lt.0) then
             c(i,k) = 0.0
            endif
 500    continue
 600   continue
          return
          end
C
C*************************************************************************
C       FUNCTION FXi
C*************************************************************************
C
double precision function fxi(c1,c2,c3,c4,ct,xkc,xskc,no3,sct,ind,model)
implicit double precision (a-h,o-z)
double precision Ksa,Ksn,kprime,Kat,Kde,mumax,cour,alpha,
           Kd,por,no3,kappa,frac,rho,Ms,Mn,Msprime
double precision term1a,term1b,term1c,term2a,term2b,term2c,qest
common /cc/ v,d,dx,Ksa,Ksn,mumax,Kat,Kde,kprime,bkc,retard(6)
common /cc/ qest,term1a,term1b,term1c,term2a,term2b,term2c
common /cc/ cour,alpha,Kd,por,tort,rmc,Xo,Kra,kappa,frac,rho
common /cc/ xkccoef,no3t,zkc,zacone,zactwo,znit,vmax
common /c/  nnodes,Ya,Yn,Ynb,Mn,Ms,Msprime
common /counter/kk
```

```
r = retard(model)
qest = (1.0-(cour*cour)-3.0*alpha)
term1a = c4-2*c3+c2
term1b = (-cour/2.0)*(c2+c4-2*c3)
term1c = (cour/2.0)*(c1+c3-2*c2)
term1 = (term1a+term1b+term1c)/(dx*dx)
term2a = (0.5)*(c4-c2)
term2b = (cour/2.0)*((-1.0)*c4+2*c3-c2)
term2c = (qest/6.0)*(c1-3*c2+3*c3-c4)
term2 = (-1.0)*(term2a+term2b+term2c)/dx
if (model.eq.5) then
        no3t = -1*term2
endif
if (ind.eq.2) then
        term1c = (cour/2.0)*(c2+c3-2*c2)
        term1 = (term1a+term1b+term1c)/(dx*dx)
        term2c = (qest/6.0)*(c2-3*c2+3*c3-c4)
        term2 = (-1.0)*(term2a+term2b+term2c)/dx
else if (ind.eq.nnodes) then
        term2 = 0.0d0
        term1a = c3-2*c3+c2
        term1b = (-cour/2.0)*(c2+c3-2*c3)
        term1 = (term1a+term1b+term1c)/(dx*dx)
endif
if (model.eq.1) then
        term2 = 0.0d0
        term3 = -kprime*ct*(xkc+xskc)
        term4 = -kappa*rho*(1.0-frac)*Kd*ct/por
        term5 = rho*kappa*sct/por
        term6 = 0.0d0
        xkccoef = 0.0d0
else if (model.eq.2) then
        d = d + rmc*Mn*(por/tort)
        xkccoef = -Xo*(por/tort)*(Kra/((Kra+no3)*(Kra+no3)))*no3t
        term3 = ((mumax*1.0*Mn)-bkc*(1.0-Ms))*xkc
        term4 = -zkc*vmax*(Msprime)*(1.0-Ms)*xkc
        term5 = -Kat*xkc
        term6 = Kde*(Ms)*xskc
else if (model.eq.3) then
        term2 = 0.0d0
        term3 = -mumax*Ms*Mn*(xkc+xskc)/Ya
        term4 = -zacone*(Ms)*(xkc+xskc)
        term5 = -zactwo*vmax*(Msprime)*(1.0-Ms)*xkc
        term6 = 0.0d0
        xkccoef = 0.0d0
else if (model.eq.4) then
        term1 = 0.0d0
        term2 = 0.0d0
        term3 = mumax*Mn*Ms*xskc
        term4 = -bkc*(1.0-Ms)*xskc
        term5 = -Kde*(Ms)*xskc
        term6 = Kat*xkc
        xkccoef = 0.0d0
else if (model.eq.5) then
        term2 = 0.0d0
```

```
            term3 = -mumax*Mn*1.0*(xkc+xskc)/Yn
            term4 = -bkc*(1.0-Ms)*(xkc+xskc)/Ynb
            term5 = -znit*vmax*(Msprime)*(1.0-Ms)*xkc
            term6 = 0.0d0
            xkccoef = 0.0d0
else if (model.eq.6) then
            term1 = 0.0d0
            term2 = 0.0d0
            term3 = kappa*(1.0-frac)*Kd*ct
            term4 = -kappa*sct
            term5 = 0.0d0
            term6 = 0.0d0
            xkccoef = 0.0d0
endif
fxi = 0.0d0
fxi =term1*d/r+term2*(xkccoef)/r+term3/r+term4/r+term5/r+term6/r
d = 0.075d0
return
end
```

H.3 Numerical predictions for solid-phase CT and solid-phase strain KC

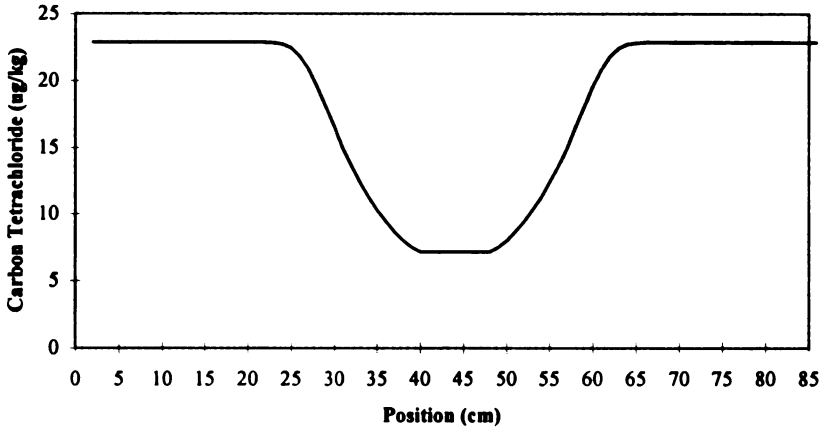

Figure H.1. Predicted carbon tetrachloride concentration profile on the solid phase on day 2 in the static model aquifer column. CT concentrations are in units of μg/kg.

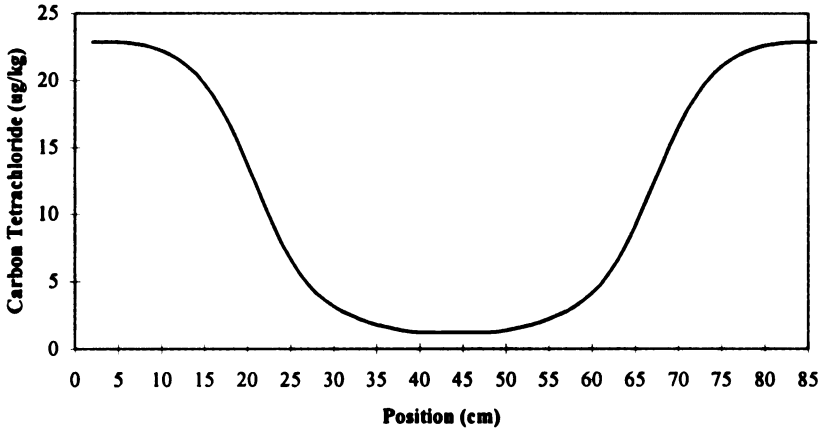

Figure H.2. Predicted carbon tetrachloride concentration profile on the solid phase on day 5 in the static model aquifer column. CT concentrations are in units of μg/kg.

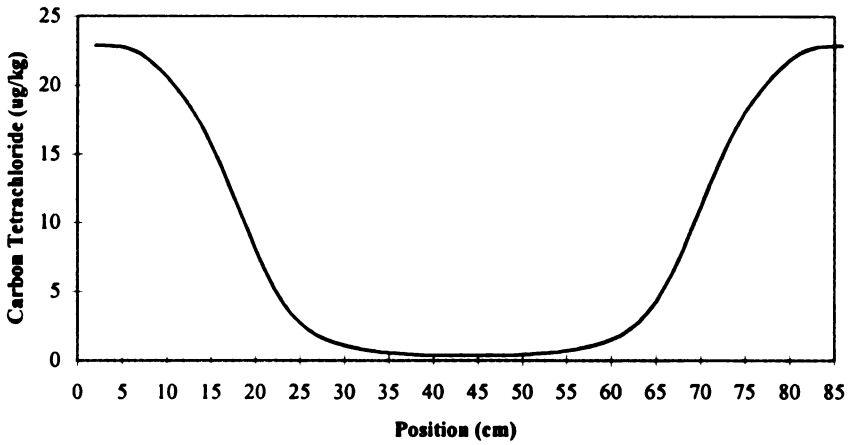

Figure H.3. Predicted carbon tetrachloride concentration profile on the solid phase on day 7 in the static model aquifer column. CT concentrations are in units of µg/kg.

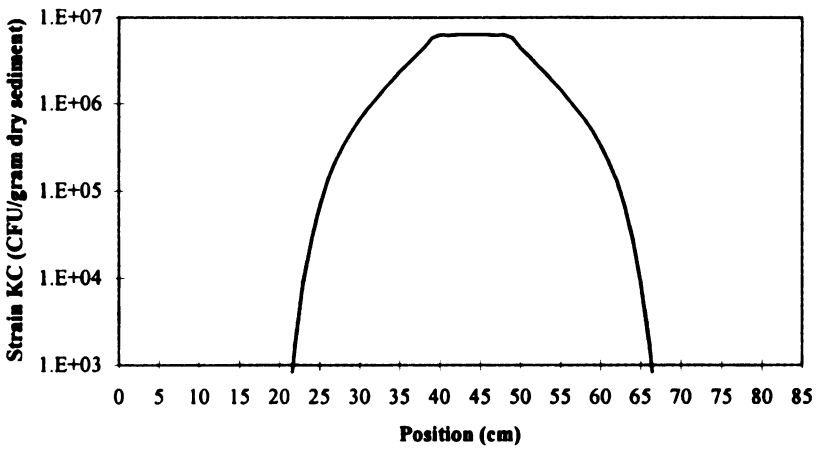

Figure H.4. Predicted strain KC concentration profile on the solid phase on day 2 in the static model aquifer column. CT concentrations are in units of CFU/gram dry sediment.

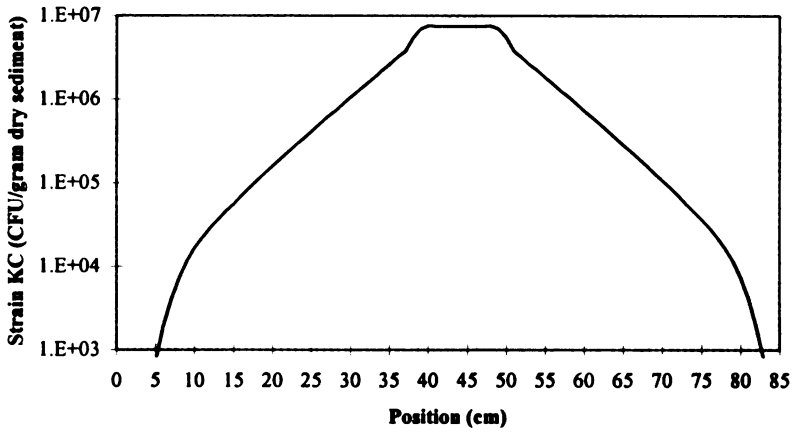

Figure H.5. Predicted strain KC concentration profile on the solid phase on day 5 in the static model aquifer column. CT concentrations are in units of CFU/gram dry sediment.

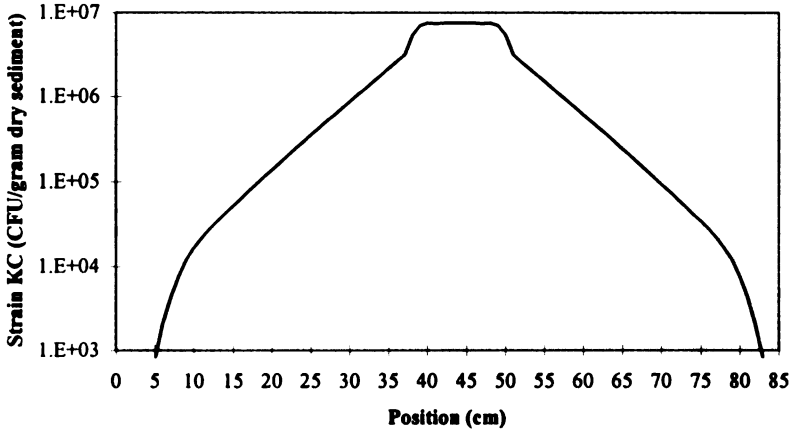

Figure H.6. Predicted strain KC concentration profile on the solid phase on day 7 in the static model aquifer column. CT concentrations are in units of CFU/gram dry sediment.

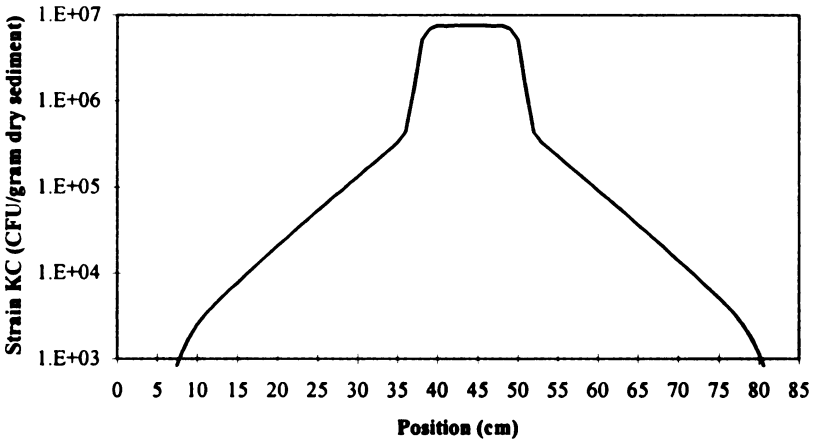

Figure H.7. Predicted strain KC concentration profile on the solid phase on day 26 in the static model aquifer column. CT concentrations are in units of CFU/gram dry sediment.

APPENDIX I

Disinfection Experiment

I.1 Disinfection Experiments

One means of encouraging success of bioaugmentation is the use of a disinfectant to remove competitors in the subsurface. The subsequent development of a stable community structure after bioaugmentation usually involves a succession of populations. Community succession begins by invasion of a habitat by microbial populations (Golley, 1977). Preemptive colonization occurs when pioneer organisms modify their habitat in such a way that invasion of their habitat by other microorganisms is discouraged. One way of providing strain KC with a competitive advantage over indigenous microflora is by disinfection of the aquifer sediments prior to inoculation and allowing strain KC to preempt colonization of aquifer sediments.

Disinfection using hydrogen peroxide (H_2O_2) was evaluated using aquifer sediments from the Schoolcraft, Michigan, field site. Twelve glass columns (Kontes Glass, Inc.), 10 cm long and 2.5 cm in diameter, were wet-packed with sediments from the Schoolcraft, Michigan, aquifer. Groundwater from the site was pumped through all twelve columns for one week to equilibrate the concentrations of indigenous microorganisms in the liquid and solid phases.

After equilibration, the columns were divided into four sets of three columns each. The columns were numbered consecutively from 1 to 12, with the first three columns belonging to group one, the second three belonging to group two, and so on. Disinfection was executed by pumping one pore volume of groundwater containing a given percentage of hydrogen peroxide (by volume) through each column. All three columns in the first group received groundwater with 0% hydrogen peroxide to serve as a control group. The second group received groundwater with 1% hydrogen peroxide, the third group 3%, and

the fourth group 5%. After disinfection, each column was flushed with one pore volume of sterile groundwater to remove any residual hydrogen peroxide remaining in the pore space. At this time, one column from each group was sacrificed and solids were obtained from both the proximal and distal ends of each column for bacterial enumeration. These analyses would provide insight into the effectiveness of removing indigenous flora from aquifer sediments using various concentrations of hydrogen peroxide.

For the remaining eight columns, one column from each group was inoculated with one pore volume of strain KC culture ($3.2\pm0.6 \times 10^7$ CFU/mL), while the second (and last) column from each group was not inoculated. After inoculation with strain KC, groundwater flow was resumed in all eight columns for a period of 24 hours. The groundwater flow rate used during this period yielded an average linear flow velocity of 15 cm/day, a rate equal to that of flow through the Schoolcraft aquifer. After this 24-hour period, bacterial enumerations were performed on samples obtained from both the proximal and distal ends of each column. Results were recorded as colony forming units (CFU) per gram dry weight of sediment.

The results of this experiment show that disinfection using hydrogen peroxide was successful at all concentrations used (1%, 3%, and 5%). Figure I.1 shows the bacterial cell concentrations for samples obtained from the proximal and distal ends of packed columns after disinfection using one pore volume of groundwater containing hydrogen peroxide. The effectiveness of even 1% H_2O_2 was apparent from the absence of any detectable concentrations of indigenous flora. High densities of indigenous microorganisms were measured in the control column (~10^6 CFU/gram dry sediment).

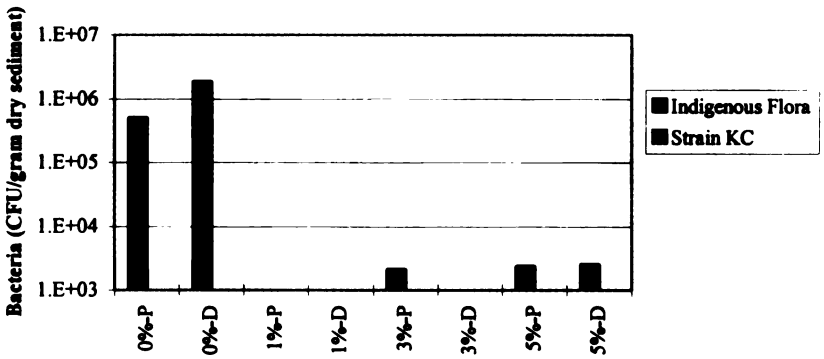

Figure I.1. Bacterial enumeration results after disinfecting the solids in packed 10-cm columns using groundwater containing 0%, 1%, 3%, and 5% hydrogen peroxide. P and D represent the proximal and distal ends of each column.

Evaluation of another group of columns shows that indigenous flora concentrations in the groundwater are too low to sufficiently invade solids after pumping for a 24-hour period. Figure I.2 shows results of disinfection, followed by delivery of about 1.5 pore volumes of groundwater containing indigenous flora. Only small concentrations (~10^3 CFU/gram) were measured in columns where disinfection was practiced. Again, the control column yielded cell densities near 10^6 CFU/gram dry sediment.

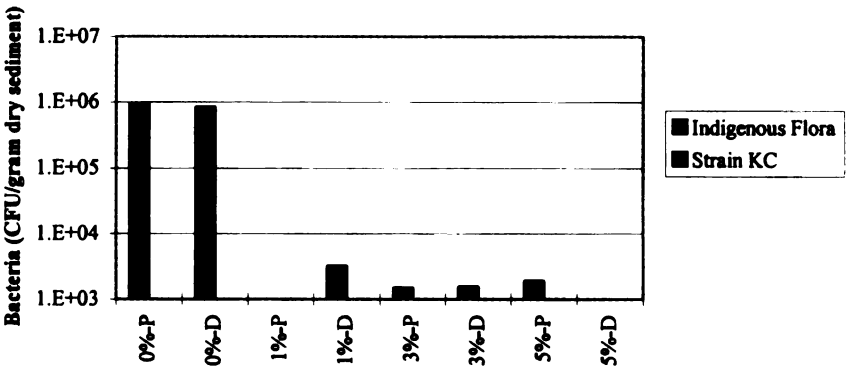

Figure I.2. Bacterial enumeration results after disinfecting the solids in packed 10-cm columns using groundwater containing 0%, 1%, 3%, and 5% hydrogen peroxide. P and D represent the proximal and distal ends of each column.

Disinfection using hydrogen peroxide, followed by inoculation using strain KC, appears to be an effective strategy for successfully colonizing aquifer sediments for the purposes of bioaugmentation. Figure I.3 shows the results of bacterial enumeration assays on samples taken from columns where disinfection and inoculation using strain KC was performed. In each of the columns analyzed, the concentration of strain KC on the solids after 24 hours of groundwater throughput was near 10^7 CFU/gram dry sediment near the proximal end of the column and ~10^6 CFU/gram near the distal end. These results show that disinfection using as little as 1% hydrogen peroxide can be used as a means for providing strain KC with an environment where successful colonization can be assured. In addition, the gradual decrease of solid-phase strain KC density over the length of the 10-cm column is in agreement with previous cell transport studies performed in our laboratory (Radabaugh, 1998).

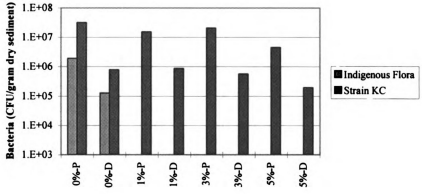

Figure I.3. Bacterial enumeration results after disinfecting the solids in packed 10-cm columns using groundwater containing 0%, 1%, 3%, and 5% hydrogen peroxide. P and D represent the proximal and distal ends of each column.

I.2 Experimental Data from Disinfection Experiment

Table I.1. Bacterial enumeration data from solid samples obtained from glass columns during the disinfection experiment.

Sample I.D.	Indigenous		KC	
	CFU	CFU/gram	CFU	CFU/gram
Col 1 - P	6.60E+05	5.02E+05	ND	ND
Col 1 - D	1.81E+06	1.88E+06	ND	ND
Col 2 - P	2.10E+06	1.91E+06	3.50E+07	3.19E+07
Col 2 - D	2.00E+05	1.28E+05	1.23E+06	7.87E+05
Col 3 - P	1.38E+06	9.63E+05	ND	ND
Col 3 - D	1.35E+06	8.38E+05	ND	ND
Col 4 - P	6.00E+02	6.07E+02	ND	ND
Col 4 - D	ND	ND	ND	ND
Col 5 - P	ND	ND	1.41E+07	1.53E+07
Col 5 - D	ND	ND	8.70E+05	8.63E+05
Col 6 - P	7.00E+02	6.73E+02	ND	ND
Col 6 - D	3.50E+03	3.18E+03	ND	ND
Col 7 - P	2.30E+03	2.11E+03	ND	ND
Col 7 - D	1.20E+03	8.93E+02	ND	ND
Col 8 - P	ND	ND	1.58E+07	2.07E+07
Col 8 - D	ND	ND	6.00E+05	5.63E+05
Col 9 - P	1.30E+03	1.47E+03	ND	ND
Col 9 - D	1.90E+03	1.53E+03	ND	ND
Col 10 - P	ND	ND	5.30E+06	4.54E+06
Col 10 - D	ND	ND	2.20E+05	1.93E+05
Col 11 - P	2.20E+03	2.37E+03	ND	ND
Col 11 - D	2.90E+03	2.55E+03	ND	ND
Col 12 - P	1.80E+03	1.87E+03	ND	ND
Col 12 - D	9.00E+02	8.56E+02	ND	ND

ND = Not Detected
P = Proximal End of Column
D = Distal End of Column

I.3 Literature Cited

Golley, F.B. (ed.). 1977. *Ecological Succession.* Benchmark Papers in Ecology 15. Dowden Hutchinson and Ross, Stroudsburg, Pennsylvania.

Radabaugh, P.D. 1998. Factors affecting the transport of *Pseudomonas stutzeri* KC. Master's thesis, Department of Civil and Environmental Engineering, Michigan State University, East Lansing, Michigan.

APPENDIX J

Microsphere Experiment

J.1 Microsphere Experiment

An experiment was conducted in order to assess the influence of size exclusion on the transport of micron-sized colloids through porous media. The effect of size exclusion was evaluated using aquifer sediments from the Schoolcraft, Michigan, field site. Two glass columns (Kontes Glass, Inc.), 50 cm long and 1.8 cm in diameter, were wet-packed with sediments from the Schoolcraft, Michigan, aquifer.

Inoculation was executed by pumping 10 mL of strain KC culture containing $6.9 \pm 1.4 \times 10^7$ CFU/mL. After inoculation with strain KC, groundwater flow was resumed in both columns at a rate yielding an average linear flow velocity of 15 cm/day, a rate equal to that of flow through the Schoolcraft aquifer. Aqueous samples were collected from the effluent of both columns after 52, 75, 91, 119, 140, and 166 hours. Samples were analyzed for strain KC and microspheres.

The results of this experiment show that size exclusion has very little influence, if any, on the "enhanced" transportability of micron-sized colloids through Schoolcraft aquifer sediment. Figure J.1 shows the strain KC concentrations in samples obtained from the effluent of both columns. The peak strain KC concentration was observed in the effluent of column 1 after 91 hours in column 2 after 75 hours. It is interesting to note that the strain KC concentration in the effluent was ~1% of the injected strain KC concentration. The transport of strain KC through Schoolcraft aquifer sediments has been the focus of research performed in our laboratory. The results of these studies have consistently shown that only 1 to 10% of the injected cells break through in the effluent of a 10 cm long glass column (Radabaugh, 1998). Therefore, the results of this study are consistent with what has been observed in previous laboratory experimentation.

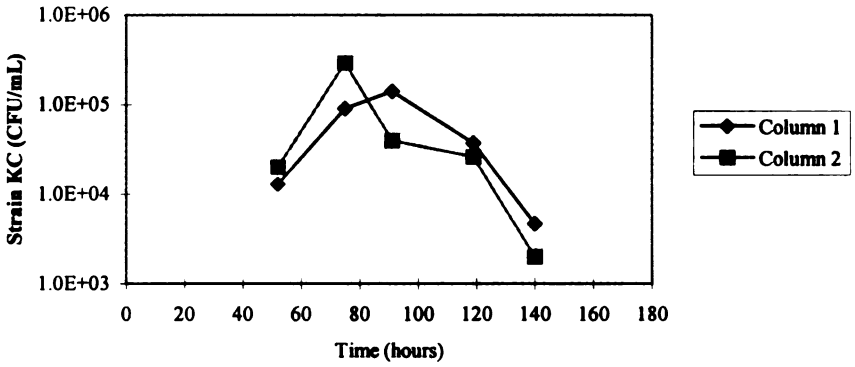

Figure J.1. Elution profile of *Pseudomonas stutzeri* KC in two model aquifer columns packed with Schoolcraft aquifer sediment.

Figure J.2 shows the breakthrough profile of the micron-sized microspheres in column 1 and column 2. The center-of-mass of the microsphere slug exited column 1 after 91 hours and column 2 after 75 hours. The microspheres migrated through the column at nearly the same rate as the strain KC cells. The only difference was that there appeared to be more dispersion of the cells, especially in column 1, as is evidenced by the wide elution peak shown in Figure J.1. The elution peaks shown in Figure J.2 are sharp, thus indicating little dispersion occurred as a result of flow through porous media.

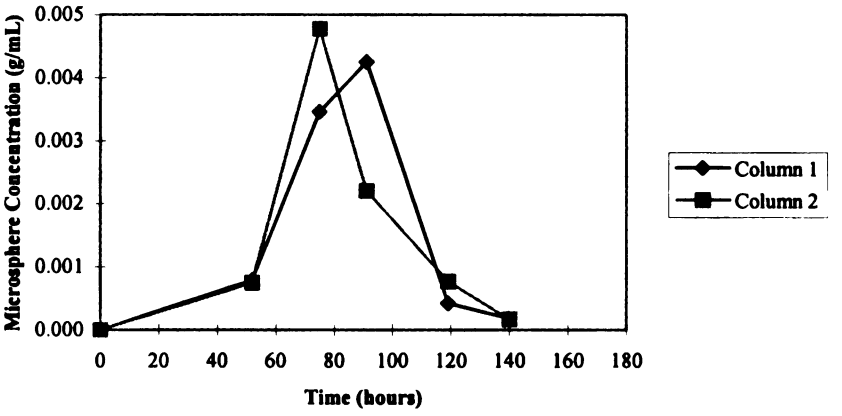

Figure J.2. Elution profile of micron-sized microspheres in two model aquifer columns packed with Schoolcraft aquifer sediment.

J.2 Experimental Data from Microsphere Experiment

Table J.1. Strain KC enumeration data from aqueous samples obtained from glass columns during the microsphere experiment. Strain KC concentrations are in units of CFU/mL.

Time (hours)	Column 1	Column 2
0	0	0
52	1.30E+04	2.00E+04
75	9.00E+04	2.90E+05
91	1.40E+05	4.00E+04
119	3.70E+04	2.60E+04
140	4.70E+03	2.00E+03

Table J.2. Microsphere concentration data from aqueous samples obtained from glass columns during the microsphere experiment. Microsphere concentrations are in unit of grams/mL.

Time (hours)	Column 1	Column 2
0	0.00000	0.00000
52	0.00079	0.00075
75	0.00346	0.00478
91	0.00425	0.00220
119	0.00042	0.00076
140	0.00019	0.00018

J.3 Literature Cited

Radabaugh, P.D. 1998. Factors affecting the transport of *Pseudomonas stutzeri* KC. Master's thesis, Department of Civil and Environmental Engineering, Michigan State University, East Lansing, Michigan.